Hes·so VALAIS WALLIS
School of Engineering

Hes·so
Haute Ecole Spécialisée de Suisse occidentale
Fachhochschule Westschweiz
University of Applied Sciences and Arts Western Switzerland

Degree Programme
Systems Engineering

Major Infotronics

Bachelor's thesis
Diploma 2019

Augsburger Nassim

Sensor of hyperpolarized ^{129}Xe inside blood

Professor
Djano Kandaswamy

Expert
Jean-Noël Hyacinthe

Submission date of the report
cf. thesis form (16.08.2019)

Valais excellence

Filière / Studiengang **SYND**	Année académique / *Studienjahr* **2018/19**	No TD / *Nr. DA* **it/2019/80**
Mandant / *Auftraggeber* ☒ HES—SO Valais ☐ Industrie ☐ Etablissement partenaire *Partnerinstitution*	Etudiant / *Student* **Nassim Augsburger** Professeur / *Dozent* **Djano Kandaswamy**	Lieu d'exécution / *Ausführungsort* ☒ HES—SO Valais ☐ Industrie ☐ Etablissement partenaire *Partnerinstitution*
Travail confidentiel / *vertrauliche Arbeit* ☐ oui / ja [1] ☒ non / nein	Expert / *Experte (données complètes)* **Jean-Noël Hyacinthe** Haute école de santé, 47 Avenue de Champel, 1206 Genève	

Titre / *Titel*

Détecteur de Xenon hyperpolarisé dans le sang

Description / *Beschreibung*

Dans la dynamique actuelle d'évolution de la médecine, d'une approche « taille unique pour tout le monde » à une approche sur mesure, dite « médecine personnalisée », il est essentiel d'avoir des outils d'imagerie moléculaire capables d'évaluer et de suivre les processus au niveau moléculaire et cellulaire.

La faible sensibilité de l'IRM rend pour l'heure très difficile – et non compétitif – l'imagerie moléculaire par IRM.

L'hyperpolarisation est un terme générique regroupant différents processus physiques d'augmentation de la polarisation et donc du signal IRM de 4 à 5 ordres de grandeur (sur un échelle logarithmique).

Le laboratoire d'IRM hyperpolarisée de la Haute Ecole de santé de Genève, travaille sur deux techniques d'hyperpolarisation.

Actuellement sur le marché on ne trouve aucun instrument utilisant l'hyperpolarisation pour faire du diagnostic (et non de l'imagerie). Un tel instrument nécessite quelques étapes :

1. La production de xénon hyperpolarisé
2. Du hardware : un détecteur pour récupérer le signal
3. Du software : Lecture du signal et lien à une base de données caractérisant les décalages fréquentiels

Le but du projet proposé est de faire un premier jet d'un **détecteur** suffisamment petit de telle sorte qu'il puisse être utilisé « at Point-Of-Care ». Idéalement, le résultat devrait être un détecteur (non optimisé au niveau de bobines, ni au niveau de la stratégie d'alignement de spins magnétiques) capable de lire le signal produit par le Xénon hyperpolarisé mis dans une émulsion PFBOC (**P**er**B**luocarbon-**B**ased **O**xygen **C**arrier, ce qui est un substitut de sang).

Objectifs / *Ziele*:
- Étude de la littérature sur le spin
- Étude sur le design d'un tel détecteur pour un puit de détection
- Réalisation d'un détecteur avec un puis « standard »
- Obtention d'un signal de relaxation dans une émulsion PFBOC

Signature ou visa / *Unterschrift oder Visum*	Délais / *Termine*
Responsable de l'orientation / filière *Leiter der Vertiefungsrichtung / Studiengang:* ..... [1] Etudiant / *Student* :	Attribution du thème / *Ausgabe des Auftrags:* **13.05.2019** Présentation intermédiaire / *Zwischenpräsentation* **13 – 14.06.2019** Remise du rapport / *Abgabe des Schlussberichts:* **16.08.2019, 12:00** Expositions / *Ausstellungen der Diplomarbeiten:* **28, 29 – 30.08.2019** Défense orale / *Mündliche Verfechtung:* **02 – 05.09.2019**

[1] *Par sa signature, l'étudiant-e s'engage à respecter strictement la directive DI.1.2.02.07 liée au travail de diplôme.*
Durch seine Unterschrift verpflichtet sich der/die Student/in, sich an die Richtlinie DI.1.2.02.07 der Diplomarbeit zu halten.

Rapport reçu le / *Schlussbericht erhalten am* ..... Visa du secrétariat / *Visum des Sekretariats* .....

Contents

HES-SO Valais-Wallis • rte du Rawyl 47 • C.P. • 1950 Sion 2
+41 27 606 85 23 • hei@hevs.ch • www.hevs.ch

Table of Figures

Glossary and Acronyms

ADC: Analog **to D**igital **C**onverter**:** it samples an analogic signal with a given resolution and sampling frequency into a digital signal

B_0: It is the static magnetic field which give the magnetization of a given atom population.

B_1: It is the sinusoidal magnetic field applied within a given time which tilt the magnetization of a given atom population.

Chemical shift: It is the nuclear resonant frequency relative to the standard B_0 given in ppm (part per million)

Cryptophane cage: a class of organic supramolecular compounds studied and synthesized primarily for molecular encapsulation and recognition. (cf. chapter Cryptophane cage for more details)

DAC: Digital **to A**nalog **C**onverter**:** transform a digital signal into an analogic signal

DNP: Dynamic **n**uclear **p**umping: one of the possible process to hyperpolarize a dipolar noble gas atom

EMF: **e**lectro**m**agnetic **f**orce

EMI: **e**lectro**m**agnetic **i**nterference

FID: Free **i**nduction **d**ecay**:** the measurement signal of the NMR after the deflection of the equilibrium magnetization of the nuclear magnetic spin

G: **G**auss unit for magnetic field 1 **T**esla= 10'000 **G**

HF: High frequency: frequency between 3–30 MHz with a corresponding wavelength of 100–10 m

HP: **H**yper**p**olarization/**h**yper**p**olarized: polarization of an isochromat in a magnetic field far beyond Boltzmann thermal equilibrium.

Isochromat: a group of spins, which resonates at the same frequency and has a quantity enough to be statistically relevant

KSPS: **K**ilo **s**ample **p**er **s**econd

LF: **L**ow **F**requency: frequency between **30-300 kHz** with a corresponding wavelength of **10km–1 km**

LOD: Limit **of D**etection**:** the effective minimum detectable quantity of FID

μ_0: induction constant equals to $4\pi * 10^{-7} \frac{V*s}{A*m}$

µC: microcontroller

MF: **M**edium **F**requency: frequency between **300 kHz – 3 MHz** with a corresponding wavelength of **1 km – 100 m**

MRI: **M**agnetic **R**esonance **I**maging

NMR: **N**uclear **M**agnetic **R**esonance

NOE: **N**uclear **O**verhauser **E**ffect: spin–spin coupling which act on T_1

PCR plate: a flat plate with multiple holes used as small test tubes

PFBOC: PerBlucarbon-Based Oxygen Carrier: blood substitute use as substrate

PPM: parts per million

RPi: Raspberry Pi: a small computer

RF: Radio Frequency: frequency between 3 kHz and 300 GHz used to communicate via electro-magnetic waves

RFPA: Radio Frequency Power Amplifier

SEOP: Spin-Exchange Optical Pumping: one of the possible process to hyperpolarize a dipolar noble gas atom

SNR: Signal to Noise Ratio

T_1: Time constant for the longitudinal magnetization to return to 63% of its equilibrium value, it is also called the spin-lattice or the longitudinal relaxation time

T_1^*: Apparent T_1 resulted through experimentation

T_2: Time taken by the transverse magnetization to return to 37% of its initial value, it is also called the transverse relaxation time. [https://www.imaios.com/fr/e-Cours/e-MRI/RMN/relaxation-rmn]

T_2' : $\frac{1}{T_2'} = \gamma \Delta B_i$ is the relaxation rate contribution attributable to field inhomogeneities (ΔB_i) across a volume containing an isochromat.

T_2^*: $\frac{1}{T_2} = \frac{1}{T_2} + \frac{1}{T_2'}$ apparent T_2 resulted through experimentation

THD: Total Harmonic Distortion

Verilog: a programming language used to configure a FPGA and its test bench

VHDL: Very High Speed Integrated Circuit Hardware Description Language: it is used to represent the behavior and architecture of a digital electronic system.

VSWR: Voltage Standing Wave Ratio: the power reflected from an antenna, which produces standing waves along the transmission line

^{129}Xe: a noble gas used as biosensor (cf. 1.3Hyperpolarized ^{129}Xe)

This list is unexhaustive but provides the core definition and acronyms used in this thesis.

HES-SO Valais-Wallis • rte du Rawyl 47 • C.P. • 1950 Sion 2
+41 27 606 85 23 • hei@hevs.ch • www.hevs.ch

1. Aim

1.1 Context

Each person's blood is unique. To characterize this uniqueness, blood has to be analyzed at the cellular and atomic level. One possible technique for this is called Nuclear Magnetic Resonance (NMR). This technique could be applied in testing which narrow-band antibiotics is most effective against targeted bacterial infections. The NMR has the potential to tackle the issue of microbial resistance globally by tailoring our use of antibiotics to increase their efficiency. Moreover, NMR technology opens doors for a high-throughput screening method for drug discovery.

1.1.1 Overall functioning

The NMR technique relies on the fact that each atom has an intrinsic "resonance frequency", which is dependent on the intensity of a generated static magnetic field (B_0), the chemical environment and the magnetic properties of the biosensor. In quadrature of B_0, an exciting sinusoidal magnetic field B_1 at the resonance frequency is produced for a given time. After the excitation phase, a weak-intensity free induction decay (FID) signal is retrieved. The spectrum of the FID signal permits to detect the kind and quantity of matter present in a given sample. This whole process aggregated in a single dimension NMR spectrometer using HP ^{129}Xe and it is the core of this project.

1.1.2 Using ^{129}Xe to offset the limitations of the existing NMR

Currently, NMR spectrometers are **expensive**, **large,** and **non-portable**. To produce powerful magnetic fields (a few tesla), large electromagnets are used and cooled with cryogenic liquid gas. Unlike conventional forms of angular momentum, spin does not arise from particle rotations, but rather form an intrinsic property of the particle itself. Their atomic nuclei exhibit a non-zero spin angular momentum and, in their ground state, have an associated dipolar magnetic moment. A nucleus exhibiting such a non-zero intrinsic angular momentum is the isotope ^{129}Xe (1/2).

In order to avoid the size and cooling problem, the magnetic fields have to be reduced and with them the size of the magnets producing the static field B_0. When, the intensity of the magnetic field B_0 is decreased, the resolution is proportionally decreased. The proposed solution to keep the resolution despite the decrease of B_0 is to use hyperpolarized noble gas, which will amplify the received signal by a factor of **100,000** without affecting the sample. ^{129}Xe is a biocompatible noble gas that can maintain its polarization for an extended period of time in blood, compared to other chemical elements. This time is called T_1. This increase in the signal intensity enables the possibility to enhance the sensitivity of the received signal (in particular, in MRI, the resolution of the images is increased). This permits a low-field NMR to work with a lower B_0 and therefore producing portable and more affordable devices.

1.1.3 Purpose of the project as a whole LEVERAGING existing NMR TECHNOLOGY for MF

The first phase of this project is to attain sufficient understanding of the current NMR system, as such to be enabled to design a simplified device. In a second phase, through the understanding of the current limitations of the existing device, the tailoring of the device, specifically for blood analysis, with the use of hyperpolarized ^{129}Xe. (which required lower frequencies than the traditional NMR) This project covers all aspects needed for the functioning of a MF NMR. Going from the chemistry to the software programing, as well as electronic design and electromagnetic/quantum physic.

Hyperpolarization techniques are not covered in this project. Hyperpolarizers are existing and can use SEOP or DNP techniques to produce HP ^{129}Xe.[1]

The geometry and the design of the magnetic generator (producer of B_1) and the magnetometer (receptor of FID) mechanism of the current NMR technology must be optimized to receive and transmit the maximal signal with the least modifications (THD and noise).

A mechanism needs to be developed to introduce the HP ^{129}Xe in the blood and replace the "depolarized" ^{129}Xe, which have a limed time of life in its Hyperpolarized form(T_1^*), while the sequence of excitation is running.

Biological cages (cf. cryptophane cages) will be used to encapsulate the HP ^{129}Xe. Chemical ligands are embedded on the outer surface of the cages. These ligands target specific blood compounds and helps determining if they are present or not by changing the atomic cloud of the HP ^{129}Xe. This will produce a frequency variation in the spectrum, called chemical shift. The HP ^{129}Xe in the cages needs to be replaced as the HP ^{129}Xe loses its polarization.

The HP ^{129}Xe has a stock of magnetization. This stock is diminished by the temperature, by the contact with surroundings atoms and by changes in magnetic field. Moreover, other geometrical variables influence the intensity of the FID and should be considered in the design of the device. Ansys Maxwell cannot be used to simulate this. There is the need to develop a finite state magnetic simulation software for HP gases with Matlab, Comsol or others to be able to optimize the design of the magnetometer and the field producer B_1. This also improves the understanding of the behavior of HP gases in their surroundings.

1.1.4 Developing a magnetometer (coil dimensioning FPGA, control signals) and integrating them into NMR technology (TO SOLVE MICROBIAL RESISTANCE)

In this thesis, a breakdown of the current technology is made as a basis for improvement to the NMR. The analysis is based on the different techniques used to generate and receive a magnetic field. In order to perform both of these functions, an air coil solenoid is designed and tested using Ansys Maxwell.

For this purpose, a physical prototype has been implemented by using existing electronic devices and chosen physical devices to test the air coil solenoid.

In a second phase, an electronic circuit board is developed to replace the existing electronic devices (the oscilloscope, the function generator and the lab amplifier). This circuit will produce the control signals and have specifications relative to the low frequencies used in the experiment. A TinyFPGA was chosen to implement the digital electronic and an analogic electronic circuit with existing IC and electronic components have been developed.

In the final stage of development, the standards on electrical safety and the electromagnetic compatibility (EMC) law in the medical environment have to be followed has depicted in section XX for the device to be commercially available (this implementation is beyond the scope of this work).

1.2 How does a NMR work?

The reference book used for this chapter provides working knowledge of how an NMR works (from the chapter 1.1 to 1.9) [2]

The **spin** is an intrinsic propriety of each nucleus. The ½ spins nuclei acts as small magnet with a North and South Pole (i.e., a magnetic dipole). Nuclei with a null spin do not have magnetic interaction. The spins larger than ½ have more poles that add more complexity and are not considered in this thesis. This thesis focusses specifically on NMR with hyperpolarized ^{129}Xe.

Nuclus	Spin	$\gamma \times 10^{-7}$ $(\mathrm{rad.T^{-1}.s^{-1}})$	Natural abondance (%)
^{1}H	1/2	26,752	99,985
^{3}He	1/2	–20,379	0,00014
^{13}C	1/2	6,728	1,11
^{14}N	1	1,934	99,63
^{15}N	1/2	–2,712	0,37
^{17}O	5/2	–3,628	0,037
^{19}F	1/2	25,162	100
^{23}Na	3/2	7,080	100
^{31}P	1/2	10,841	100
^{39}K	3/2	1,250	93,1
^{129}Xe	1/2	–7,441	26,44
^{131}Xe	3/2	2,206	21,18

Figure 1 : Physical characteristics of some usual nucleus used in NMR [2, p4]

The gyromagnetic ratio γ links the angular momentum j_n and the magnetic moment m_n together in a nucleus.

$$m_n = \gamma j_n \quad \text{[Equation 1]}$$

The angular momentum of an atom can be compared to a magnetic spinning top. This angular momentum produces a magnetic moment.

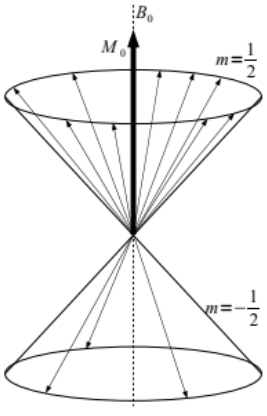

Figure 2 : Representation of the orientation of ½ spin nuclei in a static field B_0, each vector represents a nuclei on a cone and the total magnetization M_0 is the addition of all the magnetic moment of the spin. M_0 is paralel and in the same direction as B_0 [2, p5]

In the presence of a static homogeneous magnetic field B_0, the spins align along the magnetic field. However, not all spins are aligned with the magnetic field; some align against the magnetic field.

The ones aligned with the magnetic field are in a low-energy state (m=-1/2) whereas the others are in a high-energy (m=+1/2). This is illustrated in the Figure *2*.

At the thermal equilibrium and when $|\gamma|\hbar B_0 \ll k_B T$, the total magnetization follows Curie's Law:

$$M_0 \approx N\frac{\gamma^2\hbar^2 B_0}{4k_B T} \text{ [Equation 2]}$$

, where M_0 is the macroscopic magnetization, N is the number of spins , γ is the gyromagnetic moment, $\hbar$ is the Plank constant divided by 2π, $B_0$is the static magnetic field applied, k_B is the Boltzmann constant and T is the temperature in Kelvin.

This is followed by the Boltzmann's statistical distribution at the thermal equilibrium

$$\frac{n_1}{n_2} = e^{\left(-\frac{\Delta E}{k_B T}\right)}, \text{with } \Delta E = \gamma\hbar B_0 \text{ [Equation 3]}$$

, n_1 is the number of nuclei in a high energy state and n_2 is the number of nuclei in a low energy state.

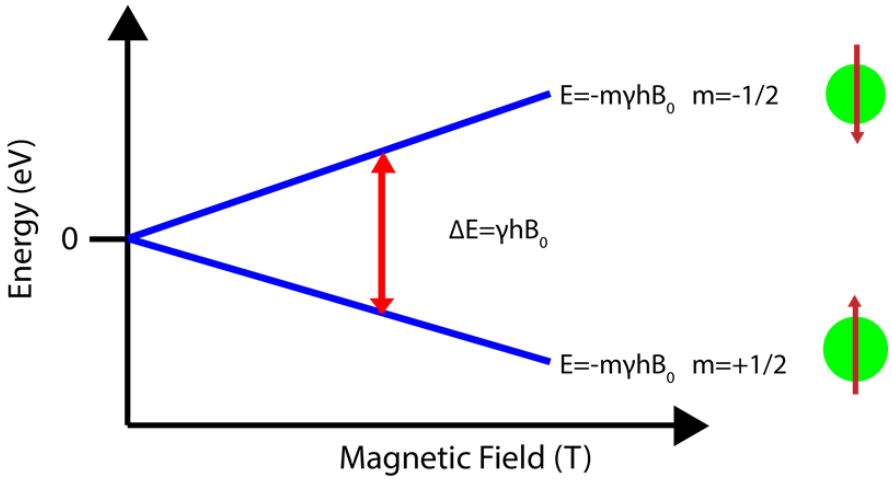

Figure 3 The splitting of the nuclear energy levels under an applied magnetic field. The green spheres represent atomic nuclei which are either aligned with (low energy m=+1/2) or against (high energy m=-1/2) the magnetic field.[3]

The difference of energy ΔE increases with the intensity of the magnetic field. In the equation of Boltzmann, this difference increases the number of nuclei in a high-energy state.

The polarization is given by the equation: $P = \frac{n_1 - n_2}{n_1 + n_2}$ [Equation 4].

When the polarization gets higher, the amplitude of the total magnetization M_0 is also amplified.

The HP ^{129}Xe is used to get a larger polarization than the one possible at equilibrium, as stated by the Boltzmann distribution. The factor of amplification between the left and right images in Figure *4* is about 10'000-100'000 allowing NMR at low field intensities. When doing NMR, we get a spectral measurement, the difference between the spectra obtained through conventional NMR and NMR in combination with HP ^{129}Xe.

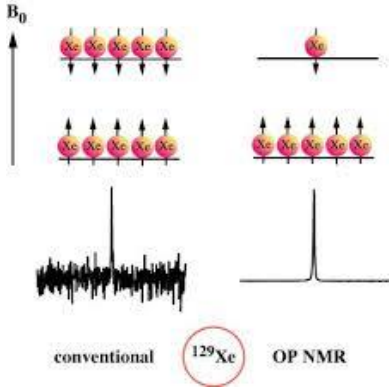

Figure 4 Spectrum difference between a conventional and Optical pumping NMR [4]

To produce this spectrum, the alignment of the vector B_0 and M_0 have to be tilted. To change this longitudinal alignment, a rotating magnetic field has to be applied at the Larmor frequency:

$$\omega_L = \gamma * B_0 \text{[Equation 5]}$$

, where ω_L is the Larmor frequency in radian, γ is the gyromagnetic constant of a given nuclei, B_0 is the amplitude of the static magnetic field apply.

The angle of excitation is the angle produces between the vectors in a rotating frame. After the excitation, the vector M_0 and B_0 returns to their equilibrium longitudinal state.

The excitation's angle equation: $\alpha = \gamma * \tau * B_1$ [Equation 6], where α is the excitation's angle, γ is the gyromagnetic moment of the atom to be excited this is also the frequency of the field B_1 , τ is the time of excitation, B_1 is the amplitude of the sine wave

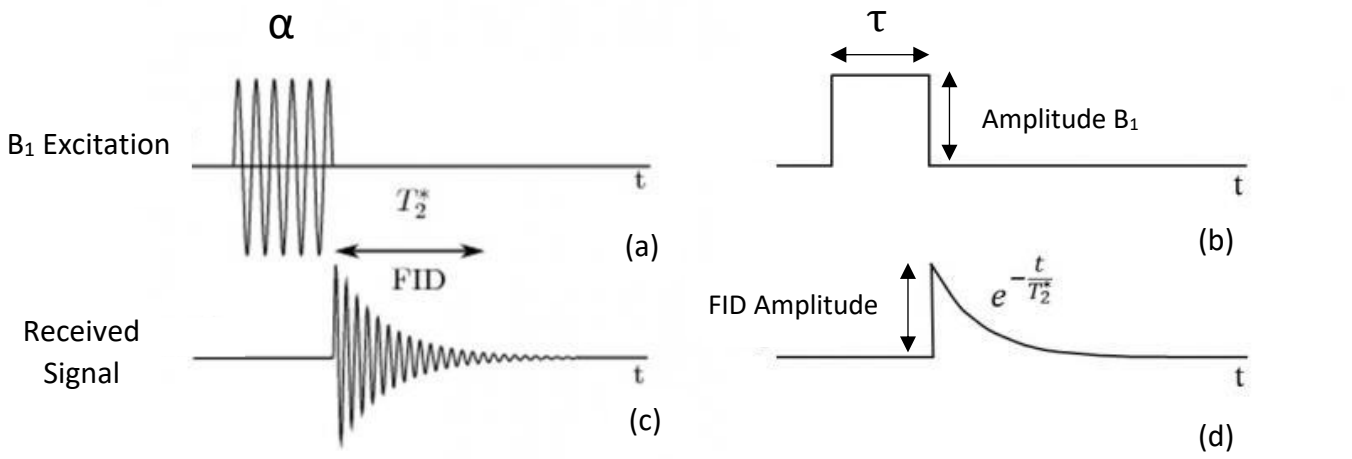

Figure 5 Graph from a sequence of excitation and reception in x-axis the time and in y-axis the amplitude (not to scale) a) the flip angle α with the sinusoidal excitation b) the flip angle envelope c) the FID received signal after the B_1 excitation d) the FID envelope[5]

The received signal after the excitation is a free induction decay (FID) which appears on the axis orthogonal to B_0 when the total magnetization M_0 returns to the alignment with B_0.

The equation of the FID is

$$A_{FID}(t) = A_0 * \sin(\omega_0 t + \varphi) * \exp\left(-\frac{t}{T_2^*}\right) \text{ [Equation 7]}$$

, where A_0 is the initial amplitude, ω_0 is the resonance frequency of the excited atoms, φ is the dephasing angle at the start, T_2^* is the time taken to retrieve the longitudinal equilibrium. T_2^* is an experimental variable which, depends on the inhomogeneities of the magnetic field.

A one-dimensional spectrum will be recovered from the FID precession. To process this signal, a Fourier transformation occurs. It has the propriety to be linear and can differentiate the different frequencies occurring in the FID. The different amplitude can be used to represent chemical shift.

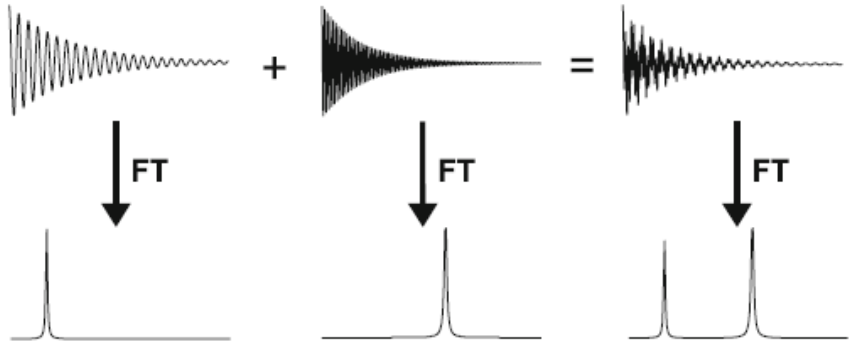

Figure 6 Linearity of the retrieved spectrum for the addition [6]

The shape of the excitation pulse is not inevitably a square in NMR. The better shape for the experiment is undefined and has to be found experimentally. Despite the unknown most suited shape, the shaped pulse chosen is a rectangle. In the electronic implementation, the modulation of amplitude of B_0 is considered.

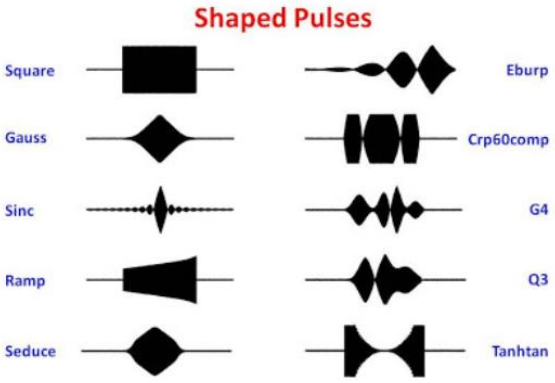

Figure 7 Different Shaped Pulses used in MRI sequences, modulation of B_1 amplitude with the same frequency [7]

There are several sequences to retrieve an FID signal. The easiest one is to excite the atoms at an angle of 90° and then read the signal directly after the excitation. The highest FID amplitude is obtained after an excitation angle **α** of 90° but when HP gases are used, another formula applied which is related to the return to the thermal equilibrium:

The magnetization of the HP ^{129}Xe (not at the Boltzmann thermal equilibrium): =

$$M(t,\alpha) = \mathrm{M_0}\exp\left(-\frac{\mathrm{t}}{\mathrm{T_1}}\right)\cos(\alpha^{\mathrm{n}-1})\sin\alpha \quad \text{[Equation 8]}$$

with n the natural non-zero number of time the excitation occurs, T_1 the time to return to the thermal equilibrium state in second , t time in second after the last known value of magnetization M(0,0), α angle of excitation in degree, M_0 the initial magnetization which is greater than the one at the Boltzmann thermal equilibrium.

With HP gases, the stock of initial magnetization $\mathbf{M_0}$ tends to return to the Boltzmann statistical thermal equilibrium. This implies that α has to be "small" to keep the effect of the hyperpolarization. The $M(t,\alpha) = \mathrm{M_0}\exp\left(-\frac{\mathrm{t}}{\mathrm{T_1}}\right)\cos(\alpha^{\mathrm{n}-1})\sin\alpha$ [Equation 8]is true until the magnetization $M(t,\alpha)$is lesser or equal than the magnetization in Curie's Law [Equation 2].

The spin-echo is a sequence of magnetization pulse: 90° pulse - 180°rephasing pulse at half time – reading of the spin-Echo after a given time. The spin-echo sequence cannot be used with hyperpolarized gases because the hyperpolarization is lost after the first 90° pulse.

In **MRI** and in **multidimensional NMR**, gradient coils are added to B_0. They change the homogeneity of B_0 at some point in space and this induces a change in the received spectrum. The sequence produces by the gradient coils and the signal processing to obtain an image are beyond the scope of the thesis. At the end, they retrieve multi-dimensional spectrum. In conventional MRI, the atoms, which are excited, are generally the protons (hydrogens atoms) because they are abundant and have a non-null spin. The Larmor frequency changes depending if the hydrogen is forming water or lipid. Selective excitation frequencies are produced to differentiate the type of tissue. This also occurs with HP ^{129}Xe depending of the surrounding nuclei, its electronic shell can be altered, and its gyromagnetic moment changes. At the end, the frequency of excitation has to be tuned to the Larmor frequency of the sample. This frequency is not well defined.

1.3 Hyperpolarized ^{129}Xe

A review paper explains in detail the advantages of biosensor principle of HP ^{129}Xe NMR [8]

Xenon exists at trace levels in the Earth's atmosphere with a concentration of 0.087 ± 0.001 ppm (parts per million) [9] It can be produced by air liquefaction. The price of xenon without isotope separation is CHF 277. - per 11 liters.[10] The abundance of ^{129}Xe among these other isotopes is 26.4% in air.

Xenon is a noble gas. This implies that it has no covalent and ionic chemical interaction with its environment since its electronic configuration is fully occupied. It exchanges his spins with the atoms around him and can create Van der Waals and London bonds. It is therefore ideal for non-intrusive analysis. Xenon is non-toxic for human and is biocompatible. It has an anesthetic effect and is neuroprotective; therefore, it is widely used in a medical setting.

Hyperpolarized ^{129}Xe amplifies the received signals up to 100'000 times. This increase in the signal is due to the fact that Boltzmann's equilibrium is no longer followed. The result obtained is that a container of ^{129}Xe atoms has more spins in the excited state (α) than in the normal state (β). This increases the total magnetization of an isochromat.

^{129}Xe has the particularity of having a dipole moment and therefore a spin ½, so they are in 2 states a high-energy state and another low energy state. Its quadrupole moment is zero. This implies

that its relaxation is slower and hence the relaxation time T1 is larger. This time T1 in a non-magnetic fluid is between 20 and 120s, whereas in human blood it is about 6-8s for arterial-oxygenated blood and 3-4s for venous-deoxygenated blood. [11] for it to be detected by an NMR spectrometer. If multiple sequences have to be made, it is necessary to recycle the “normal” ^{129}Xe and replace it with HP ^{129}Xe. The real time of loss of magnetization (T_1^*) has to be experimentally found. This time is limited by the SNR of the FID at the processing stage and the SNR has also to be determined.

Hyperpolarization techniques are being developed at the Geneva School of Health Sciences. Hyperpolarized ^{129}Xe can be transported from Geneva to Sion in liquid nitrogen-cooled boxes so that it can be used far from the production site. These boxes allow hyperpolarization to be maintained for several days. The HP ^{129}Xe at a few Kelvin box into solid state. The polarization is being lost and tends to return to Boltzmann's equilibrium.

HES-SO Valais-Wallis • rte du Rawyl 47 • C.P. • 1950 Sion 2
+41 27 606 85 23 • hei@hevs.ch • www.hevs.ch

1.4 Cryptophane cage

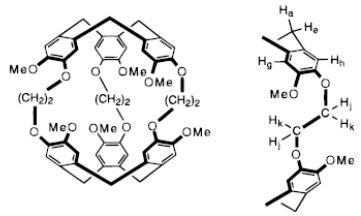

Figure 8 On the left a cryptophane cage, on the right a linker which can be attached to the cage [12]

Cryptophane cages are organic supramolecular compounds synthesized for molecular encapsulation and recognition. In this project, ^{129}Xe is encapsulated in the center. This induces a shift in the measured spectrum, called the chemical shift. This action is caused by the change of the electronic cloud of the ^{129}Xe. Chemical ligands are linked to the cryptophane cage. The final long-term goal of this project is to use specialized ligands, which link, to certain type of bacteria. Depending if the ligands are linked or not, the electronic cloud of the encapsulated ^{129}Xe is modified. A change in electronic cloud induces a change in the chemical shift and in such NMR with HP ^{129}Xe can be used as a biosensor. This effect is shown in the Figure *9*.

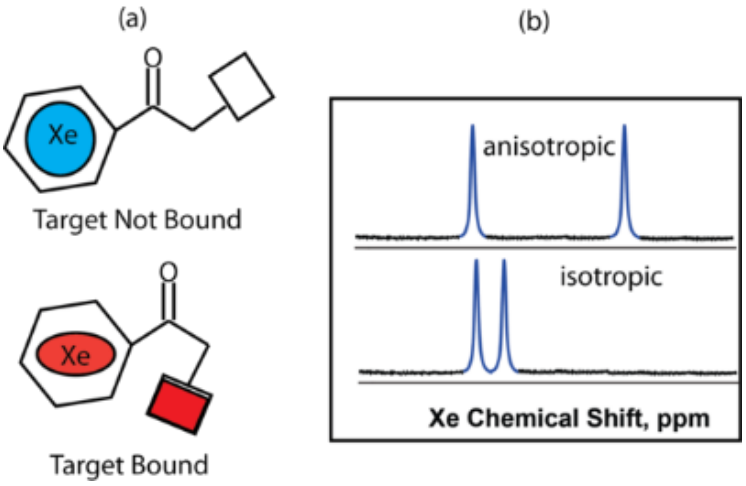

Figure 9 (a) change of the form of a molecular sensor and of the ^{129}Xe electronic cloud (b) corresponding change in the chemical shift [12]

"The hyperpolarization of xenon makes possible the observation of low concentrations biosensors. This enables to detect submicromocular concentrations by judicious signal acquisition[…] When the concentration of biosensor is lower compared to dissolved xenon, the dissolved xenon can act as a polarization reservoir if just magnetization from the caged xenon is excited (done with judiciously chosen selective pulses since the resonances are well separated). With a delay of 100 ms second between excitation pulses there is essentially full recovery of the caged xenon and many acquisitions can be done before the pool of hyperpolarized xenon is depleted and must be refreshed. This rapid, direct excitation approach allows detection down to the **hundreds of nanomolar** concentration range with natural abundance xenon and a polarization of a few percent. (^{129}Xe enrichment and higher polarization could yield an ≈ 40-fold lower detection limit) …" [13]

The above citation explains the HyperCest technique. In our project, this technique can be used to keep the SNR of the FID signal relatively constant after each excitation. The only difference needed to use this technique is to inject more HP ^{129}Xe in the blood. When the blood is saturated with “depolarized” ^{129}Xe, these techniques does not work anymore. A way has to be found to replace the saturated “depolarized” ^{129}Xe in the blood with new HP ^{129}Xe. A possibility would be to wait until the concentration of ^{29}Xe inside the sample diminishes due to “diffusion” in the surrounding air. The time of diffusion has to be defined with its variables.

This technique of relaxation is needed for time analysis and this is beyond the scope of this thesis. This technique is essential and need to be implemented in commercially available NMR spectrometer to enable the possibility to use HP ^{129}Xe inside blood. This is beyond the scope of this thesis.

2. Existing NMR device

2.1 Low-field NMR spectrometer

Currently, there is no commercial spectrometer available for NMR at LF and MF frequencies, which are using HP ^{129}Xe. There exist experimental and educational devices, which are made to handle NMR at LF (cf. 13.1Terranova-MRI, Earths field MRI & NMR teaching).

There exists an NMR spectrometer, which was conceived entirely for low frequency (30–300 kHz). Each of the electronics components are explained. However, it uses a dedicated function generator and acquisition signal cards from LabVIEW™. It is program to excite either xenon or hydrogen. It uses a single coil for measuring and producing B_1. A sample of the technical implementation is given in this section. (13.3 Low-Field NMR/MRI Systems Using LabVIEW™ and Advanced Data-Acquisition Techniques).

To implement a commercial product, it is needed to be affordable and small. In the developed main source project, the computer needs a LabVIEW™ paid license. Moreover, to run the program, a LabVIEW™ license and a supported OS are needed. In the case of a commercial product, this option is rejected but National Instrument IC can always be used without LabVIEW™. For further development, this project needs to work with open source software and a conceived electronic board to handle all the functions of an NMR.

An open source **Earth's Field NMR Spectrometer** is existent, has open hardware firmware and software, and is available on GitHub. [https://github.com/geekysuavo/pyppm]

The main drawback of this earth's field spectrometer is the magnetic interferences with its surrounding. Since it does not use magnetic shielding at LF. The LF need more material to be stopped than MF and HF.

In the first version, no attention where taken to handle electronic issues (separated mass-planes). Only one mass plane for digital, analog and power supply were designed. This resulted in unwanted magnetic field interactions induced by the not well-designed mass planes which acted as an antenna receiving unwanted external electromagnetic waves and producing also unwanted electromagnetic waves. In every stages of the design, this outside and inner noise disturbed the electronic parts of the spectrometer and especially the LNA.

This project has been improved with a version 2 which separated the mass planes and the project is still active at the time of this thesis.

2.2 Existing standalone portable NMR spectrometer HF

There are other NMR proprietary devices all-in-one spectrometer which are portable using magnetic field B_0 between 0.4 T and 2T. However, they are not suited for HP gases and needs software or/and hardware modification for ^{129}Xe (13.4 The mq-ProFiler/13.6 picoSpin™ 80 Series II NMR Spectrometer).

The NMReady-60 Pro from Nanalysis (13.7 NMReady-60PRO) is an NMR spectrometer using a magnetic field of 1.4 T already suited for ^{129}Xe. Some laboratory has already conducted some experiments by using this device with HP ^{129}Xe. [14][15][16]

A quote has been requested. The price of the device is 65'000 $. For academic usage, a reduction of 10'000 dollars is made. The device has two channels; the second channel can be configured for a different chemical compound. They also have an automatic injection technique, which is existent but does need software adjustment to insert the HP ^{129}Xe blood inside the blood before testing. This adaptation of the automation injection process introduces extra unknown costs.

2.3 Existing Small devices

2.3.1 Small Hyperpolarizer

There exists small hyperpolarizer to produce the HP ^{129}Xe before the admission. This is an optimized microfabricated platform for the optical generation and detection of HP ^{129}Xe. This hyperpolarizer enables the possibility to have a compact and affordable polarizer. With the drawback, that it provides a signal enhancement by a factor of only 5300 ± 200. [17]

2.3.2 Multipurpose IC

IC RFID transponders are small CMOS devices, which are producing an oscillating magnetic field for communication purposes. They are not effectively adapted for NMR and cannot be configured for this purpose. Although, dedicated ICs for NMR measurement are already existent with digital logic, analogic component and even an embedded microstrip antenna. [18] The only functions, which is not handle by this type of IC, are the signal processing and the field B_0 production. However, no commercially available IC where found. The main reasons why the antenna is inside the IC is to diminish thermal noise, signal distortion and cable attenuation issues also the antenna can be manufactured with more accuracy. This single device enables the possibility to connect only the power supply and a fast-synchronous communication protocol to transmit excitation sequences and to receive the digitalize FID data.

For MF frequency, the antenna is too large to be contained inside a single chip. This implies, the chip needs an external antenna which can be directly connected on top or on bottom of an IC.

2.4 Open source NMR

Open source NMR are existent. (Cf. 13.5 Opencore NMR) It is not designed to be suited for low magnetic field. It is working with a FPGA and RF electronic components. The total cost of a homemade NMR console is approximately 5'000 $ only for the hardware part. The electronics hardware can be modified to use lower frequencies. The software can also be modified accordingly.

3. Schematic diagram

The implemented device works according to the following principle diagram:

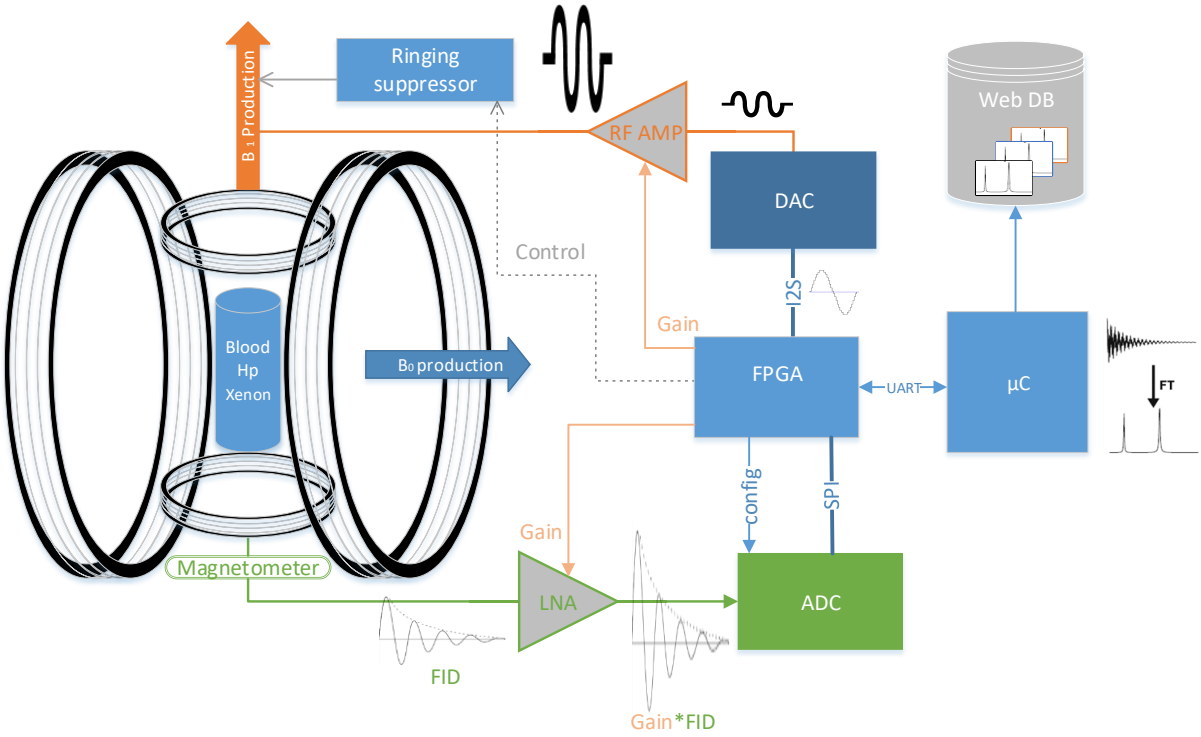

Figure 10 Schematic diagram *NMR made with Visio*

All the components are described in further details in the chapter implementation options.

To understand this schematic diagram, a sequence diagram is more suited which is shown in **Figure 46** and **Figure 47**. At first, the user has to configure the µC. Then, the other elements of the diagram have to be powered on and stabilize (e.g. B_0 has to be present and homogenous). At this time, the user can start a sequence on the µC. The µC send a start sequence to the IC and wait on the ADC. The IC tells the injector of the sample (not viewed on schematic diagram and not implemented) to add blood into the chamber, the HP ^{129}Xe and the sample are placed inside the dispositive.

During an acquisition sequence, the IC produces a digital signal of excitation, which is being converted by a DAC and amplified by a RF amplifier. This analogue power signal is sent to the B_1 magnetic producer. At the end of the excitation, a ringing suppressor is activated to suppress the energy stored in the magnetic generator (i.e. counteract the ringing). After this suppression ringing delay, an FID signal from the HP ^{129}Xe is retrieved in a magnetometer and amplified by an LNA (low noise amplifier). After this stage, the amplified signal is transformed by the ADC. This transformed signal is sent to µC since the device power on but the µC does not store the data. When the IC interrupts the µC, the µC starts saving data until the end of the interruption.

This acquisition sequence can be configured to be repeated many times. At the end of the sequences, the µC can start processing the received signal to produce the spectrum of the averaged FID by using Fourier's transformation.

The first choice made in this implementation is to use a digital reconfigurable IC and not an analogic circuit due to simplicity reasons and easier reconfigurability. The signal processing takes place on a microcontroller, which can process the signal with no time constraint.

In fact, the assembly DAC, ADC, IC and µC can be seen has an arbitrary function generator and a spectrometer for small signals such devices are existent but where not available in the college at the time of this thesis. (7.1.2 Red Pitaya STEMlab (FPGA+ µC))

4. Risk analysis

4.1 SNR

From the schematic diagram, the main risk is to receive no signal and to retrieve only noise. To solve this risk, the **SNR** has to be improved in the electronic and physical components. The noise depends from many factors. In the case of the measurement of an electromagnetic force, the most relevant factor is the measurement is the temperature, which produces thermal noise. The equation of this noise is given

$\text{Noise} = \sqrt{4k_B(R_cT_c + (R_m + R_{el})T_e) \bigtriangleup f}$[**Equation 9**], $\bigtriangleup f$: the bandwidth of excitation in radian, k_B: Boltzmann constant, R_m: magnetic impedance between the sample and the coil's surrounding, the loss produces Eddy's currents, R_{el}: is the electric coupling seen from the coil with the sample T_e: the temperature of the sample, T_c: the temperature of the coil and R_c : the resistance of the coil at the frequency of excitation

Cooling system has to be added to the device in the critical regions where the temperature adds too much thermal noise. Narrowing the bandwidth introduces also smaller noise. Introduction of an electrical shielding diminishes R_{el}, placement of the susceptibility magnetic far from the source is introducing less Eddy's current loss from the source. R_m: gets also bigger at higher frequencies.

$S_m = \omega_0 \left(\frac{B_1}{I}\right) M \sqrt{\frac{50}{R_c}}$[Equation 10], ω_0 the Larmor frequency, M the magnetic intensity, $\frac{B_1}{I}$ is the field generating efficiency of B_1, M the magnetization inside the coil, R_c : the resistance of the coil at the frequency of excitation

The amplitude of signal after the matching of the capacitors S_m is related to the frequency of excitation that implies, the frequency $\omega_0$must be maximized. The size of the sample and HP ^{129}Xe enhanced the magnetization M. The resistance of the coil must be diminished. $\sqrt{\frac{50}{R_c}}$ are the losses due to the 50 Ω impedance adaptation of the transmission cables.

From the **Equation 9** and **Equation 10**, the following equation can be deduced to know how much signal is produced depending of the excitation angle α and the time when M_0 where measured:

$$SNR(t, \alpha, \mathrm{n}) = \frac{\sum_{\mathrm{i}=0}^{\mathrm{n}} \left[\mathrm{M}_0 \exp\left(-\frac{\left(\frac{\mathrm{t}}{\mathrm{n}-\mathrm{i}}\right)}{\mathrm{T}_1} \right) \cos(\alpha^{\mathrm{i}-1}) \sin\alpha * \omega_0 \left(\frac{B_1}{I}\right) \sqrt{\frac{50}{R_c}} \right]}{\sqrt{n * 4k_B(R_cT_c + (R_m + R_{el})T_e)\Delta f}}$$[Equation 11]

This equation gives us the signal to noise ratio of a given sample in the case of HP gases.

HES-SO Valais-Wallis • rte du Rawyl 47 • C.P. • 1950 Sion 2
+41 27 606 85 23 • hei@hevs.ch • www.hevs.ch

The FID signals are summed together while the noise is multiplied by a factor $\sqrt{n}$. For simplification purposes, it is assumed that the noise is not time dependent. This produces an enhancement of the SNR by the number of repetitions.

Notice that, the range where this equation is true has to be defined but the magnetization has to be bigger than Curie's law At the thermal equilibrium and when $|\gamma|\hbar B_0 \ll k_B T$, the total magnetization follows Curie's Law: $M_0 \approx N\frac{\gamma^2\hbar^2 B_0}{4k_B T}$ [Equation 2]. It assumed that the change in magnetization is linear and the magnetic fields B_0 and B_1 are homogenous and in quadrature. In addition, the time between the repetitions is constant and has to be greater than the time of relaxation. The number of repetition n has also to be experimentally selected so that

$\mathfrak{H} * SNR(t, \alpha, n+1) > SNR(t, \alpha, n)$, where $\mathfrak{H} > 1$ is the experimental factor which has to be found by experimentation during the phase of signal processing. To find this factor, it is needed to find if the final spectrum stored on the Database has less noise than the calculated spectrum with one less excitation.

4.1.1 Impedance matching

The cables between the signal board and the coil can play a huge role on the amplitude of the received signal. In one direction, they have to transmit power-oscillating signal with a given frequency without introducing THD. In the other direction, they have to receive a small FID signal without attenuation and added THD. Since the two directions do not act the same, they do not need the same transmission cable characteristics.

In general, when coax cables are used to transmit power-oscillating signals, the input and output impedances must be matched at 50 Ω. This is a compromise between the maximal power supported in a cable and the power reflected (VSWR) which introduces THD. Notice that, the power transmitted to the B_1 producer is not the total power used to generate B_1. There are additional thermal power losses in the field generating efficiency $\frac{B_1}{I}$, which are linked to Joule losses. They induce thermal noise.

In fact, to minimize the coax attenuation on the received small FID signal, the optimal line resistance is 77 Ω. In the TV domain, RG6 CATV cables with a line resistance of 75 Ω are usually used. These cables can be used to connect the LNA and the magnetometer. In addition, the length of the cable has to be minimized to reduce the attenuation and the connector at the magnetometer side of needs to use nonmagnetic materials to not disturb the magnetic field produced and received by the magnetometer. The impedance matching and tuning circuit on the side of the B_1 producer needs nonmagnetic components to be immune from magnetic field production and to not product unwanted magnetic field. On the side of the LNA, magnetic precautions are not necessary if the LNA is sufficiently far from the magnetic field producer B_1; however, an impedance matching circuit is needed to receive more power.

In the case of transmission of RF power signal (without DC), the maximal power transmitted in (dBm) inside a coax cable is encountered for a line impedance value of 30 Ω. While, the minimal attenuation is at 77 Ω. A compromise must be found, and it is 50 Ω. Since the power transmitted by the excitation signal is greater, a 50 Ω resistance is more suited for this case.

At LF, the impedance matching has a lower importance. In fact, the length of the wave measures more than 1 km, which is bigger than the line of transmission. Another condition needs to

be respected for frequency lower than hundred kilohertz. This is the Heaviside condition, which states that if the line is designed such that R/L=G/C the line becomes absolutely distortion less [19, p65]

However, the input impedance of the receiving equipment must still be higher and preferably, in a ratio of at least 1/5 with the output impedance. This technique is currently used by RF amplifier in the audible frequency.

The formula, which gives the impedance of a coax cable, is the following:

$Z_c = \frac{1}{2\pi}\sqrt{\frac{\mu_0\mu_r}{\varepsilon_0\varepsilon_{res}}}\ln\left(\frac{d_e}{d_i}\right)$ [Equation 12], where

Z_c: characteristic impedance

ε_0 : vacuum permittivity: 8.85416 * 10-12 environ

ε_{res} : relative permittivity: 1 for vacuum, slightly more for air and air-insulated coaxial cables

μ_0 : vacuum permeability: 4π*10-7 = 1.256*10-6, μ_r: relative permeability: 1 for all non-magnetic materials (other than iron, nickel, cobalt, etc.)

d_e: outer diameter

d_i: inner diameter

The attenuation of a coax is minimal for a diameter ratio of $\frac{d_e}{d_i}$ = 3.59. In this case, and by substituting in the formula for impedance, we find a characteristic impedance of 77 Ω.

The diameter ratio that allows the most power to pass through a coax without risk of breakdown is $\frac{d_e}{d_i}$ = 1.65. Which is approximately 30 Ω [20]

4.2 Field homogeneity/External perturbation

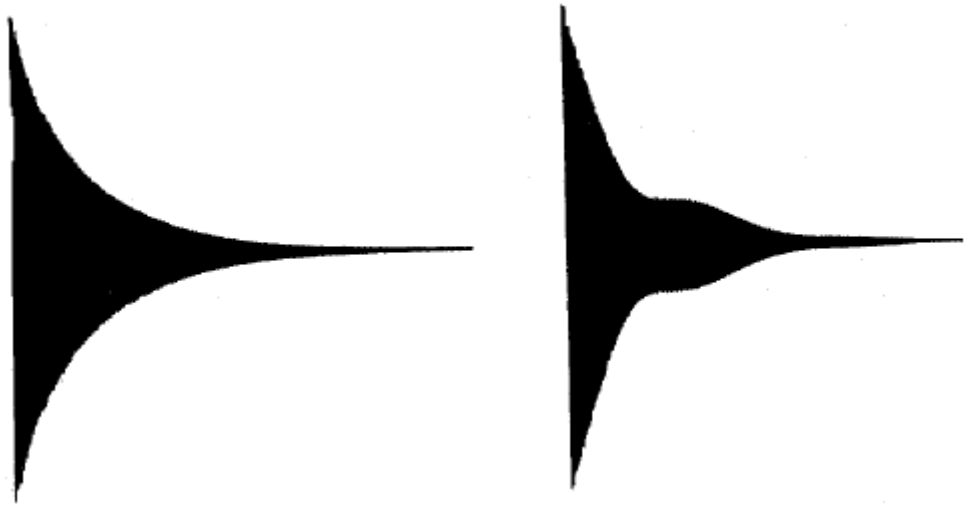

Figure 11 FID with shimming coil (left) without shimming coil (right). [21]

The second major risk is **the inhomogeneity of the field B_0**. It can change the shape of the received FID signal (i.e. the chemical shift), because the Larmor frequency in each region in space of the isochromat will be different. Each isochromat will have a different Larmor frequency. The

retrieved spectrum will be flattened. The field homogeneity $\frac{\Delta B}{B}$ is the difference of the maximal difference divided by the mean of the field in a given space and direction.

The geometrical angle between B_0 and B_1 has to be 90 degree to reduce the perturbation between the fields.

In addition, the excitation signal, which produces B_1, has to avoid distortion and glitches in the production of the exciting sine wave. VSWR of B_1 producer has to be optimal. To this purpose, the impedances must be matched accordingly. The production of the rotating field $\mathbf{B_1}$ has to be produced with the less current as possible to optimized $\frac{B_1}{I}$. With this diminution of current, the thermal noise due to Joule losses is reduced.

External disturbances in the magnetic field cause inhomogeneities in the HP ^{129}Xe. If they are not aligned with the vector of HP ^{129}Xe polarization and if they are at the resonant frequency of the HP ^{129}Xe, they diminish its T_1 and its polarization. Magnetic shield can prevent these EM perturbations. In addition, external EM waves can produce undesired frequencies in the received spectrum; all the electronic devices have to be shield against the external perturbations to suppress these undesired signals.

4.3 Electronic device

Electronic devices are also prone to external noise disturbances. They need to be shielded accordingly.

For electronic devices, the generation of the excitation pulse has to avoid distortion and glitches. The function generator needs a good resolution and a good clock stability.

The DAC has to convert the signal with the less noise and time drift as possible. The power amplifier has to amplify the signal without adding harmonics and distortion

The power amplifier has also to be optimized after the generation of the first signal. In addition, a dedicated IC is needed inside the power amplifier to avoid glitches in the excitation signal.

Multi-processor micro controller (μC) with OS are prone to glitches in the production of time sensitive signals. The time taken by each instruction in a μC is not always the same. They are dependent from the pipelined used of instruction by jump prediction etc. Therefore, a dedicated IC is needed with synchronization and **hard real-time**.

In fact, the thermal noise is preeminent and puts the limit of the reception. The components have to be fewer thermal sensitive as possible, to prevent thermal noise. It can also be needed to cool certain parts of the electronic circuit.

The interaction between the HP ^{129}Xe and the blood diminishes the HP ^{129}Xe polarization. The physic and chemistry of this interaction are hard to analyze and are not treated in this thesis, but they give critical times and diminish the T2* time of the FID signal. Also, a magnetic schema of the HP ^{129}Xe and its container will be needed to determine its magnetic susceptibility and one of the interactions to analyze.

4.3.1 Quantization noise

The quantization noise depends of the number of samples per second and the resolution. The resolution can be seen on the y-axis and the sample par second in the x-axis. This effect is unwanted especially for low amplitude receive signal. For this purpose, the more resolution has an ADC the less noise will be produced.

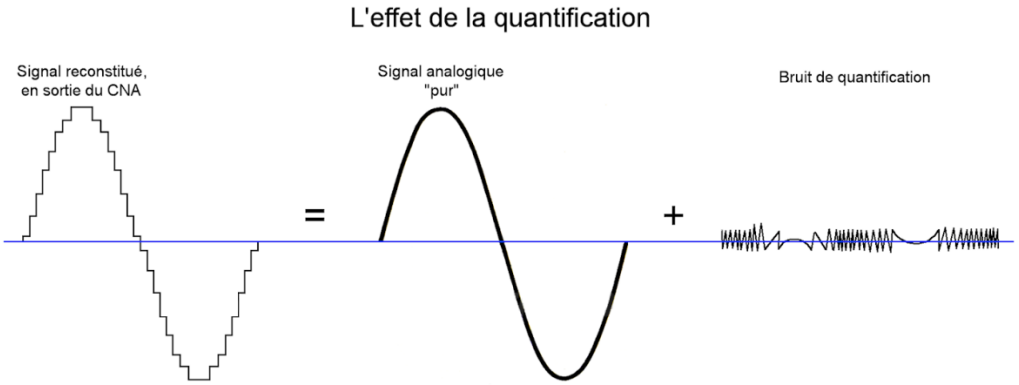

Figure 12 Quantification noise (vintage-audio-laser.com)

On the right, the quantification noise is represented and added to the received digital signal to produce the digital quantized signal.

5. Specifications and sizing

5.1 Physical and chemical specifications

It was stated that a chemical shift of at least **50 ppm** (parts per million) should be detectable for chemistry purpose. A chemical displacement of 50 ppm corresponds for a Larmor frequency of 50 kHz to detect a frequency variation of 2.5 Hz. This corresponds to differentiating a frequency of 50'002.5 Hz from one of 50 kHz in the retrieved spectrum without overlap. This gives us directly the sensitivity of detection in $\frac{ppm}{\sqrt{Hz}}$. A spectrometer has to be found and/or made for such sensitivity. It was decided to make a device working at low magnetic field but stronger than the earth's magnetic field.

The only parameters given to design the electronic spectrometer were: "the T_2^* which is equal to roughly 5-10 [ms] and the angle of excitation is **2°**. They depend on the temperature (thermal agitation), the magnetic field strength and gradient, the size of the sample, the partial pressure of the xenon in the mixture and the **magnetic susceptibility** of the container (glass or plastic). Also, the signal depends on both magnetization (i. e. hyperpolarization rate and relaxation, intensity and homogeneity of B_1, in short physics) and electronics (Q of the antenna, noise of the preamplifier etc...)". Dr. Jean-Noël Hyacinthe gave these parameters and the explanations. The physical part was not treated and only the electronic perturbations are treated. When the NMR spectrometer is functional, it will enable the possibility to test the HP ^{129}Xe with all the interactions between the physical parameters.

B_0 > Earth's magnetic field $\approx 50\mu T$

Security Factor = 80

$$B_0 \min = 50\mu T * 80 = 4mT$$

$$f_{B_1} \min = \frac{\gamma_{Xe}}{2\pi} * A_{B_0} \min = \frac{74.521*10^6[rad/T]}{2\pi} * A_{B_0} \min = 47'108\ [Hz]$$

$$B_1 = \frac{\alpha}{\gamma_{Xe}*\tau},\ \alpha \approx 0.035\ radian, \gamma_{Xe} = 73.997 * 10^6 [Hz/T]$$

τ : = excitation time (to be the smallest as possible and $\tau < T_2^*$)

$$\tau * B_1 = \frac{\alpha}{\gamma_{Xe}} = \frac{0.035}{73.997 * 10^6} = 4.73 * 10^{-6}[s * T]$$

This implies that B_1 for a time of excitation of 1 millisecond is equal to $4.73 * 10^{-3}$[T].

The intensity of B_1 and the time of excitation τ are independent from B_0

When using such low frequencies, it is not possible to use the same components as in high frequency. The length of the line needed to make $\lambda 4$ or rat-race circuits are too long. The component will be prompt to EMI and large signal attenuation. Components working at small frequency are needed to be implemented.

In the existing NMR spectrometer at the Geneva School of Health Sciences, they are using a transmission reception probehead (solenoid with litz-wire) with a frequency of approximately 50 kHz same frequency and their main problem is during the shutdown of B_1.

At that moment, they need to measure the received signal, the magnetic power stored in the coil has also to vanish. This stored power is reemitted at the frequency of resonance of the coil, which is approximately the same as the excitation pulse. A solution has to be found to fight against this ringing issue.

A solution to this issue is to use a quality factor damper to transform the quality factor Q within a given time and retrieve a signal after the dissipation of the energy. The stored energy in the coil will be faster dissipated. With is solution, more signal can be retrieved from the FID without noise.

Another solution is to use two different coils one for transmission and one for reception. They need to be in quadrature to avoid mutual inductance effect. A geometry can be found to solve this issue.

In fact, by the end of the project, it was discovered that the field $\mathbf{B_0}$ intensity does not require to be low. It was thought at the beginning of the project that if the magnetic field B_0 is not aligned with the polarization of the HP ^{129}Xe during the injection phase, too much polarization would be lost. This can be compared as a small angle of excitation from the Equation 6 where B_0 is the field of excitation and τ is an infinitesimal short time of excitation, which is unknown. This phenomenon can be found experimentally by measuring the loss of polarization at the injection of the Xe^{129} process. In fact, there is a magnetic gradient before coming to the center of the magnetic field producer B_0. This gradient diminishes the total polarization of the HP ^{129}Xe.

The intensity of this effect is existent but considered to be not preeminent. In fact, in an NMR spectrometer, the higher the B_0, the more signal can be retrieved without being affected by external noises.

5.2 Magnetic specifications

In the specification, it was also stated that the device could use PCR experimental plates with few holes. In fact, each sample needs its own B_1 producer and B_1 magnetometer. Moreover, each of this component needs its own coaxial cable and its own alimentation supply. That is why, in a first phase, PCR plates with only 8 holes (2x4) are considered. The design of the B_0 producer has to take this geometrical aspect into consideration.

An equivalent electric circuit can be made from the HP ^{129}Xe and blood; with its noise, its characteristic impedance and a simulated FID signal. The magnetometer can be coupled with an ideal transformer to the sample. The magnetometer has also an equivalent impedance and noise. This gives us an equivalent circuit with an oscillating voltage and an equivalent impedance. However, the simulation needs given parameters for each of the components. The different noises and the FID are not constant. In addition, the FID diminishes with the T_1^* of the HP ^{129}Xe. This implies that the LNA needs to be modulated in amplitude between each excitation to use all its amplitude range without saturating.

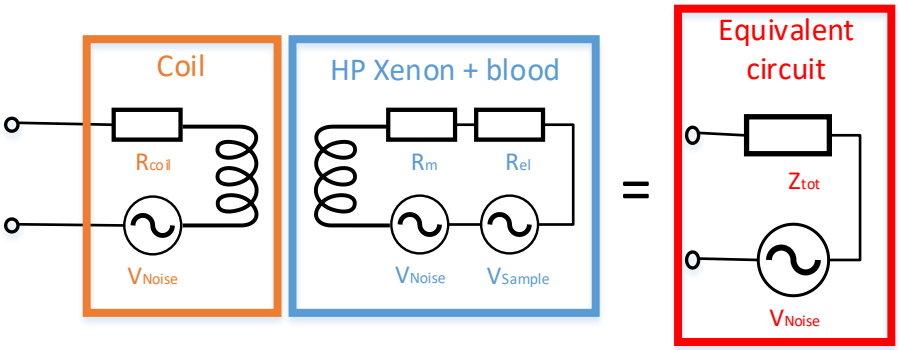

Figure 13 Equivalent electric circuit of the coil and the sample

HES-SO Valais-Wallis • rte du Rawyl 47 • C.P. • 1950 Sion 2
+41 27 606 85 23 • hei@hevs.ch • www.hevs.ch

The equivalent magnetic circuit of the HP ^{129}Xe in blood should be also simulated. For this specification to be aimable, a magnetic simulation environment with finite element should be developed with the physical equation related to hyperpolarized gases. This is not in the scope of this thesis.

5.3 Electronic specification

The signal generator needs a small clock jitter to not distort the signal at the production. This timing is unknown, but it needs a true real time producer to be insignificant in the toolchain. That is why a dedicated IC has to be designed to produce the sinusoidal signal and control the other parts of the circuit. The received signal has also to be synchronized to not add additional jitter.

The AC power amplifier after the signal generator needs to stop exciting the B_1 producer at a known time. Furthermore, the MF power amplifier needs to be switched off without producing additional ringing on the magnetic coil receiver. At its outside stage, it needs a matching electronic circuit.

The LNA has to be protected against too high input signal and has to be tunable in amplitude. It needs this functionality because each FID signal has a different amplitude, which is decreasing due to the diminishment in polarization after each excitation. This phenomenon is depicted in [Equation 11] The time to change the amplitude range of the LNA is larger than T_2^*. (5-10 ms). This implies that a DC/DC converter controlled by an IC has to be realized to adjust the gain of the LNA during this short period of time.

The most crucial part in the electronic component are the LNA and AC power amplifier. The non-linearity of the components inside the power amplifier are diminishing their output voltage. It is mandatory to control their temperature and to have passive and active component adapted to the task.

chapter, the different implementation options of the schematic diagram are explained.

5.4 Field B_0 production

The intensity of the magnetic field B_0 produces the magnetization of the sample by aligning the magnetic moments of the spin. This gives also the Larmor frequency at which the sample will be excited. $\omega_L = \gamma * B_0$[Equation 5]

Field B_0 must be as **stable** and **homogeneous** as possible. It is possible to produce this field with the help of a permanent magnet or an electromagnet. The field B_0 stability can be influenced by thermal changes and gradient in temperature, by the stability of the current supply, by external field perturbations and by the magnetic susceptibility of the atoms inside the produced magnetic field. To monitor the stability of a magnetic field, this parameter has to be measure or optimized.

In the following section, the specifications of different magnets are compared. The shielding of the magnetic producer has also to be taken into account, to stop the external perturbations.

The picked choice is explained at the end of this chapter.

5.4.1 Superconductor magnet

In classical IRM, superconductor magnets are used. They need to be cooled to a temperature near the absolute zero to amplify the produce magnetic field. The cooling system needs liquid nitrogen and/or helium near the absolute zero to operate. The whole system is inside a dewar and

takes a lot of space. In the meantime, the whole superconductor magnet has to be magnetically shielded to avoid undesired magnetic interaction. Shimming coils are also needed to homogenize the magnetic field. This solution is costly and hard to miniaturize.

5.4.2 Permanent magnet

Permanent magnets exist in different materials, shapes, and geometries. The field produces at the center is high. The main problem of permanent magnet is their poor temperature stability. Temperature control and thermic insulation are required to keep the field stability. Also, if the temperature become too high, a demagnetization occurs at the Currie temperature. This implies that the magnet needs a sufficiently high Curie temperature and a high coercivity to keep its magnetic domains in the same direction. These hard magnet characteristics can be found inside Neodymium magnets ($Nd_2Fe_{14}B$) which are usually the more affordable hard magnet (i.e. magnet with high coercivity) with a high remanence (i.e. strength of a magnetic field measure in Tesla). They are also generally used in existing benchtop NMR spectrometers. Their principal characteristics are their high coercivity and their relative low-cost compare to other magnets.

5.4.3 Iron discs and ferrite magnet

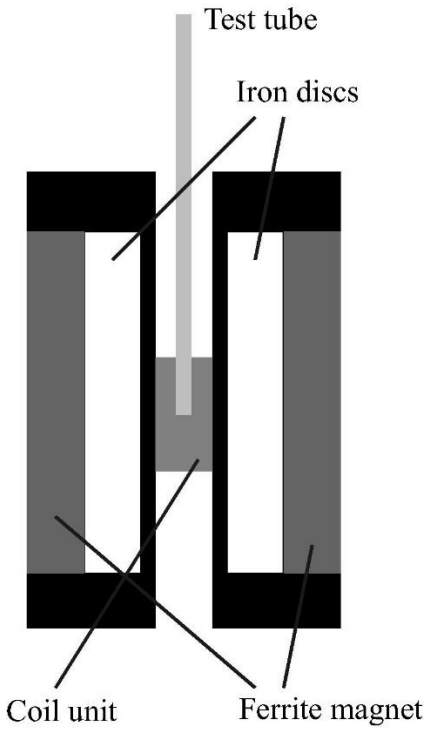

Figure 14 Sketch of our NMR magnet system. The black part is a magnet base on which the ferrite magnets and iron discs are set with their magnetic attractive forces. The coil unit contains the magnetometer and the field B1 producer. [22]

A pair of two commercial ferrite magnets with iron discs was developed. The total cost of material and machining is about $400 with a field of about 85 mT and a 90 Hz frequency resolution in spectra at about 2.4 MHz Larmor frequency. The resolution in ppm of the magnet is equal to 2.4 MHz /90 Hz =37.5 ppm [22]

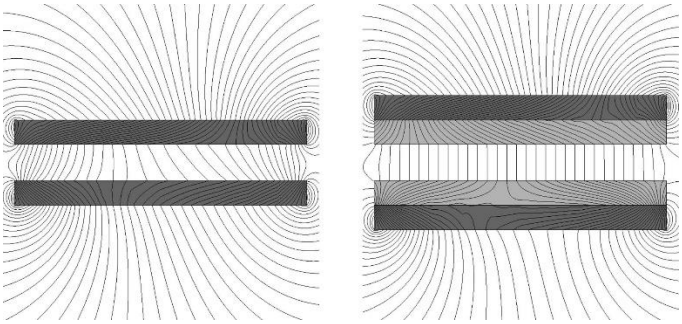

Figure 15Iron disks can homogenize a field. Sketches of flux lines with (the right panel) and without (the left panel) iron discs (gray discs) are shown. These are simulations calculated with FEMM [22]

The field homogeneity can satisfy the requirement by the addition of the iron disks. With this kind of setup, it is not possible to insert standard PCR plates. Only one test tube can be tested at the time. The resolution of 37.5 ppm is inside our specification. This geometry and materials have to be tested with smaller magnets and multiple magnets to be used with PCR standard plates.

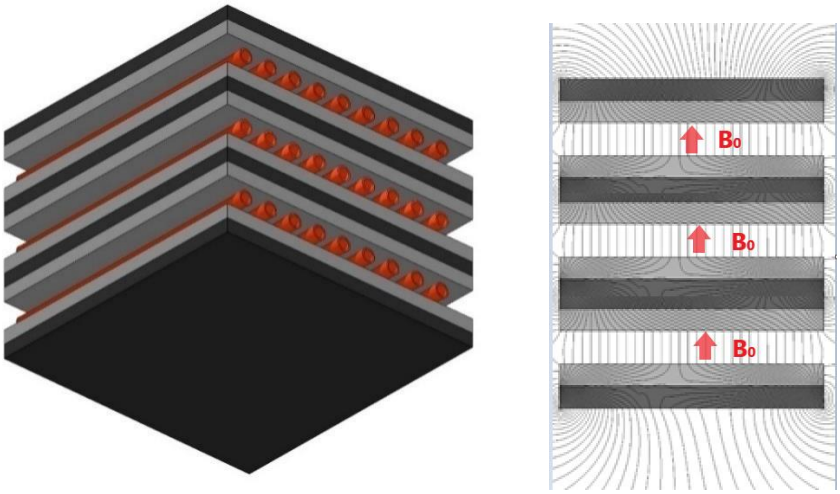

Figure 16 arrangement of ferrite magnets in black with multiple iron plate in grey, the test tubes containing the HP ^{129}Xe and the magnetometers and B_1 producer are represented in orange

This arrangement has to be tested first with test tubes and afterwards with PCR plate. The cost and the homogeneity of the field with multiple plate as to be found but it has to be approximately the same than the research paper above.

5.4.4 Halbach array.

The arrangement using Halbach array is described in the annexes. (cf. 13.9 NDFEB HALBACH ARRAY)

In addition to Halbach array, shim magnets between the arrays can be added to increase the field homogeneity this is already used in actual NMR spectrometer. [23]

With the Halbach arrays, it is possible do define a paving of magnet and holes. The magnetometer and producer of B_1 will be inside the holes. PCR plates could be insert inside the magnetometer and the field producer. The zone of interest, where the magnetic field is the most homogenous, is found at the center of the hole. In fact, the test tube needs to be as large as the zone of interest. If they are too large, they will have a lesser homogeneity and distort the signal. This phenomenon is produced by the fact that at the edges of Halbach array, the field lines are less straight.

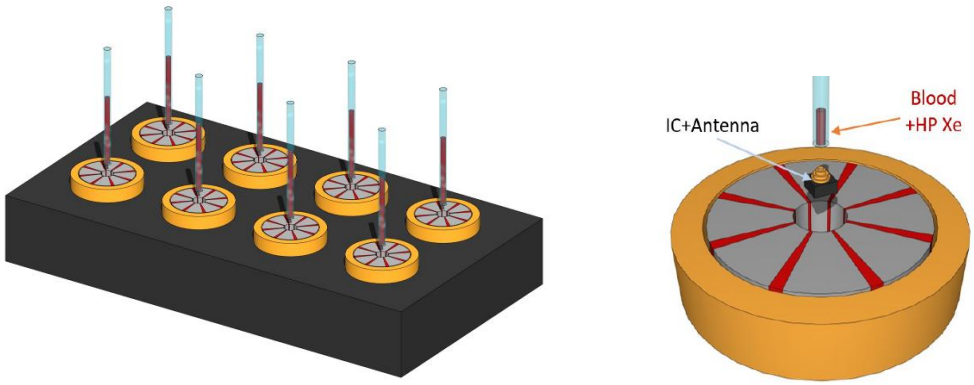

Figure 17 8 Halbach arrays with each 8 shimming magnets, inside a plastic plate. Shimming magnets are depicted in red and Halbach array in grey.

This solution is costly because the Halbach arrangement has to be aligned and mechanic shim magnets have to be added between the arrays in every region to produce the most homogenous field as possible. This arrangement can be easily tuned by the fact that if the coils are tested at the same time with the same sample, it is possible to map the field homogeneity of each coil (i.e. where to move the mechanic shim coils to have a better retrieved signal). The main problem of this device is that it needs many magnets and is prone to temperature variation. The intensity of the magnetic field in each hole will be slightly different. The price of such device and the true intensity of the field have to be found. In the existing benchtop NMR spectrometer, only one sample at the time is measured in a test tube. In this arrangement, the size of the magnetometer and B_1 producer has to be reduced. Due to time constraint in the manufacturing of the magnet, this solution has not been developed but needs a lot of work to be properly made.

5.4.5 Helmholtz coil

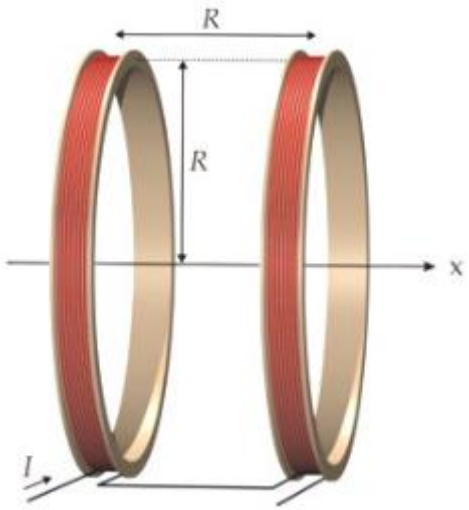

Figure 18 Helmholtz coils schematic drawing [24]

Helmholtz coils are two-winded coils producing a magnetic field from a current supply source. Their radius is the same as their distance interval. The magnetic field B at the center of the Helmholtz coil is $\mathrm{B} = \left(\frac{4}{5}\right)^{3/2} \frac{\mu_0 NI}{R} = \frac{0.8991*10^{-6}NI}{R}$[Equation 13]

, where μ_0= the permeability constant = $4\pi * 10^{-7}$[Tm/A], I coil current in ampere, R coil radius in meter and coil interval in meter, N number of windings for one coil (the same for the two coils).

From the Helmholtz coils are two-winded coils producing a magnetic field from a current supply source. Their radius is the same as their distance interval. The magnetic field B at the center of the Helmholtz coil is $\mathrm{B} = \left(\frac{4}{5}\right)^{3/2} \frac{\mu_0 NI}{R} = 0.8991 *10{-}6NIR$[Equation 13, when the space and radius of coils are small, the more field intensity can be produced. The field production efficiency is given by this equation:

$$\frac{\mathrm{B}}{I} = \left(\frac{4}{5}\right)^{3/2} \frac{\mu_0 N}{R} = \frac{0.8991*10^{-6}N}{R}$$ [Equation 14]

To amplify the field production efficiency, the number of windings have to be increased and the radius of the coils and the distance between them have to be reduced.

To simulate the field in all region, a finite element simulation has to take place by using Biot-Savart Law with given mesh and limit conditions. In addition, the temperature of the support and the isolation of the wire have to be taken into account during the simulation. To be able to find the homogeneity of the field and its associated thermal noise. In fact, in such a setup, shimming coils in different axis are needed to be implemented.

5.4.6 Shield

If too many external magnetic disturbances are encountered, the device must be shielded in order to restore its homogeneity and stability. It is also important that the current supply is stable to maintain the field stability in case of using shim coils in permanent magnet or electromagnets.

Shim coils are not used in the project, but they can permit to amplify the homogeneity of B_0. They have to be placed around given axis to change the magnetic field homogeneity. Each shim coil in each axis need its own stable current supply to homogenize the magnetic field. In the annexes, there is an example of such a commercial setting. (13.8 Helmholtz coils for field homogeneity)

In fact, the spectrometer can work at **earth magnetic field** and the field B_0 will be produce by the earth ferrous core. In this case, care must be taken to the inclination of the field compare to the geographic position on earth. The sample and the B_1 producer have to be in a good inclination with the earth magnetic field. This solution is more prompt to fluctuation, than producing an external magnetic field and has a geographic and time dependency. Other magnetic field producers can alter the received signal. At the condition of using the earth's magnetic field only, the device has to be shielded in a Faraday's cage or far from perturbations to prevent inhomogeneity. Nevertheless, Eddy currents can be produced in the magnetic surroundings environment. They need to be encircled in protective shielding sheet (e.g. aluminum) to not produce magnetic field lines too far from the magnetic producer. Also, the lower the frequency the more shielding is needed to stop external magnetic waves.

5.4.7 Choice of implementation B_0

As part of the project, it was decided to produce the field B_0 by using two Helmholtz coils cooled by ambient air. Since permanent magnets do not allow the field strength to be varied and can have different magnetization in each of their magnetic domains, they are also prompt to disturbance due to temperature variations. Despite, Halbach Array could produce greater and more homogenous magnetic field for B_0, YX magnetic a Swiss company can produce such of this magnet. [https://www.yxmagnetic.com/en/halbach-cylinder-496.html]

Due to time issue, the magnet was not produced but it can be by partnering with an external company. Due to its special arrangement, the price needed to produce them is unknown. In addition, the intensity and homogeneity need to be simulated with varying the space between the different parts. The simulation can be done with COMSOL. Finally, the calibration and the testing of the shimming magnets needs that all the other parts of the spectrometer are functional.

The main disadvantage of Helmholtz coils are their heat production and the shimming coils needed to homogenize the field in different axis. The main advantage is their possibility to produce a high field intensity.

The main disadvantage of the chosen Helmholtz coils is their heat production. However, they were directly available at the HES-SO Valais-Wallis. The goal, at that moment, was to implement the same dispositive as the one in the Geneva School of Health Sciences which is also the same dispositive as the main source of this project (13.3 Low-Field NMR/MRI Systems Using LabVIEW™ and Advanced Data-Acquisition Techniques)

A global homogeneity test of the static field was made by using a Hall sensor device. In fact, to map with accuracy the magnetic field, it would have been needed to measure some point in space with a given magnetometer and a software to represent the magnetic field. While it was not the optimal solution, the field has not been mapped. In fact, while the device was not shielded, its field lines influence the susceptible magnetic surrounding, by inducing Eddy current. This effect is hard to characterize and can be suppress by shielding the device.

5.5 Field B_1 production

In NMR, B_1 is a rotating magnetic field, with appropriate frequency, amplitude, and phase to generate a detectable NMR signal, which has to be switched on and off.

It is possible to produce this field with a rotating hollow permanent magnet at the Larmor frequency. The problems are the smooth stop and start, the high **mechanical rotation** frequency, and the fact that the magnetic field is always present even when the spinning magnet stops moving. This solution is not applicable in NMR spectrometer due mainly to the last issue because the field B_1 will change the inclination and the intensity of the static total magnetic field which gives the Larmor Frequency.

Since B_1 is a rotating field, an oscillating magnetic field generator in only one direction can produce it. It is also possible to add other directions in quadrature with the field B_0. To avoid mutual induction between the magnetic producers, they have also to be in quadrature with B_0. In this configuration, a maximum of two coils in quadrature can produce the field B_1.

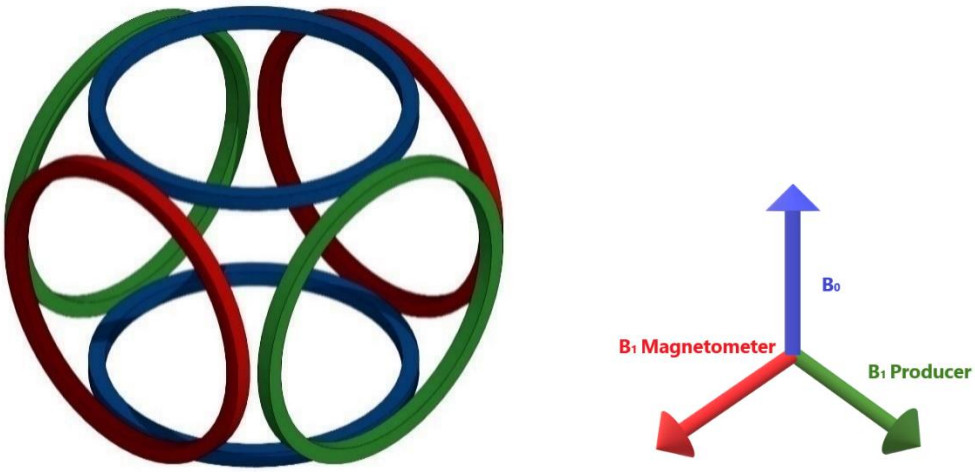

Figure 19 Schematic diagram of B_1 producer in quadrature with B_0 and the magnetometer

In Figure 19, the B_1 Magnetometer can also be the B_1 Producer. In fact, if the magnetometer does not have mutual inductance issue, it is possible to put them on the normal plan of the vector B_0.

5.5.1 Magnetic field generation by using special antenna.

In this chapter, a study is made to implement an NMR probehead, which can be as well a magnetic generator of a magnetic producer. The reference of this chapter is a book explaining the design of a magnetometer and a magnetic field producer by using Ampère's law (using EMF) for different geometry.

To design a unidirectional magnetic producer, it is needed to produce a magnetic flux ϕ. The Ampère's law states that a variation of a current in an inductance produces a magnetic flux ϕ and an induced tension:

$$L\frac{dI}{dt}^{\cdot} = \phi = -U_{ind} \text{ [Equation 15]}$$

The larger the inductance, the larger the magnetic flux is in an ideal case. In fact, the magnetic field is far from perfect

But for a real solenoid this is not true anymore. In fact, it has a parasite parallel capacitor and an inner resistance. This can be seen as a parallel resonant tank.

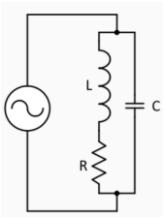

Figure 20 Equivalent circuit of a Solenoid

The characteristic impedance of a real solenoid: $Z = \left((sL + R) \,//\, \frac{1}{sC}\right) = \frac{sL+R}{s^2CL+sRC+1}$

The below figure and explanations are taken from the reference book, they stated also that an experimental comparison has to take place to be more accurate:

	$I = \sqrt{2PQ\omega C_{eq}}$	V_{peak}	C_{eq}
 Helmoltz coils	$\frac{8\pi I}{5d}$	$\frac{I}{2C\omega}$	$2C$
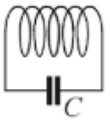 Solenoid (or loop gap)	$\frac{2\pi n I}{\sqrt{d^2 + len^2}}$	$\frac{I}{C\omega}$	C
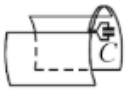 Saddle coil	$\frac{3.46nI}{\sqrt{d^2 + len^2}} \frac{len}{d}\left(1 + \frac{d^2}{d^2 + len^2}\right)$	$\frac{I}{2C\omega}$	$4C$
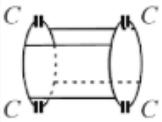 AGR	$\frac{3.39I}{\sqrt{d^2 + len^2}} \frac{len}{d}\left(1 + 0.835\frac{d^2}{d^2 + len^2}\right)$	$\frac{I}{2C\omega}$	C
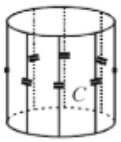 Birdcage (low-pass)	$\frac{4\zeta I}{\sqrt{d^2 + len^2}} \frac{len}{d}\left(1 + \frac{d^2}{d^2 + len^2}\right)$	$\frac{I}{\beta C\omega}$	$\frac{\beta^2 C}{N}$
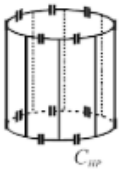 Birdcage (high-pass)	Same as above replace C by αC_{hp}		
 Circular surface coil	$\frac{2\pi n I}{d}$	$\frac{I}{C\omega}$	C

Figure 21 Estimation of the rotating frame magnetic field at the of various probe geometries. The length l and diameter d are in mm. n is the number of turns N is half the number of legs in the birdcage case. V_{peak} is the peak voltage across the capacitor for a given transmitted power P. The total current is obtained from the value for C_{eq} given in the last column. C is the capacitance value used in the design. [25, p688]

"Figure 21 summarizes the equations that allow estimation of the expected magnetic field amplitude for a given probe (assuming known dimensions, the Q factor when loaded with a sample, and the incident power P delivered by the transmitter). This evaluation is done for a given product PQ(the RF B_1 field amplitude is proportional to the square root frame in gauss, when the probe dimensions are in mm and the current I second column provides the voltage expected across the tuning capacity, parameters [$\beta = \frac{I}{I(2N)}$) that depend on the number of legs . The figure gives numerical values for a b and ζ as a function of the total number of legs..." [25, p688]

From the Figure 21 the current inside different geometries of coils is:

$$I = \sqrt{2PQ * 2\pi f_{exc} C_{eq}}$$

This current has to be taken into account in the calculation of the joule loses.

« Note that the signal strength also depends on the field generating efficiency of the B1 coil: $\frac{B_1}{I}$.

Although S is the signal induced into the B_1 coil alone, because it is common to tune and match the NMR probe to 50 ohms, the actual measured signal S_m becomes: $S_m = \omega_0 \left(\frac{B_1}{I}\right) M \sqrt{\frac{50}{R_{AC}}}$, where$R_{AC}$ is the resistance at the frequency of excitation. This resistance is not the same as at DC because of skin effect." [26]

To optimize the process of magnetic production, the Q factor has to be optimized at the frequency of excitation.

The equation of the Q factor is the following $Q = \frac{\omega_0 L}{R_{AC}}$ *[Equation 16]*

, where ω_0 is the frequency produced in radian, L is the inductance in Henry and R is the resistance at ω_0 in Ohm. To optimize this factor, the resistance has to be reduced. A geometrical and material optimization of this factor has to be found. In addition, a tradeoff has to be found between the used frequency (in our case 50 kHz [cf. 5. Specifications and sizing]) and the geometry of the coil.

The $\mathrm{R_{AC}}$ is linked to the skin effect when the current travel at high frequency (i.e. the current is only present at the frontier of the coil).

The quality factor (Q-factor) of the B_1 producer and the bandwidth involve a tradeoff. On one hand, a high Q-factor results in a large signal-to-noise ratio (SNR) and a longer ring-down time (longer system recovery time from the pulses). On the other hand, the higher the Q-factor is the smaller the bandwidth of transmission will be. For the application in NMR, the Bandwidth of transmission and reception is narrow. It implies a large quality factor and to use electronic adaptation to keep it high.

The magnetic field producer has to be designed to fit outside a test tube, which contains the blood and the HP ^{129}Xe. The **geometry** and the **material** of the coil are investigated in the chapter 6.2 Air-coil design.

5.5.2 Helmholtz coil and surface coil and solenoid

The magnetic field produced by Faraday induction on a multiple loop of wire is represented by the following equation:

$$B = \mu_0 \frac{\mathrm{N*I}}{length}$$ [Equation 17]

, with N number of windings, I the current transmitted inside of the solenoid

The inductance of a solenoid is given by the following equation:

$$L = \frac{N^2 \mu_0 S}{length}$$[Equation 18]

, where S is the surface at the base of the solenoid, with N number of windings, I the current inside of the solenoid.

The Q factor can be found by the following equation and condition above and below.

The design of a solenoid with multiple turns and a single wire can be made by using HMwaves calculator for RF Inductance for Single-Layer Helical Round-Wire Coils: [https://hamwaves.com/antennas/inductance.html] A usual rule is that the optimal quality factor is obtained when the windings are separated by a factor 3/2. This is mainly for physical purpose to diminish the parallel capacitor. The radius of the winding should be almost equaling the skin depth at the used frequency. The type of material used to make the winding also influence the final inductance.

$Q = \frac{7.5*\mathrm{D}}{1.03+0.4(\,D/length)} * \sqrt{f_{MHz}}$ all the dimensions are in millimeter the ratio D/length maximized the Q factor when it is between 0.7 and 2.0. From the equation above, the Q factor gets larger when the frequency is increased. [25, p88]

S parameter and Spice model are usually given by the manufacturer of the coil for the range of frequency used. It is also possible to use this source to find out how to realize a probehead.[27]

5.5.3 Birdcage/Saddle coil/ AGR

The birdcage has a quadrature excitation. The birdcage coil is a volume coil. Volume coils are preferred over surface coils in some design. A very important point is that volume coils have a bigger homogenic field compared to a surface coil and thus volume coils can produce a homogenous B_1 field in the volume of interest. So that the nuclei can be uniformly excited, and a homogenous image can be obtained.

The birdcage coils physically consist of multiple parallel conductivity segments equally spaced parallel to z-axis. These parallel conductive segments are called legs or rungs. The size of the cages has a dependence with the frequency of excitation. For a 1 MHz cage, the diameter and the length of the cage will be to large (20 centimeters for our application). Saddle coil and AGR have almost the same size issue.

5.5.4 Final choice

Helmholtz coils are the chosen method to produce the field B_1. It is the same as the B_0 method of production. This is due to the simplicity of implementation and the fact that they were directly available in the physic laboratory. This is not the greatest choice especially because they produce ringing and are not optimized for the frequency needed to be excited.

Depending of the frequency, another generator, which can also be a magnetometer, has to be chosen. The main problem with this kind of dual function is the stored energy released after the excitation. B_1 field producers have intrinsic ringing at commutation due to its stored energy released.

For the sake of this project, a small coil design needs to be implemented and its S factor need to be characterized.

5.6 B_1 Magnetometer

The magnetometer is used to measure the precession of the FID after the phase of excitation. A common method for measuring the FID is to measure the electromotive force (EMF):

$$EMF = -\frac{d\phi}{dt}, \text{[Equation 19]}$$

The change of the total magnetization of the spin given by Bloch's equation creates an EMF. This variation produces also an induced tension following Faraday's law. In this chapter, different types of magnetic detection are analyzed.

5.6.1 Introduction and comparison

There exist different types of magnetometers, which uses different types of physical proprieties.

They need a good resolution to detect small variations in a magnetic field. This is given by $\mathrm{B_{min}}\ [\frac{\mathrm{T}}{\sqrt{\mathrm{Hz}}}]$ which is the minimal magnetic field detectable by a device for a given frequency. Note that the smaller the frequency, the less sensitivity is obtainable for measuring a magnetic field. It introduces a spectral density noise in a specified magnetic field.

They need also to detect sufficiently large amplitude signal to be usable. B_{max} [T] is the maximal field intensity detectable for a given magnetometer. In our case, it should be larger than 10 mT for alternating magnetic field.

ΔB $[\mathrm{ppm}/\sqrt{Hz}]$ is their precision in part per million. It might be as small as possible.

The maximal bandwidth of a spectrometer BW [Hz] does not need to be especially large at low frequency.

The $f_1/_f$ knee frequency of our magnetometer must be greater than the frequency of excitation plus the maximal chemical shift plus a security factor. For some magnetometer, this variable is irrelevant because they theoretically do not have a maximum detectable frequency.

With all these parameters in mind, it is possible to make a choice on the final magnetometer design. The Figure 22 gives a comparative of the different magnetometers technology with the factor explained before. Also, in this chapter different type of magnetometer technology are explained, the type explained are only the most significant for this project. Others explanation can be found in the reference of Figure 22.

To choose our magnetometer, we have to set an interval. Let the range of detection be between **1nT and 1uT**. This implies for a frequency of 50[kHz], $B_{min} = \frac{1[nT]}{\sqrt{50[\mathrm{kHz}]}} \approx 4.47p$ this value has to be greater than the B_{min} values in the table in **Figure 22**. Also, B_{max} has to be greater than 1**uT** suited for the application. Let the resolution to be better than 50. The SERF and the Mems tunneling have not a sufficiently high resolution ΔB. **The final funding is that the more suited magnetometer for this task are the Squid, the pick-up coils and the optically pumped.**

equivalent noise in magnetic field/ absolute error /linearity/measuring range/directivity/bandwidth, i.e. its ability to capture rapid changes in magnetic field/thermal stability (in T/°C) gradient tolerance, i.e. its ability to make a reliable measurement in the presence of a magnetic field gradient.

To calibrate a magnetometer, Helmholtz coils are usually used.

Magnetometer	B_{min} [T/$\sqrt{\text{Hz}}$]	B_{max} [T]	ΔB [ppm/$\sqrt{\text{Hz}}$]	BW [Hz]	$f_{1/f}$ [Hz]
SQUID (at 4 K)	1 f	10	0.2	1 G	10
Pick-up coils	20 f	>10	1	1 G	10-1 000
SERF	70 f	100 n	1 000	100 k	–
Optically pumped	100 f	100 μ	<0.01	100 k	–
Electron precession	500 f	100 m	<0.01	1 G	–
MEMS (tunneling)	2 p	10 m	200	10 k	100
Nuclear precession	10 p	>10	0.01	100 M	–
Magnetostriction (magnetoelectric)	10 p	10 m	100	50 k	–
EMR	10 p	>10	10	1 G	10
Flux-gate	30 p	10 m	50	10 k	–
AMR,	100 p	5 m	100	100 M	10
GMI	100 p	100 μ	50	10 M	–
GMR	100 p	100 m	100	1 G	1-100 k
MTJ	100 p	10 m	200	1 G	10 k
MEMS (Lorentz force)	1 n	10 m	100	1 G	100
Magneto-optical	1 n	>10	1 000	10 M	–
BJT magnetotransistor	10 n	1	100	1 M	10
Hall plate	100 n	1	10	1 M	10 k
Magnetodiode	100 n	1	100	1 M	1 k
MAGFET	1 μ	1	100	1 M	1 k

Figure 22 Summary of magnetometer techniques with corresponding performance characteristics. Here, B_{min} stands for a measurement sensitivity, B_{max} for a maximum operating magnetic flux density, ΔB for a precision, BW for the maximum bandwidth and f_1/f for the $1/f$ knee frequency [28, p47]

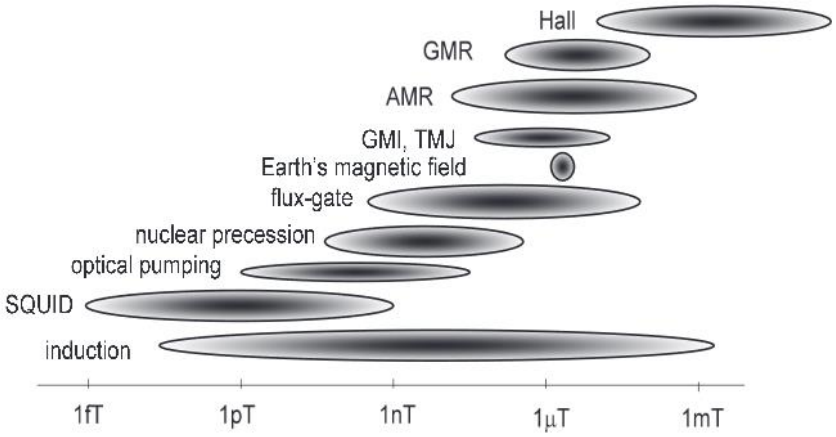

Figure 23 Typical area of applications of the main magnetic field sensors [29]

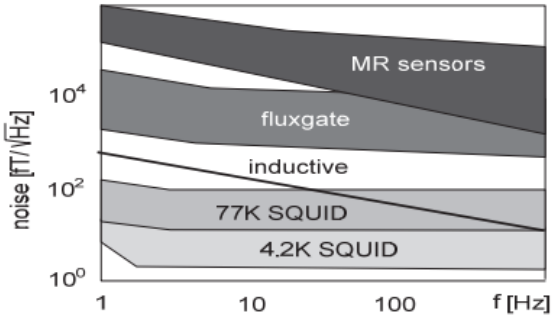

Figure 24 Comparison of resolution of several main magnetic field with their frequency [29]

5.6.2 Hall Effect sensor

The Hall Effect sensor can receive a magnetic field from 50mT to 30T. It is not suitable for high oscillation frequencies. This method cannot be used to test the field B_1.

"The sensitivity of a Hall plate depends on the material chosen the best sensitivity can be reach at 100 pT/√ Hz One of the most simple structures with which to observe the buildup of Hall voltages is a rectangular plate in which a drive current is fed into two ends of the plate and sense nodes are placed perpendicular to this axis.

To have a high-power efficiency, the substrate should have a small number of charge carriers with high mobility. Materials that best fulfill these requirements are semiconductors, especially gallium arsenide, indium antimonide, and silicon.

The sensitivity of a Hall plate depends on the material chosen. Indium antimonide-based sensors offer the highest sensitivity, reaching 100 pT/√Hz.

If silicon is chosen for the material, the sensitivity is clearly higher, typically on the order of 100 nT/√Hz. Hall plates are influenced by 1/ f noise and typical 1/5 noise knee frequencies are between 1 and 10 kHz, depending on the material. Above the sensitivity limit, measurement precisions about 10 ppm/√Hz are typically obtained. In theory, there is no maximum value for field strengths that can be detected with Hall plates, and measured flux densities as high as 23 T have been reported. Measurement bandwidths are limited by sensor noise and are typically not above 1 MHz." [28, p47]

5.6.3 Optical-pumping magnetometer

Measuring Field Strength with an Optically Pumped Magnetometer needs to use laser and Rubidium. It is the same process used to Hyperpolarized Xenon. The only drawback is its higher possible magnetic field detection. The hyperpolarized gases would be hardly detectable.

5.6.4 SQUID

SQUID magnetometry is the most sensitive magnetometry technique. Superconducting materials and Josephson junctions are used. The junctions allow receiving magnetic field variations by tunnel effect. The variations that are detectable are very small.

The disadvantage of this technique is that superconducting materials must be used and a cooling device close to absolute zero is required.

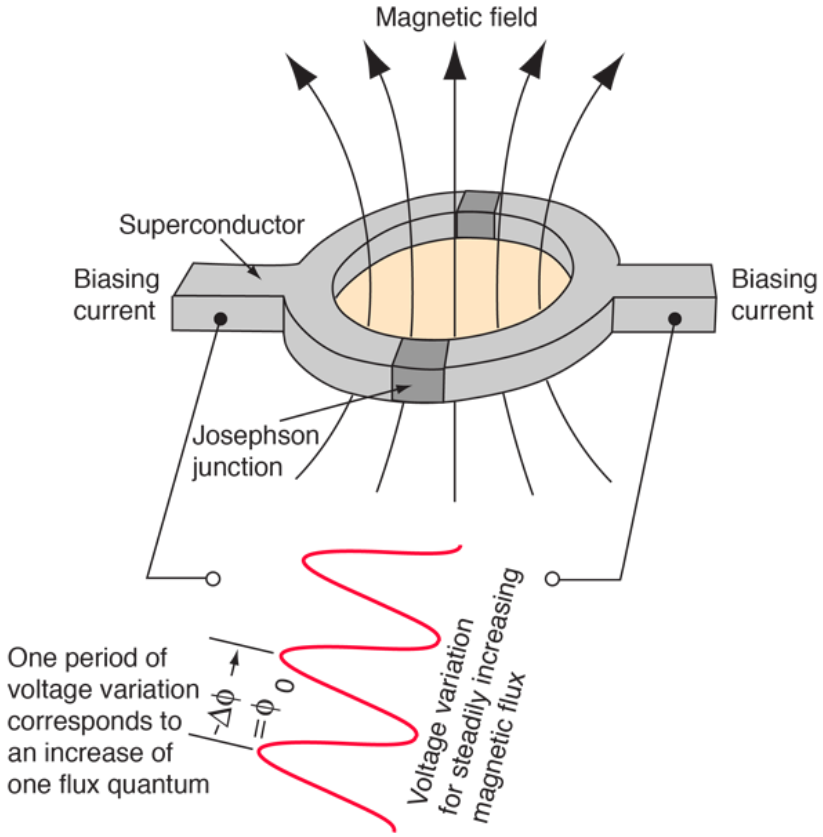

Figure 25 Josephson Junction [30]

5.6.5 Inductive coil

Inductive coils in air follow Faraday's law and produces induced voltage.

Inductive coils are the most efficient and easy to use. In fact, the explanations on how to generate the B1 field can be taken up again by defining that a variation in magnetic flux generates an induced voltage across an inductive coil.

The energy stored inside a coil is $W = \frac{1}{2}LI^2$. This energy will be given back as soon as the end of the excitation. This forms unwanted ringing effect.

5.6.6 Final choice

The magnetometer chosen for the application is the inductive coil due to its simplicity and its possibility to act at the same time as a magnetic producer and a magnetic generator. Adverse self-induction and mutual induction effects are existent in this kind of setup. A quadrature geometry needs to be implemented to counteract this undesired effect. There are still different types of magnetometers, with each their own specific features. It is needed to find if the ^{129}Xe of our application can use any commercially IC NMR spectrometer to implement the end application.

HES-SO Valais-Wallis • rte du Rawyl 47 • C.P. • 1950 Sion 2
+41 27 606 85 23 • hei@hevs.ch • www.hevs.ch

5.7 ADC (Analog to Digital Converter)

The ADC must be able to comply with the Nyquist-Shannon sampling theorem. This implies that the sampling frequency must be at least twice as high as the excitation frequency.

$2 * f_{Larmor} \leq f_s$[Equation 20], f_s: sampling frequency in Hertz

In order to increase the resolution and to process the received signal without reconstitution signal algorithm like interpolation, the sampling frequency must still be multiplied by a factor of at least 5 (this is given by experimentation). In addition, the more samples are taken and the lower the quantization noise will be.

There exist multiple different techniques to retrieve a signal; the most used are the SAR and ΣΔ converters. The Figure 26 compares both techniques. The ΣΔ is be more suited for NMR spectroscopy mainly for its lower noise production.

TABLE 2: KEY ATTRIBUTES OF Δ-Σ AND SAR ADCs

ADC type	Resolution (bits)	Max. speed	Advantages	Disadvantages	Applications
SAR	8-18	10 M	• Fastest • Low power • Inexpensive • Can use a multiplexer	• Less resolution • Greater noise	• Data acquisition • Industrial control • Battery-powered
Δ-Σ	8-32	1 M (192 ksamples/s, typical)	• Lowest noise • Highest resolution • No S/H amplifier needed	• Slowest • Moderate cost and power consumption	• Instrumentation • Audio • Medical

Figure 26 Difference between SAR and ΣΔ ADC [31]

The ADC has of course quantization noise which is needed to be reduced by taking more acquisition data and to have a better resolution. If the frequency of the ADC is not high enough to comply with the sample frequency, a RF mixer is needed. The RF mixer need a carrier wave to be generated at the excitation's RF frequency. and a signal has to be generated t frequency which is lower than the emitting frequency has to be sent to downsize the excitation frequency. The electronic circuit is represented below.

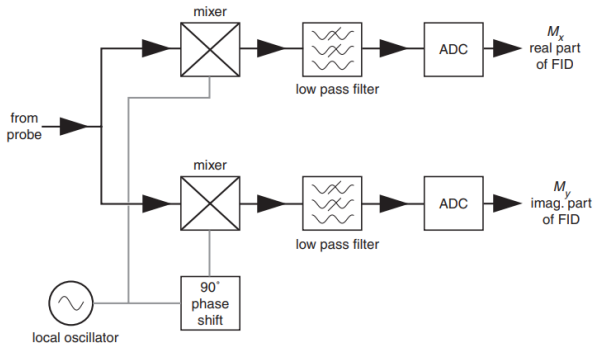

Figure 27 downsizer of an NMR [32]

This process is the same which is made in oscilloscope and this could be a good inspiration. The problem with the downsizer is that the element is not perfect and some default in the mixer induces undesired retrieved frequency.

5.8 DAC (Digital to Analog Converter) + AC Amplifier

The AC power amplifier produces the field B_1. It is needed to be able to amplify sinusoidal signals that are in a frequency range of 50 kHz for our application. The less THD and a high dynamic range are required. The slew rate of the AC amplifier must be bigger than the slope of the oscillating sine wave.

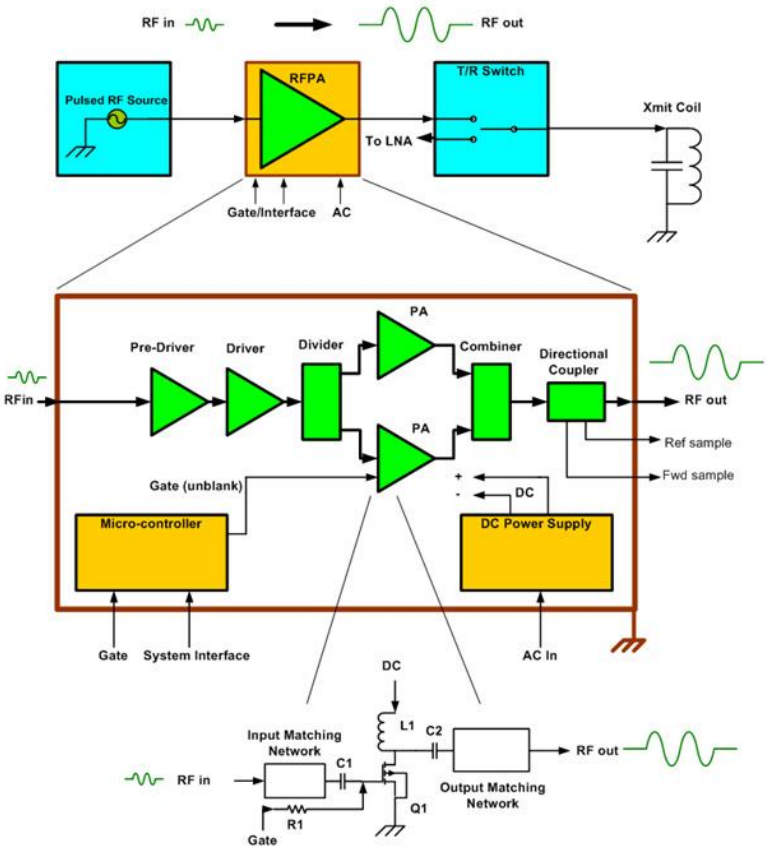

Figure 28 Schematic diagram of an AC amplifier [33]

On the figure above, all the part of a RF amplifier for NMR are represented. In fact, it is needed to have more power amplifiers to reduce undesired effect listed in the Figure 29 before combining the amplifier and the data. Each power amplifier has its own matching network and grounding which are decoupled for each power amplifier. In fact, all the undesired effect produce by the power amplifier cannot be filtered outside the amplifier.

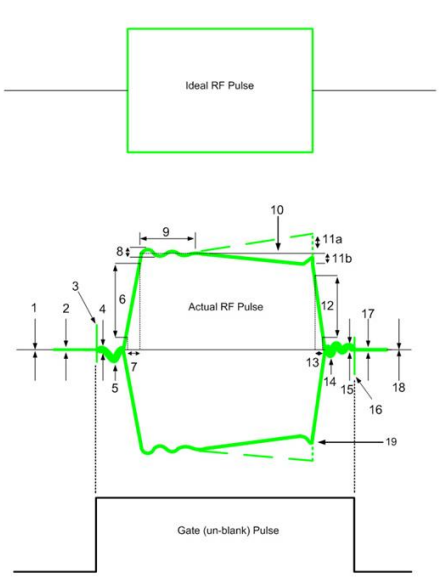

Measurement	Dimension
1. Forward coupling (measured)	db
2. Reflected coupling (measured)	db
3. -50 db atten. (measured)	db
4. -10 db atten. (measured)	db
5. Test power output	dbm
6. Vp-p at -10db attenuator output	volts
7. Rising transition duration	nsec
8. Falling transition duration	nsec
9. Pulse overshoot	%
10. Pulse tilt	%
11. Input forward power	dbm
12. Input reflected power	dbm
13. Input return loss=(11-12)	db
14. Gain= (5-11)	db
15. QPower (-10 db pad @position#1)	dbm
16. Power (-10db pad @position#2)	dbm
17. Gain compression/expansion (15-16)	db

Figure 29 Real pulse produce by a AC amplifier[33]

The amplifier can produce harmonics, which has to be attenuated. (THD+N) It needs also a protection against reflected waves at the stage of amplification. In the audio frequency range, audio amplifier and audio communication protocol can be used.

To produce an analog signal from a digital signal, the easiest solution, is to convert our wave with a ΔΣ converter made inside an FPGA and to use a low-pass filter. This solution is not optimal because it is depending of the cut-off frequency and the order of the low pass filter at the output of the FPGA. In addition, the SNR and the THD+N are not computable with this kind of solution.

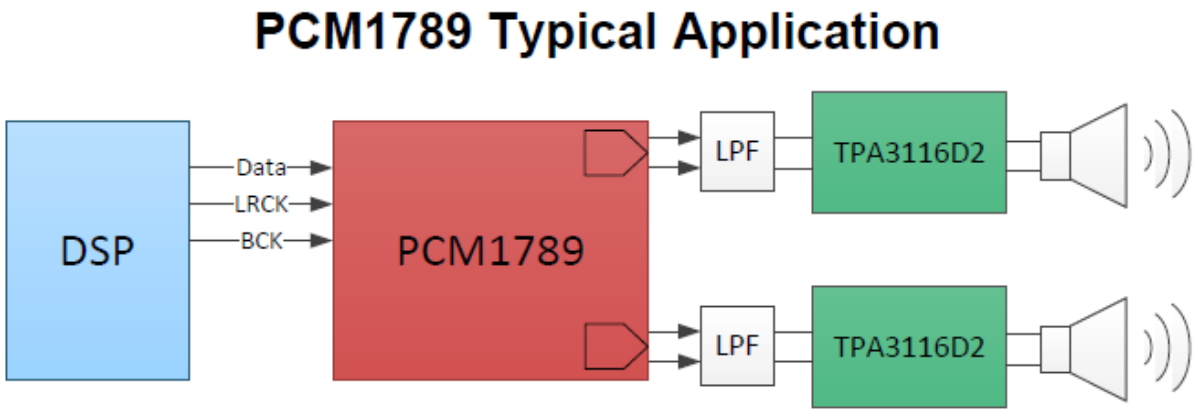

Figure 30 Circuit representing the generation of amplified signal for high sound quality application [35 p33]

5.8.1 Purepath® Digital Audio Power TI amplifier

PurePath® is a technology developed by Texas Instrument for the audio range of frequency up to 100 kHz. A digital signal communicates protocol (SPI, I2S or Hardwire) produces an analog signal. The component works digitally and converts the signal in the analog domain via an H-Bridge. Its SNR is about 112 dB, its THDn (Total Harmonic Distortion plus Noise.) is about 93 dB Its THD, and SNR are well for this kind of small amplifier. External amplifiers are needed if not enough power is transmitted. This it is shown in the

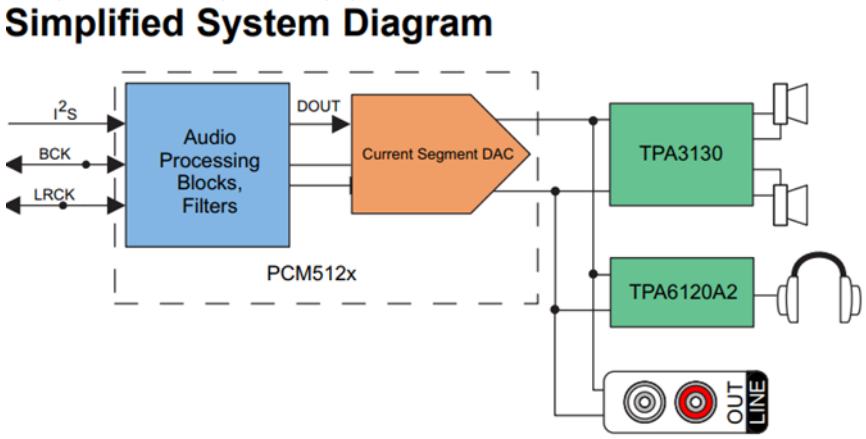

Figure 31Figure 31.

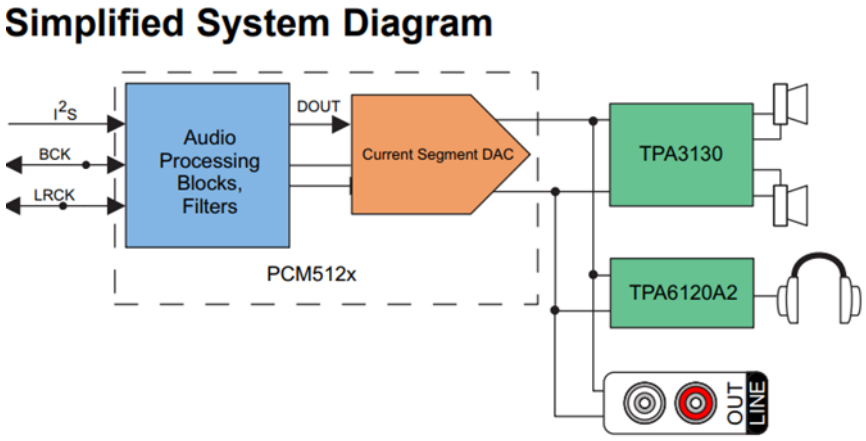

Figure 31 Simplified system Diagram of a Purepath® Digital Audio Power TI amplifier [36]

Purepath® enables the possibility to have a development board with an integrated software to find undesired perturbations and counteract them. The possibility is given to have a development board with an integrated software to test the performance of the board.

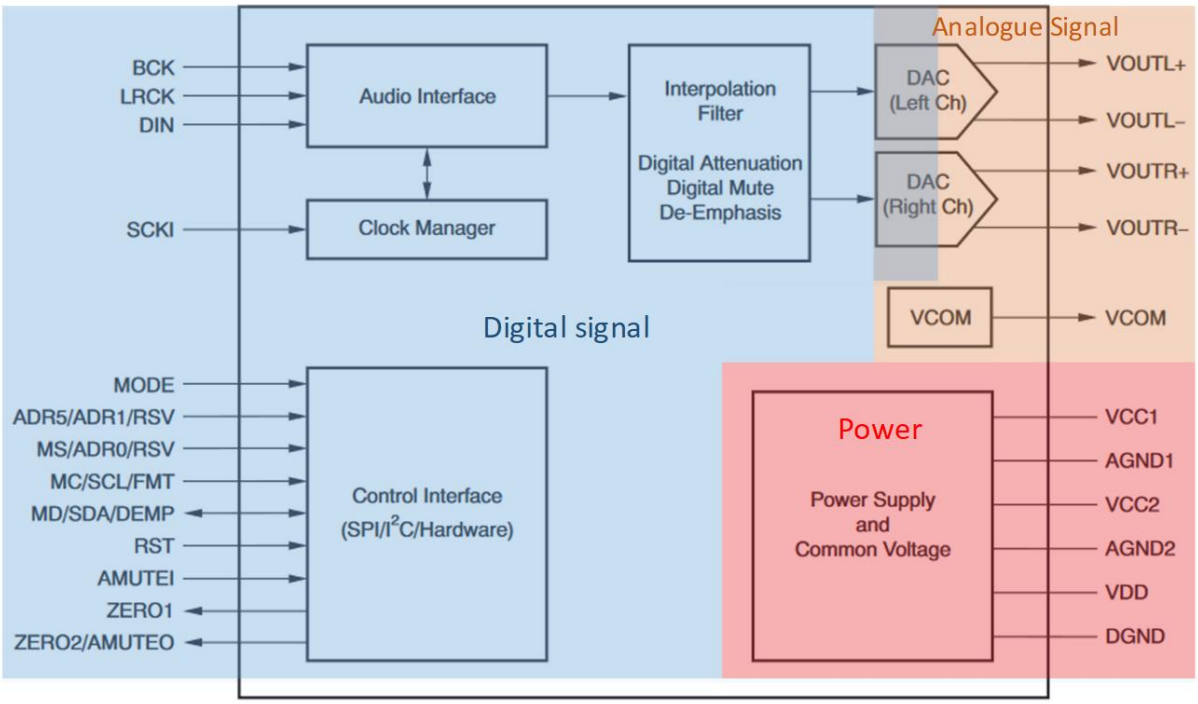

Figure 32 Block diagram of a stereo DAC with its different stages [35 p.13]

In this schematic, there are digital signal, analog signal and a power part. The digital and analog alimentation are not coupled. And each output has its own power supply.

5.9 LNA (Low Noise Amplifier)

The function of an LNA is to amplify the received precession signal (FID) without adding additional noises and distortion. It is the most crucial part of the electronic device. Ideally, it needs to amplify signal in the required needed bandwidth and can support high input signals amplitude without failing. A protection is needed at the input stage of the LNA in case of high input. The tension at the LNA needs to be tunable in amplitude. For this purpose, a DC/DC converter is required. The power supply of the LNA needs to be constant to amplify the signal without additional distortion.

For a clear understanding of the disturbance and implementation of an LNA, the reference book gives a lot of good practice. [19, p128-137]

A dedicated LNA has been chosen to tackle this function, it has a low VoltageNoise:1.1 nV/√Hz and a low THD: –136 dB (G = 1, ƒ = 1 kHz) and a sufficient slew rate: 27 V/µs for the application. Normally it is used in the power amplifier stage after a DAC or to drive a 16 bits ADC. In fact, for simplicity reason, this ADC is used in both applications.[38]

5.10 µC (microcontroller)

The µC have the function to give an interface to the end user (i.e. via a GUI or an external web app), to configure an excitation sequence on an IC and to process the FID signals. In the case of multiple excitations, the different signals have to be added and average by the scale of their noise to enhance the SNR. (Cf. [Equation 11])

To produce a power spectral density of the FID signal, it is possible to use either inverse Laplace transformation or Fourier transformation on the signal. The inverse Laplace transformation works well only for known signal function. If the signal has undesired modulation in amplitude(cf. 4.2Field homogeneity/External perturbation), Fourier transformation is a better suited option in this condition.

To send NMR data format on a server or to process the FID signal remotely, the µC needs an internet interface. Additionally, a data format has to be chosen. NMReDATA can be a format adapted for this purpose since it is a standard data format between companies in the frame of NMR. It defined a protocol to store data of 1D spectrum. A converter to this format from the received process spectrum has to be implemented.

The choice made in this thesis is to use a **Raspberry PI** because it has an OS to run multitask. It can run C/C++ and Python languages and others. It has an internet interface (can be access via SSH), GPIO, SPI master interface and a GUI. Its main advantage is its wild use in software development, which is linked to its well documented and numerous libraries. The alternative would have been to use an **Arduino** but its lack of Ethernet port, OS, multitask possibility as well as its lower CPU and communication speed has led to not choose it.

5.10.1 Raspberry Pi 3B

The RPi is a small computer that is widely used in development equipment. It is possible to install a Raspbian OS (operating system). It can be commanded either by a CLI, by a GUI or via a remote SSH. Raspbian is a free open-source OS composed of a Linux kernel (distribution Debian), which is made especially for the RPi. The raspberry pi can store a data server like any computer with less consumption. A web interface can be implemented on the Raspberry Server (i.e. Tomcat) to view the process chemical shift on any connected device.

The RPi has protocol communication port implemented (i.e. SPI master, I2C master, GPIO) that can allow it to communicate with an IC. This communication can be used to transfer information and reprogram an FPGA. In fact, it is also possible to directly reprogram the FPGA from the RPi via a free toolchain. This can be done remotely by sending command via SSH. In the current project, it has been tested without success. It is also possible via VNC® Connect to share the screen of the Raspberry PI if the GUI is installed. This has been tested with success.

"The RPi SPI runs at APB clock speed, which is equivalent to core clock speed, 250 MHz. This can be divided by any even number from 2 to 65536 for the desired speed. The datasheet specifies that the divisor must be a power of two, but this is incorrect. Odd numbers are rounded down, and 0 (or 1) is equivalent to 65536. A divisor smaller than 2 is therefore impossible.

This makes the frequency range be from 3.814 kHz to 125 MHz, with 32768 steps in between." [40]

The above citation taught us that the maximal clock speeds of the SPI bus is equals to 125 MHz; this frequency is suited to have a fast communicate with IC.

The only problem is that the speed of the bus is dependent of the time taken by each instruction executed by the RPi. The clock speed of the SPI does not give the true sampling frequency of the SPI bus.

This solution limits drastically the accuracy due to timing variations. The solution is to use the RPi's DMA to store the received data. The only issue with this process is the pulling time of the ADC, which has to be constant and the synchronization between the excitation and the reception of the data on the DMA

To avoid timing issue, the RPi reception process was transferred to a FPGA, which stores the data from the DAC and send them to the RPi. It has been decided to implement this function inside the FPGA and to transfer the digitalized signal from the FPGA to the RPi via an asynchronous communication protocol, which can be full duplexed. This implies that the FPGA handles all the real-time signals.

5.11 IC/FPGA

A field-programmable gate array (FPGA) is an integrated reprogrammable logic circuit (IC). The main advantage of a FPGA is that the clock is constant, and the time taken for each action is always the same. It is true real-time. The FPGA can generate arbitrary digital signals and can implement communication protocol with better time accuracy than µC (microcontroller).

In fact, FPGA could also process the FID signal after it has been stored. However, since FPGA has a limited memory and is better at doing only one thing at the time, it has to be reprogrammed without an µC at runtime. This is why it is more convenient to process the signals on a µC, which has more flexibility and more programming languages and libraries. In addition, FPGA have finite logic blocks, which are used by each implemented algorithm and functionality. It needs to change its memory at runtime in that case. This is in effect possible but can produced undesired effect.

If FPGA cannot contain the entire logic blocks, a more expensive FPGA with more logic blocks is needed. The algorithm cost has to be reduced. The memory in the case of a FPGA is not an issue for our project, because it can be stored on an internal memory (BRAM). If more memory is needed, a dedicated logic block has to be used to communicate with the external memory (DRAM).

There are many FPGA boards and configurations. In fact, for this project a TinyFPGA BX was chosen because it was directly available, it is affordable (~$40) and it is small.

As already said, a µC has to configure the FPGA. For this purpose, a communication is needed at the time of implementing the algorithm of the FPGA. Another communication is needed at runtime to receive and transmit messages in both directions.

5.12 FPRF Field-programmable RF

The **field-programmable RF** (FPRF) is a radio frequency transceiver IC which has the possibility to change the frequency of operation. It can generate and receive signal with accuracy. It is possible to have dynamic filter and mixer.

This technology works in a bandwidth of **100 kHz – 3.8 GHz**.

A developed project has made a base NMR spectrometer using this technology. [41] In this project, it exposes, that the RX and TX could be synchronized, and an external computer could program a LimeSDR (a FPRF). The LimeSDR produces the sequence of excitation and receive the signal from the LNA. An external RF power amplifier and LNA are needed as well as a RF duplexer for using an only coil.

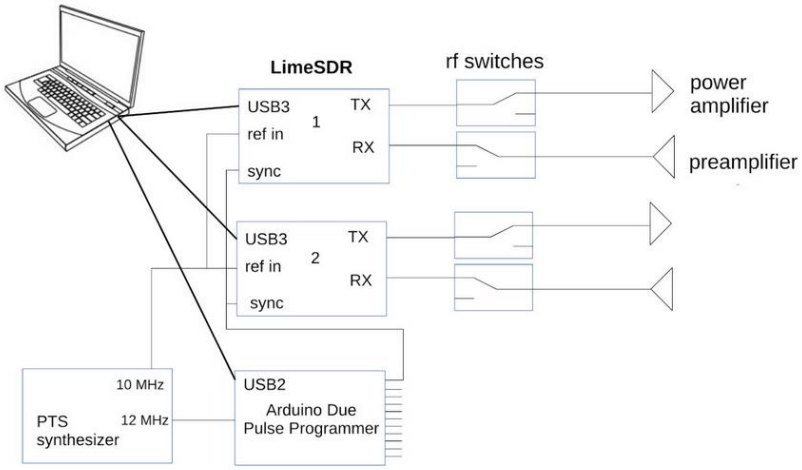

Figure 33 Schematic diagram of the NMR spectrometer working with a FPRF [41]

At the moment, the signal of excitation and reception is between 1 MHz and 10 MHz, this could have been the perfect suit for the experiment. The TinyFPGA could be used in adequation of this system to produce the real time clock.

5.13 RPi with FPGA and PMOD DAC and ADC

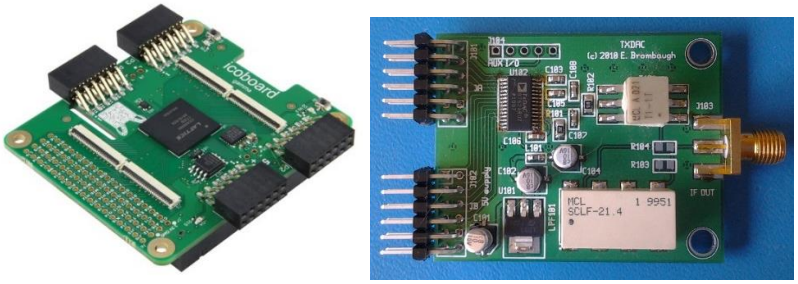

Figure 34 right: Icoboard FPGA left: TXDAC Pmod AD9760 10-bit 100MSPS TXDAC 12-bits [37]

The icoBoard contains a Lattice FPGA with 8k LUT, 100 MHz max. clock, 8 MBit of SRAM and is programmable in Verilog by a complete open source FPGA toolchain. (the same as the TinyFPGA Bx)

The icoBoard is pin-compatible with the Raspberry Pi and can use external boards to link the RPi with outside circuit. This can provide an all in one development circuit. It will be always needed to have a low noise amplifier, a matching circuit and RFPA. To be used in the application.

6. Tasks implemented

6.1 Test with existing devices without optimization

In a first phase, existing devices were tested according to the bellow one setup.

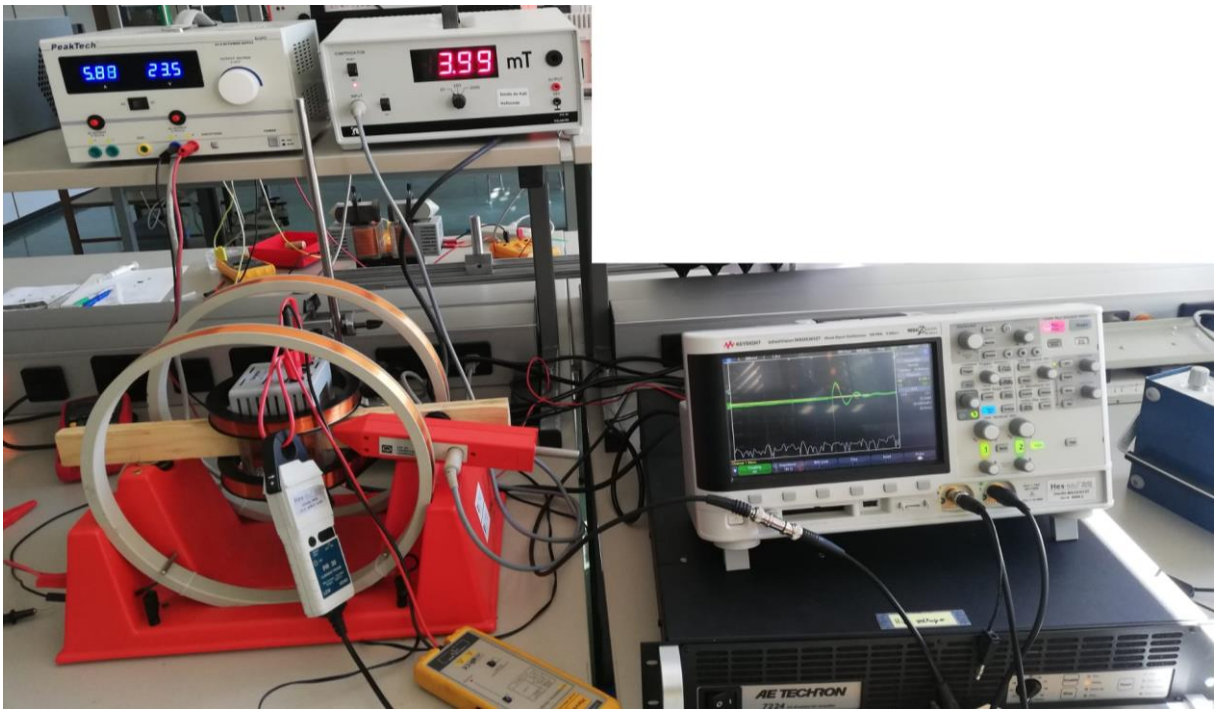

Figure 35 Existing setup with power amplifier and console

From the implementation options, an existing Helmholtz coils pair setup was tested to generate the field B_0. This setup was chosen because it was directly available at the physic laboratory. The setup can generate a field of 4 [mT] with a current of 6 amperes. Each coil resistance is 4 Ohm. A lot of the heat is generated in this setup due to joule losses. (50 degree where measured) Their homogeneity was basically tested using a Hall probe in several places and seemed satisfactory for a first trial.

For the B_1 generation, two other Helmholtz coils in quadrature of B_1 where used. They were also available in the physic laboratory. Their resistance AC where not tested. A commutable capacitor where added to change their resonance frequency. While changing this resonance, it seemed that the Q factor changes accordingly. For test purpose, a signal generator, which is also a function generator, produces an excitation signal of 50 kHz 5V peak-peak, which is then amplify by an RF amplifier. The cable between the function generator and the power amplifier where connected by using a 50 Ω coax cable and their input and output were matched accordingly. However, the output of the amplifier was not meant to be matched while in the audio domain the impedance matching is not considered. The test where conduct with the variation of a lab tunable capacitor. Since the magnetometer from the physic lab was not able to measure a frequency of 50 kHz, test measurement where conducts at 50 Hz which is the frequency of the test magnetometer. It was then tried to find a magnetometer at a frequency of 50 kHz.

No magnetometer above a frequency of 10 kHz was available at the college. It would have been possible to use a RF field meter available at the college but the bandwidth of the field meter available is 50 - 3500 MHz. This is not suited to measure the field produced. It was decided to not buy a field meter but rather to produce a test coil align with the magnetic producer and measure mutual induction effect. This solution was far from optimal since the true characteristic of the made coil with litz wire was not the one expected. During an experiment to test the magnetic field produces by the coil at a frequency of 50 kHz and a power transmitted of approximately 5 watt, the support of the coil made of PCV was deformed by a measured temperature greater than 60 degrees on the outside of the coil produced by Joule's law

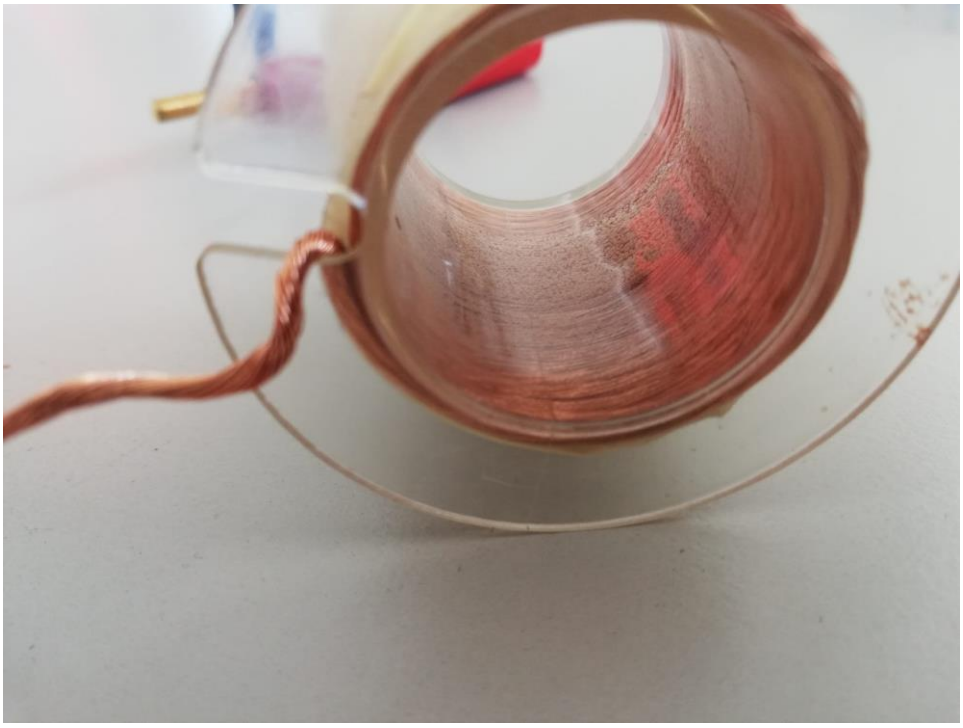

Figure 36 The effect of thermal induction on the support of the made coil with Litz wire

It was discovered that the support of the coil could not stand too high temperature. Another coil with another support could have been built with known dimensions but this is far from optimal. The solution to this problem was to buy a standard coil, which can give standard measurement. Since the optimization of the magnetic field was not meant to be mandatory, the coil was not bought. In addition, during the test it was found that the frequency does not have to be so low and are in the HF range. For HF other specifications are required, they are explained in the chapter 6.2 Air-coil design.

Another experiment was conducted to characterize the mutual inductance of the magnetic producer and the magnetometer in quadrature. At first, test coils were aligned with the magnetic field produced by our pair of small Helmholtz coils. The power of amplification given by the RFPA was then measured to obtain a received power value in the magnetometer coil of **1mW**. When this value was acquired, the coil was turned to be in quadrature with the pair of small Helmholtz coils to avoid mutual induction. This had led to find that the litz coil has a lesser directivity than coil with normal winding. (i.e. they received more signal than other coil geometry, thus they normally wouldn't) This effect is certainly due to the geometry of the coil, but this was not found in the literature. Due to time issue and change to HF, these tests were not documented. In fact, to procure useful tests, a test chamber would be needed for LF which is not available in the college. While, when using MF and HF

coil antenna, the directivity can be measure in an anechoic chamber available in the college and the ground design of the coil differs (c.f. chapter 6.2 Air-coil design).

The Keysight InfiniiVision Msox3012T is an oscilloscope and function generator. It can create sinusoidal signals from 5 Volt peak-peak.

A differential probe was used on the cables to find the output voltage on the litz- wire coil magnetometer.

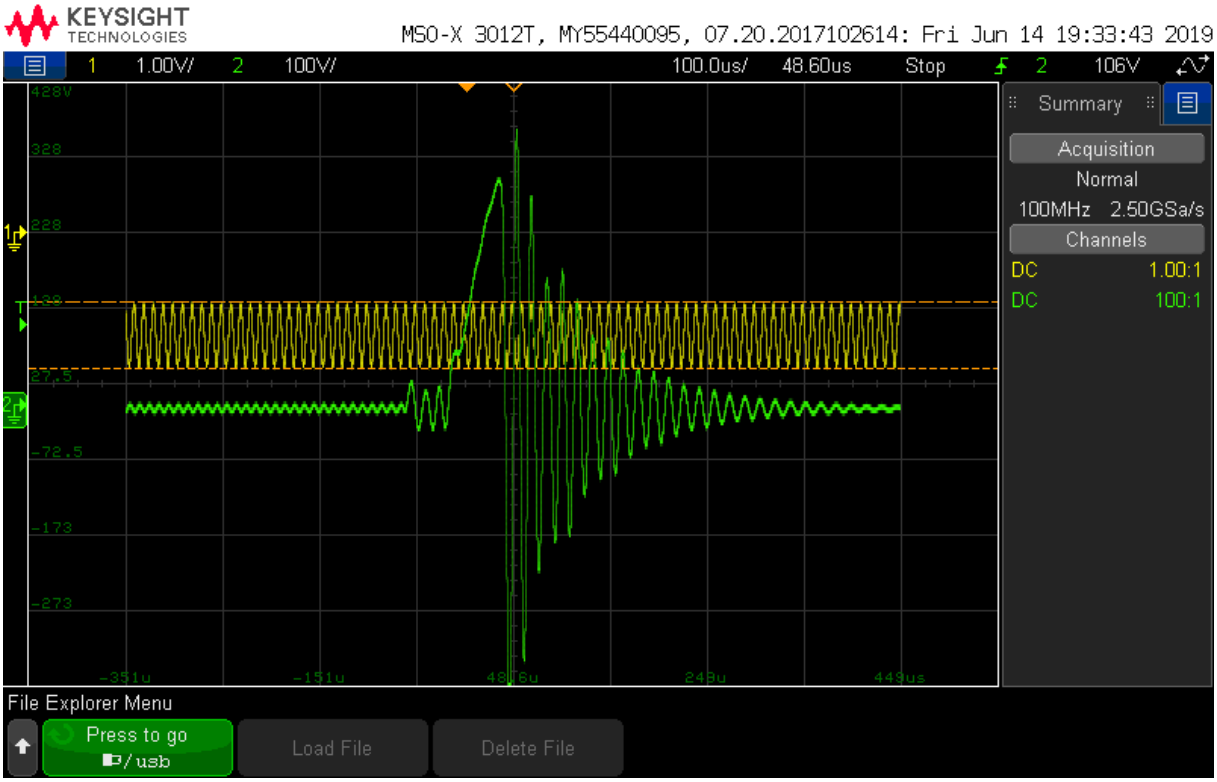

Figure 37 Test of ringing with the lab setup at 50 kHz; in yellow, the signal generated by the oscilloscope; in green, the ringing issue on the receiver part when the power amplifier is stopped and its energy is transmitted to the coil.

The figure above shows how the power amplifier produces a ringing effect at the moment it is power off. The beginning of the signal was not really understood but it is thought that the transfer function of the RFPA since it is not impedance matched produces this undesired signal.

A last experiment consisted to find the undesired effect of ringing. As the ringing and the mutual inductance between the coils. The main problem of this setup is the lack of a sequencer to trig the function generator and stop the signal generator and the power amplifier. In fact, to trig on this value, the stop signal where given by hand. The spectrometer used to generate sequences and to received signal were already used by another thesis. It was decided to produce a sequencer before other testing.

The function generator from the oscilloscope could be an arbitrary wave generator. In fact, it has been tried to change its generated waveform to produce the sequence of excitation. But the software from Keysight needed a license. It has been tried to hack the program without success and no exploit where found.

6.2 Air-coil design

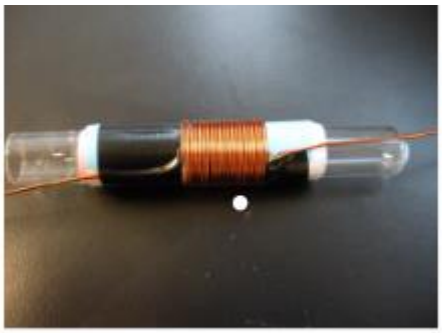

Figure 38 Photo of a coil made around a test tube [42]

The pick-up coil needs to encircle a test tube its size needs to be as small as possible.

The chosen magnetometer is a solenoid with Litz-wire in the air. This device can produce and receive magnetic field.

A first magnetometer was made by using Litz wire.

The air-coil has the propriety that the inductance does not change with the carried current. Its ferromagnetic cores counterpart is less linear and saturate at high frequency.

The Q-factor has to be optimized to transmit and receive the maximum signal. For this purpose, litz-wire are used. It is a special type of multi strand wire used to transport alternating current. The litz-wire is designed to reduce the skin effect and proximity effect losses in conductors used at frequencies up to about 1 MHz. The result of these winding patterns is to equalize the proportion of the overall length over which each strand is at the outside of the conductor. This has the effect of distributing the current equally among the wire strands. This reduces the total resistance. The skin effect is not reduced but there is more volume which transmit the alternating current.

The used frequency for a given Litz wire is given by the manufacturer. Also, the support of the winded litz-wire has an impact on the magnetic field produce. The skin-effect is reduced in litz-wire compare to a normal wire of the same thickness. At low-frequency the skin-effect has also an effect on the received signal produce by magnetic field. The litz-wire gives a better-quality factor.

The software used to simulate coils where Maxwell from Ansys. It is actually It's possible to simulate a litz wire with its isolation and also the component which makes the Litz add the support of the coil. It's also possible to simulate the effect of the plastic and other materials on the coil. Actually, it is hard to simulate litz-wire and the thermal noise induced in one coil. It is also possible to simulate the coil by using NMRP [19] is a program specially made to design a coil.

The design was made for a 50 [kHz] magnetometer since this is not anymore, the frequency used, this has not been documented.

6.3 Impedance Matching/ Coil tuning

To generate the most signal, it is crucial to know the actual Q factor of a coil, in fact, this changes when the coil is near the sample due to magnetic coupling. A circuit with an excitation coil and a pickup coil can be realized to determine the actual Q factor and the frequency at which it is at his highest.

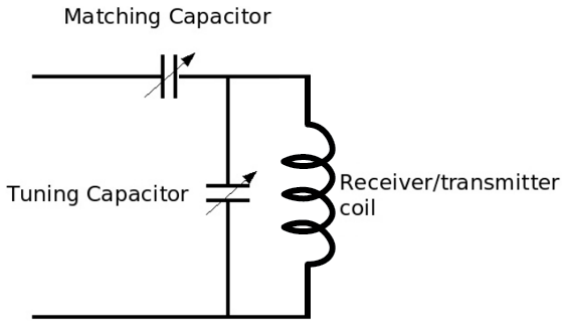

Figure 39 Impedance matching and tuning using capacitors

The coil has to be tuned and matched to oscillate at a given frequency. The capacitor has to be variable. The value of the variable capacitor has to be changed by a human operator with a screwdriver. There exists the possibility to use varactors (variable capacitor) without this drawback.

They can be designed as a mechanical setup of rotating disk inside a cylinder. This mechanical setup takes space and need to be rotated by a small motor or a human. There exists also tunable capacitor based on MEMS technology, but they are not commercially available yet. Finally, the most used technology at the time in radio tuning are PN junction acting as a capacitor whose capacitance value varies with the reverse voltage applied to its terminals. The drawback of the last technique is the variable tension produced by the capacitor values. Moreover, the power supply needs to be stable and connected to the same ground has the resonant circuit. With a varactor, a DC power cable is added near the magnetometer or/and producer B_1. The stability in frequency of the varactor is nonlinear since this is a diode optimized for this application. It is needed to choose a varactor from a supplier and inspect its electric stability.

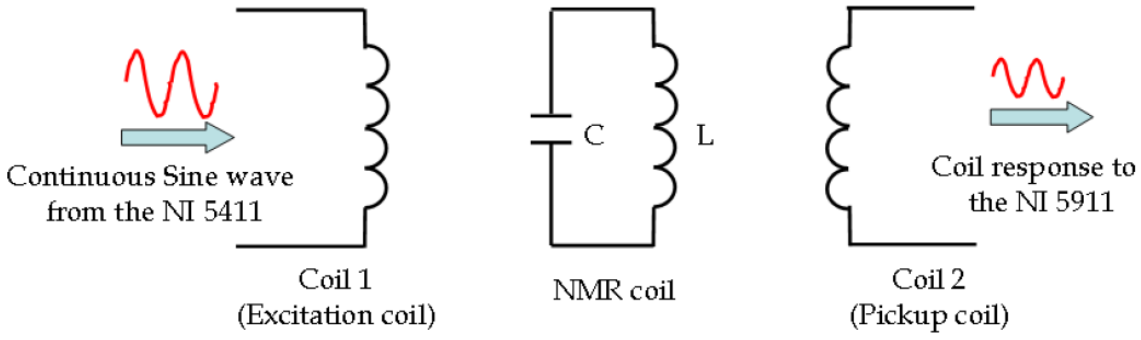

Figure 40 A method for tuning the NMR coil inside the magnet. [0, p35]

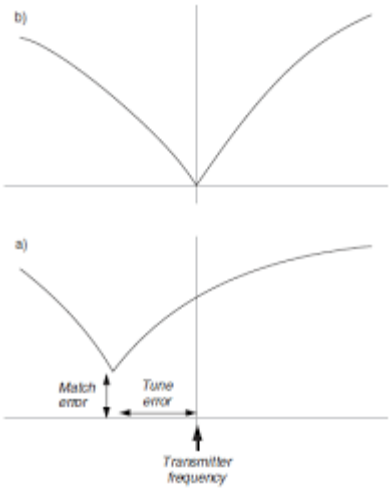

Figure 41 a) missed tune and missed match coil B) tune and match coil [6]

In the Figure 41, the tuning capacitor is tuned to the resonance frequency while the matching capacitor changes the depth of the coil's resonance. This also diminishes the bandwidth frequency of excitation.

6.4 Ringing suppressor

6.4.1 Ringing (transient switch on/off)

"After the field switching, there is transient effect which appear the stored energy in the coil spreads out on the sample with a time constant $\tau = \frac{2Q}{\omega}$ after 10-20 time constant, the ringdown is generally insignificant. At high frequencies, this time is typically a few microseconds or less. However, in the Earth's field apparatus it is **25 ms!** […] but unless one uses a non-Faraday form of detection […] this result in severe SNR loss. An alternative solution is to **actively damp** the ringdown for a short time following the RF pulse. High Q coils also restrict the bandwidth at low frequencies" [26]

The ringing suppressor need to change the quality factor of the circuit for a period of time which is lesser than 10*τ. To do so, it is needed to amplify the resistance or to reduce the inductance.

In fact, the method for measuring the Q-factor of a resonator is the ring-down method." [43] Since at small frequencies, a ringing occurs, it is needed to diminish this unwanted effect.

6.4.2 Q factor damper

To reduce the effect of ringing, it may be necessary to use a Q factor attenuator. It has the possibility to stop the oscillations of the sample.

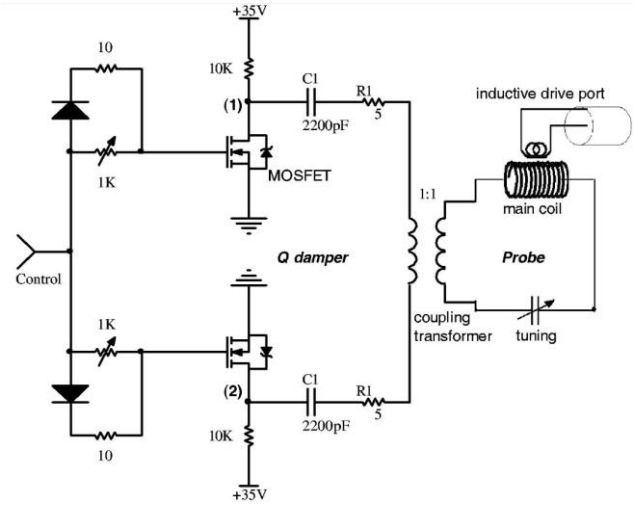

Figure 42 Q Damper electronic circuit [44]

To suppress the ringing effect, a Q factor attenuator was realized using LTSpice to stop the undesired oscillations. The circuit changes the impedance of the coil; this implies that the oscillation is damped. This work well when the frequency is constant, and the component used inside the application are ideal. It has not been tested with variation of the electronic component and is therefore not suitable before further research.

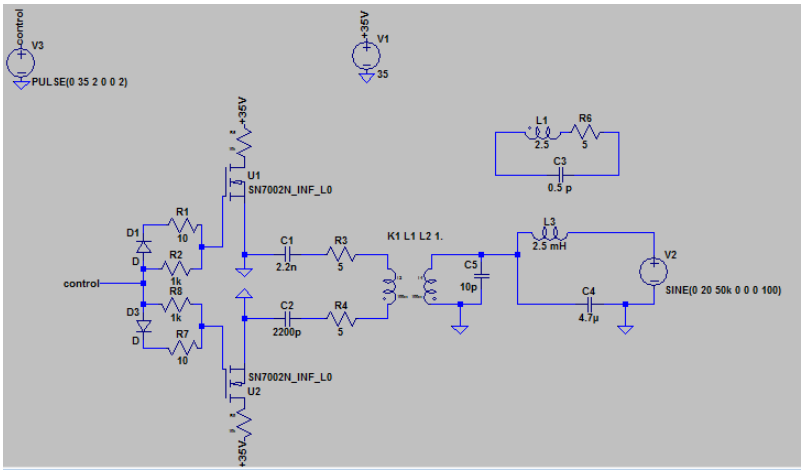

Figure 43 LT Spice circuit of a Q-Damper with a coil

This circuit changes the impedance of the coil when the circuit is not activated the inductance of the transformer is added to the coil. When the circuit is activated the Q, factor is diminished at the exciting frequency.

7. Electronics implementation

From the main source of this project, the following figure gives the electronic functions to be implemented.

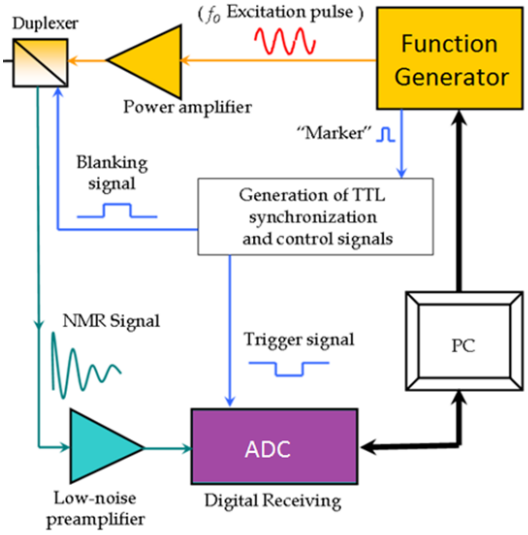

Figure 44 Schematic diagram of the electronic implementation [0]

A FPGA will be configured to handle the generation of TTL synchronization and control signals. The FPGA will also act has a function generator. On the previous schematic, the different power supplies of each component are not shown. Their stability is crucial for the analog devices as their bias current. The last thing to be implemented is the PC, which has to configure and start the function generator and to receive/process the NMR signals.

The duplexer enables the coil to receive and transmit signals on a single coil. This has not been implemented because we are using two separate coils.

In this chapter, the digital and analogic electronic worlds are being explored.

7.1 Existing Spectrometer

7.1.1 Lab spectrometer

Lab spectrometers are too expensive for the application. The one at the HEVs in the electric lab was already used in another project and is not suited for MF.

7.1.2 Red Pitaya STEMlab (FPGA+ µC)/OpenScope

Red Pitaya is an arbitrary pulse generator and oscilloscope. It can be configured as a spectrometer and can do the function of the ADC, DAC, µC and IC. The software and the firmware are open source. (vendor hardware) More details about this board are given in the annexes

7.1.3 ScopeFun

ScopeFun is an arbitrary signal generator and oscilloscope entirely open source software, hardware and firmware. At the time of this thesis, this device was under development with a

crowdfunding ending the 6 August 2019. Part of this circuit can be analyzed and implemented to design a RF board hardware and or to change the firmware code to be used as a console before transmitting the data to a μC for signal processing.[45]

From the software prospective view, it is made to run on standard OS (Windows, Linux, and Mac) It can be connected remotely on a server over an IP network. A Python API reads samples and controls the ScopeFun directly. In this thesis, the same applies in the usage of our μC to store the retrieved FID Data on a remote server.

7.2 FPGA implementation

7.2.1 Introduction

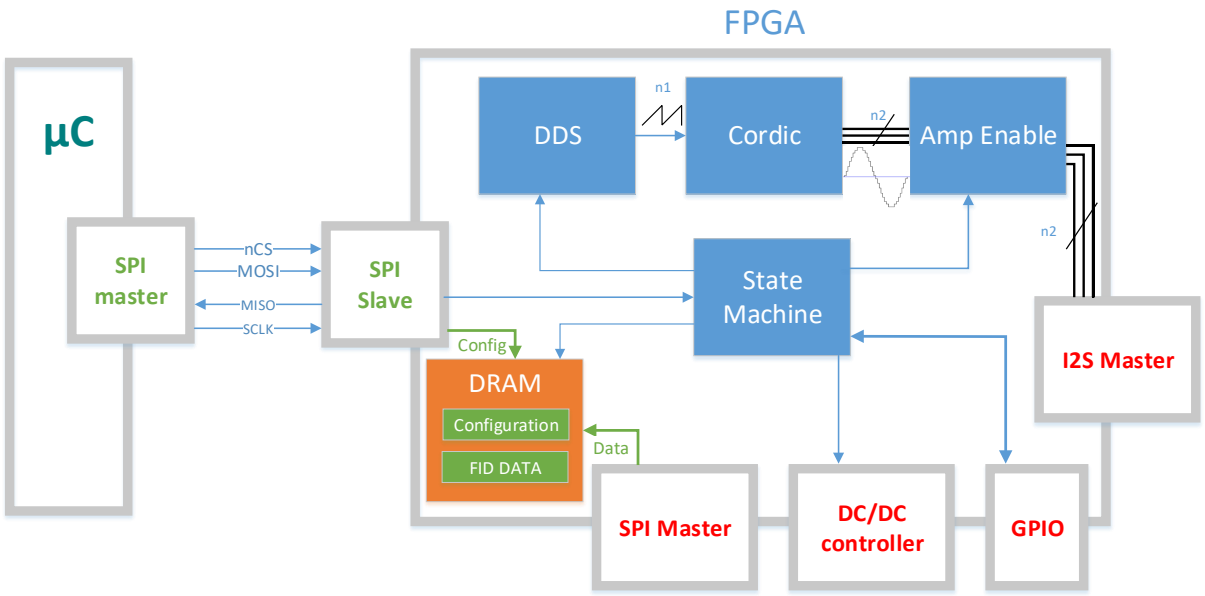

Figure 45 FPGA implementation diagram

The above diagram represents the function block of the FPGA and their relations. The central block is the central state machine which gives instructions to all the other blocks. The state machine received the configuration from the µC and gives command to all the other blocks. The interfaces give the possibility to the FPGA system to communicate with the external IC like the ADC and DAC and the µC. The communication has to be real-time. The FPGA configures also via GPIO the mode of the ADC and the DAC. The FPGA needs also to change the gain of the LNA during a sequence of transmission this can be done by controlling a DC/DC regulator. The DDS produces a saw tooth, which has to be transformed into a sine signal. It can be either done by taking values from a LUT or to use a Cordic pipeline algorithm. The pipeline algorithm has some latency before being usable. In our application, the Cordic algorithm can be always running. That implies that the State Machine has to wait on the restart of the sawtooth counter before enables the signal to be sent to the I2S master. The Cordic output signals can even be reused at the stage of reception if an IQ modulation is needed.

The communication from the microcontroller to the FPGA can be any protocol. It is not mandatory to have a real time or fast protocol for this application.

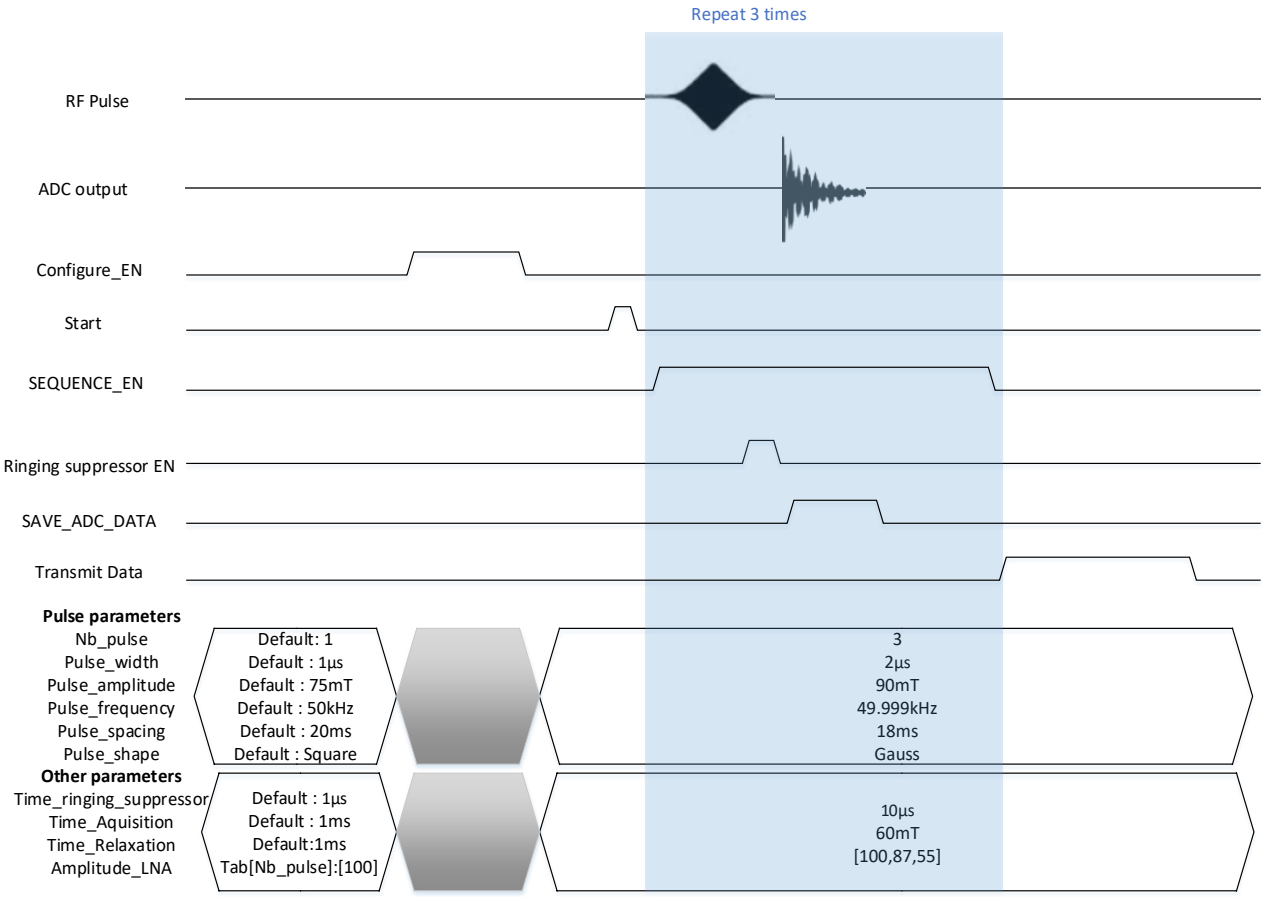

Figure 46 Time diagram of a pulse sequence

The above sequence timing diagram gives an understanding of what the central state machine is doing. The sequence can be modified by modified in code.

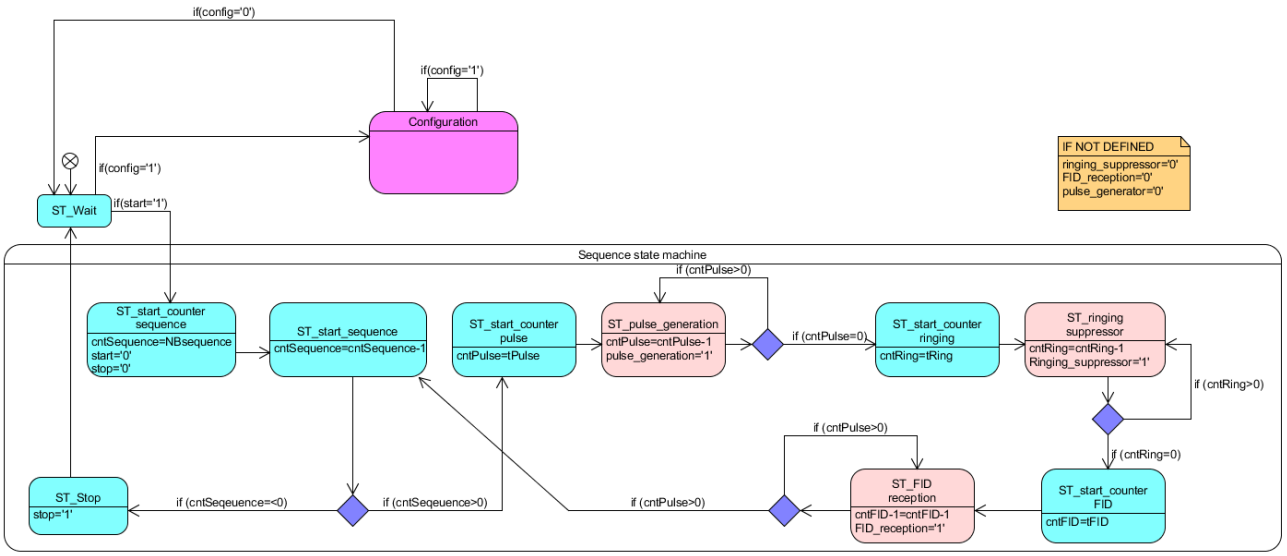

Figure 47 State machine of the FPGA

7.2.2 Installation on a PC

A TinyFPGA BX were chosen because it was available at the college, it was affordable, it is open source, it can run a SoC (System on Chip) like RiskV and the TinyFPGA EX where not available at the moment of this thesis.

For the installation of the TinyFPGA BX, there is a User Guide, which can be found at the following web address [https://tinyfpga.com/bx/guide.html]. There is also a GitHub repository with all the needed files. [https://github.com/tinyfpga] This installation is made without using license. To facilitate this installation, a virtual image on a Linux machine on Ubuntu was made to use the already installed program. The image can be mounted on VMWare.

The free open source environment of development uses a Verilog language. It is not possible to use VHDL to program the TinyFPGA in the opensource environment. The solution to use VHDL is either to code with a translator to Verilog (it is not well suited for big design) or to install Lattice Diamond. The installation of Lattice can be followed on this website: [http://mondzeu.ch/wikis/EDA/index.php?title=Install_Lattice]. The main problem with this setting is that an account and a free license file are needed to synthetize with VHDL designer. Lattice Diamond is installed on the Virtual Machine.

7.2.3 State Machine

The control signals are produced by the FPGA to synchronize external devices. The time at which they have to be activated. The activation sequence of the control signals has to configurable. The code made is a simple state machine.

7.2.4 DDS

The DDS is a simple counter which is incremented each n1 clock and produces a sawtooth signal.

7.2.5 Cordic algorithm

The Cordic algorithm enables to use less storage than a LUT (look up table) In the case of hardware without multiplier, this algorithm is not needed. This algorithm gives a digital sine wave as output, other trig functions can also be produced.

The core concept of this algorithm is to use division by two instead of using costly division by non-two number.(i.e. division by two is a right shift and takes only an instruction) For this purpose, the Cordic produces pseudo rotation, which needs to be scaled to the factor of their input. A table of these rescaled scales is saved. And it needs to multiply by the factor of the scale the before value.

From the figure below, we see the phasors moving. The green line has at first the length of the first sine at 90°. The green line is each time divided by two and added in quadrature to the last phasor it has constructed. Either on the left or on the right. The size of the phasor is then readjusted by multiplying factor of their rotation

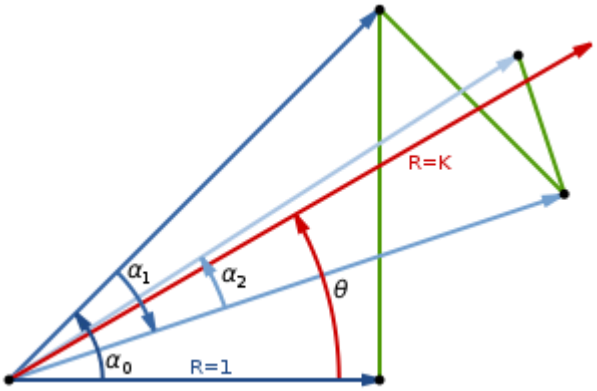

Figure 48 Graphic representation of the Cordic algorithm [34]

The resolution given by the Cordic algorithm is represented by two factors, n1 and n2. In fact, n1 is dependent of the ramp of the sawtooth and can be easily modified. While the factor n2 is dependent of the number of intermediate gates used int the Cordic algorithm. To change n2, in the case of a FPGA, it has to be reprogrammed because the gate has to be regenerated. In fact, it is not needed to reprogram the FPGA at runtime for this purpose.

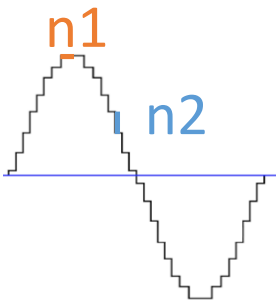

Figure 49 The factor n1 represents the frequency resolution and the factor n2 represent the amplitude resolution

7.2.6 I2S/I2C/SPI

The code for the SPI, I2S and the I2C were reused from existing project. Test benches were made to find their true output.

7.2.7 BRAM/DRAM

The TinyFPGA has BRAM and DRAM blocks. These blocks are used to store the data from the ADC. This memory blocks are volatile. In fact, to store the data and avoid memory capacity issue, a TinyFPGA EX is more suited than the BX because while it has an already implemented SD card.

7.2.8 UART

The TinyFPGA has already an USB access via its bootloader. It is possible to send data on the bus at runtime with a software adaptation. This has not been tested due to time issues but has been implemented.

A **USB program** driver has to be developed so that the FPGA can be connected to any computer and not only a Raspberry PI for the data processing. This task is not mandatory. In fact, with the TinyFPGA BX it is already possible to use the UART message via the USB port.

7.3 Power Supply and DC/DC converter

Power supply has to be used to power all the part of the circuit. In the current project, the power supplies are external. Depending of the power transmitted to the B_0 producer from the RFPA, the power amplifier has to be external and has its own power supply. In the design of the board, the ADC and DAC have two different DC power supply, one analogic and one digital also they have their own ground. This is made in the purpose to not distort the analogic signals. In fact, it is possible to use isolator IC connected to the two grounds at the stage of the direct alimentation input to use 2 direct components.

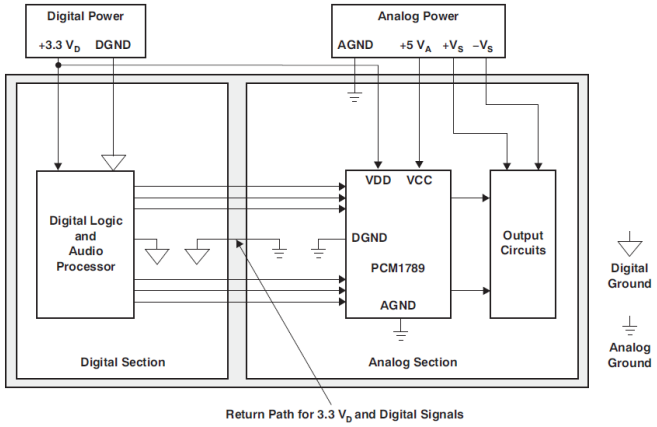

Figure 50 Recommended PCB Layout [59]

On a single board, it is important to separate the power supply, the analogic signal, and the digital signal in separate mass plane to reduce the possibility of ground loops. The data bus has to be surrounded by capacitor between the mass planes to avoid EMI (electromagnetic interferences). The command signal did not require any further modification to go from one world to another. A star point connecting the mass plan is needed at the center of the board plan to reference all the mass planes at the same ground. In fact, the star point in the middle reduces the size of ground loops and EMI radiation.

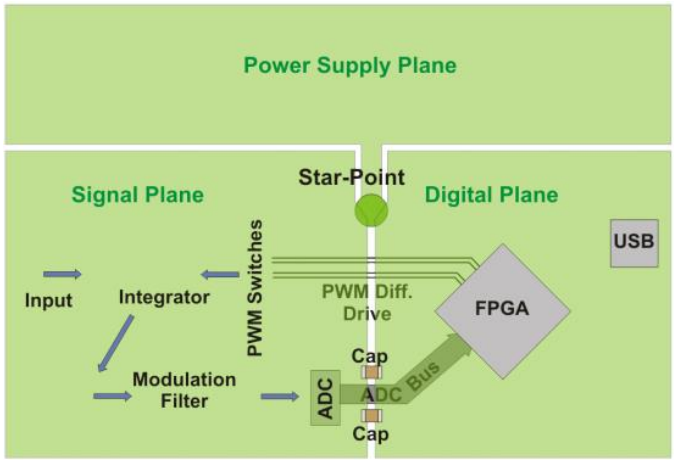

Figure 51 Practical board layout [46]

7.4 Analog circuit implementation

A schematic diagram of an analogic circuit was made on Altium Designer according to the components given by the different data sheets. The routing needs still to be made and care must be taken on the separation of the mass planes. This implementation has been made for a 50 kHz Larmor frequency. The filter and the power amplifier passive component are not well suited for other frequency. Cross over diodes are used in the implementation of the circuit to stop unwanted DC bias voltages.

The design circuit needs in addition, a power supply regulator and component to decouple the analogic and numeric power supply. The choice of the impedance between the components where chosen according to the test schematic of the circuit vendor. And the IC amplifier were simulated by using the S-parameter of the vendors. In fact, the simulation is not usable since it was implemented with ideal component. No care was taken to conduct simulation with measuring errors and real component. A study with fault in the component has to be conducted to constrain the component. It can be conducted with a Red Pitaya and it bode analyzer.

In fact, this circuit has been realized before finding out that the B_0 magnetic field is needed to be greater to diminish the size of the coils. The study of this component is useful for the audio domain.

7.5 Raspberry PI implementation

It was stated that the Raspberry PI needed a user interface to be able to show directly the end-results of the Fourier transformation to the user. The software, which processes the signal, does not need to be real time. The stored values from the ADC bus can arrive directly on the Raspberry port without interface. Following is the installation process of a Raspberry with Raspbian OS and its GUI (graphical user interface) (these steps can also be followed to install a Raspberry PI without user interface):

1. To start, the Raspberry PI needs a screen connected via an HDMI cable, a 5v power supply with a USB B port, an empty SD card, a mouse and a keyboard with an USB port. Another PC is needed to install the OS.
2. The Raspbian OS with desktop has to be download from another PC at the following address: https://www.raspberrypi.org/downloads/raspbian/
3. balenaEtcher has to be install from the following address: https://www.balena.io/etcher/ to flash the OS on the SD card. If the SD card is not suited for the OS, the installation program will tell it. The rest of the installation process is straightforward.
4. The SD card has to be installed inside the Raspberry and the needed device of the task 1 can be connected.
5. The Raspberry PI can be installed and is ready to be used.

Due to time issues, the Raspberry has not been implemented but the requirement are explain in the chapter 5.10 µC (microcontroller)

7.6 Communication protocol between FPGA and Raspberry PI

A communication protocol between FPGA and Raspberry PI has to be implemented over the UART. The communication protocol can be either Full duplex or Half duplex. Since the transmission of the data from the FPGA takes almost all the time. It will be a good idea to store packages on a SD card before sending the results. On the TinyFPGA BX, there is no SD port, it would be needed to use the TinyFPGA EX which has a SD port which simplifies the electronic implementation. At the time of this thesis, the TinyFPGA EX was not available. The communication between the PI and the FPGA has not been fully developed but was started. Since the memory of the TinyFPGA BX is not sufficient to store all the data from the SPI bus, it was decided to wait the availability of the TinyFPGA EX with its SD port.

8. Discussion

When producing an NMR spectrometer working with HP ^{129}Xe in the blood, it is needed to specify the polarization and the number of HP ^{129}Xe encapsulated into cryptophane cages. This gives the maximal signal received. The frequency of excitation will be narrowed to the frequency of rotation of the HP ^{129}Xe encapsulated. This is the limiting factor for designing the pickup coil and the LNA. The RFPA also needs to produce the exact amount of frequency to not diminishes the relaxation T_1 of the HP ^{129}Xe or to not change enough the tilt angle. The other parts of the electronic design do also need to not distort the received signal but are less crucial.

9. Conclusion

Our findings noted that to use PCR plates to characterize the content of the blood, it is needed to have small hard permanent magnets in a round Halbach array arrangement with the possibility to add shimming permanent magnet to enhance the field homogeneity. To use PCR plates, it is also needed to have a monolithic small-dedicated IC with an integrated stacked inductor for both magnetic field generation and reception and the capability to have analogic, digital and power stages. The IC needs also a communication protocol to configure a sequence and to receive data from a µC which will process the data and store them on a Data base.

Each test tube of the PCR plate will have its own IC spectrometer and Halbach array arrangement. The IC could be mounted on a PCB with a single bus of communication and controlled alimentations with non-susceptible magnetic materials.

A study of the HP ^{129}Xe was conducted to understand its electronic specifications. Along as an extensive study of the possible noise and distortion sources encountered by electronic devices.

A development bench has been set up to work at low frequency (~50 kHz). As well as a development board. This has led to rethink how to produce the field B_0 since the thermal noise produced by electromagnet are too high, it has made us think to use small round Halbach arrangement instead.

A schematic circuit working at a frequency of 50 kHz has been prototyped, realized and analyzed by combining existing IC and passive component. The routing has not been performed. It is needed to take care to route the component with care to separate the mass planes.

In the scenario of using a single coil for both excitation and reception, a ringing suppressor circuit has been simulated.

Finally, this thesis has paved the way to the feasibility of a small portable NMR spectrometer for high-throughput blood screening method.

10. Outlook

The tasks implemented in this project were meant to conceptualize an NMR spectrometer working with blood and HP ^{129}Xe. There are still some aspects needing to be prototyped.

The need further optimization to work with MF determined by the static magnetic field B_0. The kind of coil used can be almost the same as a LF RFID tag emitter. However, RFID are not authorized to use MF, and some have soft magnets.

The electronic functions design in the electronic board of this project can be implemented on a test board if a further project needs low frequency or is working in the audio domain as the application was thought at the beginning to work at a frequency of 50 kHz.

The digital part does not need further changes. Only the analogic part needs to be tailored according to the excitation frequency used. In a magnetic field B_0 between 0.5 and 1 Tesla, the frequency of excitation is between 1 and 10 Megahertz. Since these frequencies are not in the ISM spectrum, they need to be contained inside the device.

A modelling environment software to characterize HP ^{129}Xe and its interactions is not yet existent, it could be implemented by using a finite element software like **Comsol Multiphysics** with integration of magnetic susceptibility and equations related to Bloch's equations and hyperpolarization. To model the loss in magnetization at the injection process and to model an antenna interacting directly with HP gases.

Halbach Array could produce greater and more homogenous magnetic field for B_0, YX magnetic a Swiss company [47] can produce customized magnets. Due to time issue, the magnet was designed but not prototyped. The shimming magnet were not tested, and their design need further research.

An IC can be produced to handle all the functionalities of a small NMR spectrometer without the signal processing and the B_0 production. Em Microelectronic collaborates with schools to implement such devices. However, the minimal number of pieces to be produced is around 100'000. AMS is an Austrian company also specialized in IC production. They have the possibility to produce series of minimal 100'000 IC with each its own electronic circuit. Little variations could be introduced in each analog component to optimize the functionality of the end NMR spectrometer on a single chip.

A signal processing software has to be developed to amplify the SNR in the frame of multiple excitation sequences. It needs to use the appropriate window and a Fourier transformation algorithm. FluidFFT library can be used for this purpose. The result needs to be linked to a database for storing the FID spectrum. A file format for this purpose needs to be used; NMReDATA could serve as an adapted format since it is standard data format between companies in the frame of NMR record. It can be used as it is in the frame of 1D spectrum excitation. A converter to this format from the received FID has to be implemented.

The norm for Medical devices (ISO 13485) has to be respected as well as the general requirements for the competence of testing and calibration laboratories ISO/IEC 17025 to be used in the medical environment. This norm demonstrates that the results are valid. Furthermore, since EM wave are produced, EMC standards also need to be observed.

11. References

[0] Aktham Asfour, Low-Field NMR/MRI Systems Using LabVIEW and Advanced Data-Acquisition Techniques

[1] Polarean 9800 129Xe Hyperpolarizer (http://www.polarean.com/129Xe_hyperpolarizer.html) (viewed the 07.06.2019)

[2] DECORPS Michel, Imagerie de résonance magnétique, EDP Sciences May 2011 (ISBN : 978-2-7598-0000-1)

[3] Derrick Kaseman (UC Davis) and Revathi Srinivasan Ganesh Iyer (UCD), **Figure 14.5.1,** version Dec 15, 2018 https://chem.libretexts.org/Courses/University_of_Arkansas_Little_Rock/UALR%3A_CHEM_3572_-_Physical_Chemistry_for_Life_Sciences_(Siraj)/Text/14%3A_Spectroscopy/14.05%3A_Nuclear_Magnetic_Resonance (viewed the 07.06.2019)

[4] New Mexico Tech infohost.nmt.edu (viewed the 06.06.2019)

[5] Els Fieremans. Diffusion Weighted MRI in Brain White Matter http://www.diffusion-mri.com/phd/PhDch2.html (viewed the 06.06.2019)

[6] Physical Basics of NMR, Rolf Pohmann 2011, page 18

[7] Glenn Facey, Shaped Pulses (version May 31, 2011) http://u-of-o-nmr-facility.blogspot.com/2011/05/shaped-pulses.html, viewed the 06.07.2019

[8] Leif Schröder, Xenon for NMR biosensing - Inert but alert, (2011)

[9] *Shuen-Cheng Hwang, Robert D. Lein, Daniel A. Morgan, Kirk-Othmer Encyclopedia of Chemical Technology, Hoboken, Wiley, 2005, 5e ed. (*ISBN 978-0-471-48511-7, LCCN 2003021960, DOI 10.1002/0471238961.0701190508230114.a01*)*, « Noble Gases »

[10] Xenon in Merck catalog, https://www.sigmaaldrich.com/catalog/product/sial/00472?lang=fr&region=CH&cm_sp=Insite-_-prodRecCold_xviews-_-prodRecCold3-1, (viewed the 18.07.2019)

[11] Rao M, Stewart NJ, Norquay G, Griffiths PD, Wild JM. High resolution spectroscopy and chemical shift imaging of hyperpolarized (129) Xe dissolved in the human brain in vivo at 1.5 tesla. Magn Reson Med. 2016;75(6):2227–2234. doi:10.1002/mrm.26241, page 784

[13] David E Wemmer, Hyperpolarized Xenon-129 Magnetic Resonance (Chapter13), Royal society of Chemistry 2015

[14] Shchepin, R. V.; Birchall, J. R.; Chukanov, N. V.; Kovtunov, K. V.; Koptyug, I. V.; Theis, T.; Warren, W. S; Gelovani, J. G.; Goodson, B. M.; Shokouhi, S.; Rosen, M. S.; Yen, Y-F.; Pham, W.; Chekmenev, E. Y. “Hyperpolarizing Concentrated Metronidazole 15NO2 Group over Six Chemical Bonds with More than 15% Polarization and a 20 Minute Lifetime” Chem. Eur. J. 2019, 25, 1-9.

[15] Barskiy, D. A.; Ke, L. A.; Li, X.; Stevenson, V.; Widarman, N.; Zhang, H.; Truxal, A. Pines, A. “Rapid Catalyst Capture Enables Metal-Free Para-Hydrogen-Based Hyperpolarized Contrast Agents” J. Phys. Chem. Lett. 2018, 9, 2721−2724 See Supplementary Information

[16] Halse, M. E. “Perspectives for hyperpolarisation in compact NMR”, Trends in Analytical Chemistry, 2016, 83, 76-83

[17] Kennedy, D. J. et al. An optimized microfabricated platform for the optical generation and detection of hyperpolarized 129Xe. Sci. Rep. 7, 43994; doi: 10.1038/srep43994 (2017)

[18] Hossein Pourmodheji, TOWARDS CMOS NUCLEAR MAGNETIC RESONANCE SPECTROSCOPY: DESIGN, IMPLEMENTATION AND EXPERIMENTAL RESULTS, master thesis, November 2015

[19] Joël Mispelter, Mihaela Lupu, André Briguet NMR Probeheads for Biophysical and Biomedical Experiments Theoretical Principles and Practical Guidelines, (2nd Edition) ISBN: 978-1-84816-662-2

[20] Yves OESCH, HB9DTX, Pourquoi 50 W ??? http://www.yvesoesch.ch/publicat/50ohm.pdf, (viewed the 04.07.2019)

[21] LECTURE COURSE: NMR SPECTROSCOPY, Zebre Olivier, page 27

[22] A simple and low-cost permanent magnet system for NMR, K. Chonlathep, T. Sakamoto, K. Sugahara, Y. Kondo, Journal of Magnetic Resonance, Elsevier, February 2017

[23] Blümler, Peter & Casanova, F. (2016). CHAPTER 5: Hardware developments: Halbach magnet arrays. 10.1039/9781782628095-00133.

[24] Design & Development of Helmholtz Coil for Hyperpolarized MRI, Excerpt from the Proceedings of the COMSOL Conference 2010 India, https://www.comsol.jp/paper/download/62250/bhatt_paper.pdf (viewed the 28.07.2019)

[26] Eccles Craig. (2017), Low Field NMR Methods and Applications, Elsevier Ltd. 10.1016/B978-0-12-409547-2.05099-X.

[27] Dustin D. Wheeler, Mark S. Conradi, Practical exercises for learning to construct NMR/MRI probe circuits, https://doi.org/10.1002/cmr.a.21221,2012

[28] Pekka Tapani Sipilä, Real-Time Magnetic Field Monitoring in Magnetic Resonance Imaging, 2011

[29] PRZEGLĄD ELEKTROTECHNICZNY, ISSN 0033-2097, R. 89 NR 10/2013

[30] R Nave, SQUID Magnetometer http://hyperphysics.phy-astr.gsu.edu/hbase/Solids/Squid.html (viewed the 24.07.2019)

[31] Lou Frenzel | What’s the Difference Between SAR and Delta-Sigma ADCs? (May 04, 2016) https://www.electronicdesign.com/adc/what-s-difference-between-sar-and-delta-sigma-adcs (viewed the 24.07.2019)

[32] Lectures by James Keeler How the spectrometer works http://www-keeler.ch.cam.ac.uk/lectures/understanding/chapter_5.pdf (2011) (viewed the 22.07.2019)

[33] Introduction to NMR/MRI RF Amplifiers (2012) CPC (NMR amplifier vendor) http://www.cpcamps.com/introduction-to-nmr-mri-amplifiers.html(viewed the 12.08.2019)

[34] https://en.wikibooks.org/wiki/Digital_Circuits/CORDIC

[35] Texas Instruments, “PCM1789 24-Bit, 192-kHz Sampling, Enhanced Multi-Level ΔΣ, Audio Digital-to-Analog Converter”, PCM1789 datasheet, OCTOBER 2008–REVISED AUGUST 2015, page 33

[36] Texas Instruments, PCM512x 2-VRMS DirectPath™, 112-dB and 106-dB Audio Stereo DACs with 32-Bit, 384-kHz PCM Interface, AUGUST 2012–REVISED OCTOBER 2018, page 1

[37] https://shop.trenz-electronic.de/en/TE0887-03M-icoBoard-Version-1.1-with-8-MBit-SRAM?path=Trenz_Electronic/Modules_and_Module_Carriers/special/TE0887/REV03/Documents

[38] Texas Instruments, "OPAx211, OPAx2111.1-nv/√Hz Noise, Low Power, PrecisionOperationalAmplifier", OPAx211datasheet, Revised September 2018, page 1,6,18

[39] Surface Mount Switch 50Ω SPDT, Absorptive DC to 4.6 GHz, Minicircuit

[40] What SPI frequencies does Raspberry Pi support? (2014) [https://raspberrypi.stackexchange.com/questions/699/what-spi-frequencies-does-raspberry-pi-support] (viewed the 18.07.2019)

[41] Michal, CA. *A low-cost multi-channel software-defined radio-based NMR spectrometer and ultra-affordable digital pulse programmer*. Concepts Magn Reson Part B. 2018; *48B*:e21401. https://doi.org/10.1002/cmr.b.21401

[42] Clarissa Lynette Zimmerman Low-field Classroom Nuclear Magnetic Resonance

System (February 4, 2010) page 54

[43] Iacopo Giangrandi, Measuring the Q-factor of a resonator with the ring-down method

[44] Peshkovsky AS, Forguez J, Cerioni L, Pusiol DJ. RF probe recovery time reduction with a novel active ringing suppression circuit. J Magn Reson. 2005;177(1):67–73. doi:10.1016/j.jmr.2005.07.004

[45] Open Source All-in-One Instrumentation on Crowd supply https://www.crowdsupply.com/scopefun/open-source-instrumentation(viewed the 14.07.2019)

[46] J. Pickering Analogueto Digital and Digital to Analogue Converters (ADCs and DACs): A Review Update https://cds.cern.ch/record/2038672/files/arXiv:1607.01589.pdf page14 (viewed the 22.07.2019)

[47] Halbach Cylinder, YX Magnetic Switzerlandhttps://www.yxmagnetic.com/en/halbach-cylinder-496.html(viewed the 31.07.2019)

[48] Terranova-MRI, Earths field MRI & NMR teaching system, Magritek https://www.labx.com/item/terranova-mri-earths-field-mri-nmr-teaching-system/510873#description(viewed the 18.07.2019)

[49] profile NMR-Mouse, Magritek http://www.magritek.com/wp-content/uploads/2013/12/MOUSE-2012-web-1.pdf

[50] Kea NMR and MRI Spectrometer Consoles, Magrikek http://www.magritek.com/products/kea/(viewed the 02.07.2019)

[51] the mq-ProFiler, Bruker BioSpin 01/17 T137095 https://www.bruker.com/fileadmin/user_upload/8-PDF-Docs/MagneticResonance/TD-NMR/minispec_mqProFiler_T137095.pdf (viewed the 05.07.2019)

[52] minispec mq-Series user manual version001, Brucker http://www2.chem.uic.edu/nmr/downloads/bruker/en-US/pdf/e1400012.pdf(viewed the 07.07.2019)

[53] Kazuyuki Takeda, OPENCORE NMR: Open-source core modules for implementing an integrated FPGA-based NMR spectrometer, Journal of Magnetic Resonance, Volume 192, Issue 2,2008, Pages 218-229,ISSN 1090-7807, https://doi.org/10.1016/j.jmr.2008.02.019. (http://www.sciencedirect.com/science/article/pii/S1090780708000670)(viewed the 06.07.2019)

[54] picoSpin™ 80 Series II NMR Spectrometer, Thermo Scientific™ https://www.thermofisher.com/order/catalog/product/912A0832(viewed the 12.08.2019)

[55] NMReady-60PRO, Nanalysis,http://www.nanalysis.com/nmready-60pro(viewed the 12.07.2019)

[56] HC9 350mm Helmholtz Coils, Barington instruments http://www.bartington.com.cn/presentation/hc9-350mm-helmholtz-coils/index.html(viewed the 30.06.2019)

[57] NDFEB HALBACH ARRAY, bunting https://e-magnetsuk.com/neodymium_magnets/products/ndfeb_halbach_array.aspx(viewed the 24.05.2019)

[58] ScopeFun, Open Source All-in-One Instrumentation, https://www.crowdsupply.com/scopefun/open-source-instrumentation(viewed the01.08.2019)

[59] Texas Instruments, “PCM1789 24-Bit, 192-kHz Sampling, Enhanced Multi-Level ΔΣ, Stereo, Audio Digital-to-Analog Converter”, PCM1789 datasheet, OCTOBER 2008–REVISED AUGUST 2015, page 33

12. Credits

Special thanks to the following people for helping me realizing this project:

- Dr Djano Kandaswamy, supervising professor, HEVs
- Dr Jean-Noël Hyacinthe, expert, Hes-Geneva
- Lê Thanh Phong Kevin, physic doctoral student, Hes-Geneva
- Alexandra Andersson, RF electronic professor, HEVs
- Dr Joseph Moerschell, analogic electronic (DAC, ADC) professor, HEVs
- Dr François Corthay, digital electronic professor, HEVs
- Christian Costa, EMC & Electromagnetic simulation advisor, HEVs
- Medar Rieder, Radio Amateur and ultra-low power embedded systems professor, HEVs

In addition, I wanted to thank the collaborators of the HEVs for providing me materials and advices.

13. Annexes

13.1 Terranova-MRI, Earths field MRI & NMR teaching system [48]

Figure 52 Terra-Nova NMR teaching device [48]

The Terranova-MRI is a teaching device working thanks to the earth's magnetic field for B_0. B_1 is produced by an air coil solenoid. It can contain sample up to 75 mm in diameter. It uses no cryogenic technics and no permanent magnets. The sample has to be aligned with B_0 to produce the best signal.

a) b)

Figure 53 a) Alignment of the coil in quadrature of the earth's magnetic field. b) Alignment of the probe to the earth magnetic field B_0 [48]

The spectrometer can tune the probe capacitance to adapt the resonance frequency of the transmitter-receiver solenoid. Added shimming coils can change the homogeneities of the B_1 field in this device. The sequences of the spectrometer can be chosen. In theory, the program should be able to retrieve a spectrum of the HP ^{129}Xe. This being said, no source stated that the Terranova-MRI had been tested using the HP form of ^{129}Xe.

13.2 Profile NMR-Mouse one-sided NMR

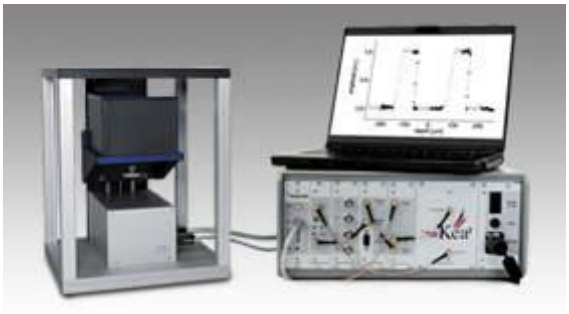

Figure 54 on the left an NMR-Mouse (which contains a permanent magnet for B_0 and a RF coil for B_1) on the right a personal computer standing on a Kea² spectrometer. [49]

"The Profile NMR-MOUSE is a portable open NMR sensor equipped with a novel permanent magnet geometry that generates a highly uniform gradient perpendicular to the scanner surface. Given this field profile, a flat sensitive volume is excited and detected by a surface RF coil placed on top of the magnet at a position that defines the maximum penetration depth into the sample. By repositioning the sensitive slice across the object, this scanner produces one-dimensional profiles of the sample structure with a spatial resolution better than 5 µm. The gradient of the sensor can as well be utilized to measure molecular self-diffusion coefficients. By applying spin or stimulated echo sequences liquids with a wide range of viscosities can be fast and accurately measured. The Profile NMR-MOUSE system includes a high precision lift and a fully digital mobile spectrometer Kea."[49]

The Kea² is an NMR Spectrometer console with a bandwidth from 1 to 100 MHz made by Magritek. This spectrometer cannot be used at lower frequencies and therefore cannot be used for this project.

"Kea² uses no intermediate mixing frequencies — meaning no quadrature issues. Kea²'s digital transmit circuit performs direct waveform synthesis. The receive module directly digitizes the NMR signal at 100 MHz for a high quality, low noise NMR signal. This is the same technology used in most modern high field NMR spectrometers but is available with Kea for a fraction of the price." [http://www.magritek.com/products/kea/]

13.3 Low-Field NMR Systems Using LabVIEW™ and Advanced Data-Acquisition Techniques [0]

A Low-Field NMR/MRI Systems Using LabVIEW™ was developed at the Grenoble University. In this thesis, some of the features of this technology are optimized to work with HP ^{129}Xe. This source provides detailed breakdowns of the implementation of the electronic components and their circuits. This permits us to reproduce, enhance and adapt for the use of HP ^{129}Xe. The complete signal-processing program is explained along with the code interface node of LabVIEW™. The device is broken down, from the user interface to the physical environment. The below flowchart demonstrates the above-mentioned electronic circuits [0]

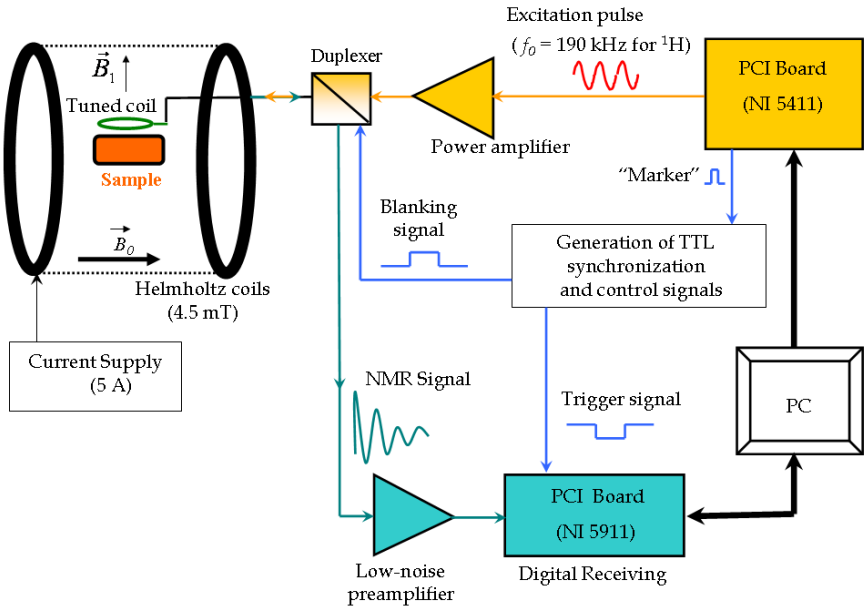

Figure 55 The hardware architecture of the low -field NMR systems

The static field B0 of about 4.5 mT is produced by a pair of Helmholtz coils. The excitation pulse (at about 190 kHz for 1H) is generated by the transmitter (arbitrary waveform generator board NI 5411 form National Instruments). This pulse is amplified by a power amplifier and sent, via the duplexer, to the well-tuned coil (at the working frequency of 190 kHz for the 1H) which generates the excitation field B1. At the end of the excitation pulse, this same tuned coil detects the weak NMR signal. This signal is transmitted to a low-noise preamplifier via the same duplexer. The amplified signal is then received by the receiving board (A digitizer board NI 5911 from National Instruments) for digitalization and processing. A monostable-based circuit generates TTL control and synchronization signals from a single and very short (about 10 ns) TTL pulse ("Marker") that could be generated from the NI 5411. At least, two signals are necessary. Since the same coil is used for both transmitting and receiving (i.e. a transmit-receive coil), a "blanking signal" is required to control the duplexer. This signal "blanks" the preamplifier input during the excitation pulse and it isolates the transmitting section from the receiving one during the NMR signal detection. Another control signal (trigger signal)

is necessary for triggering the signal acquisition with the receiving board.

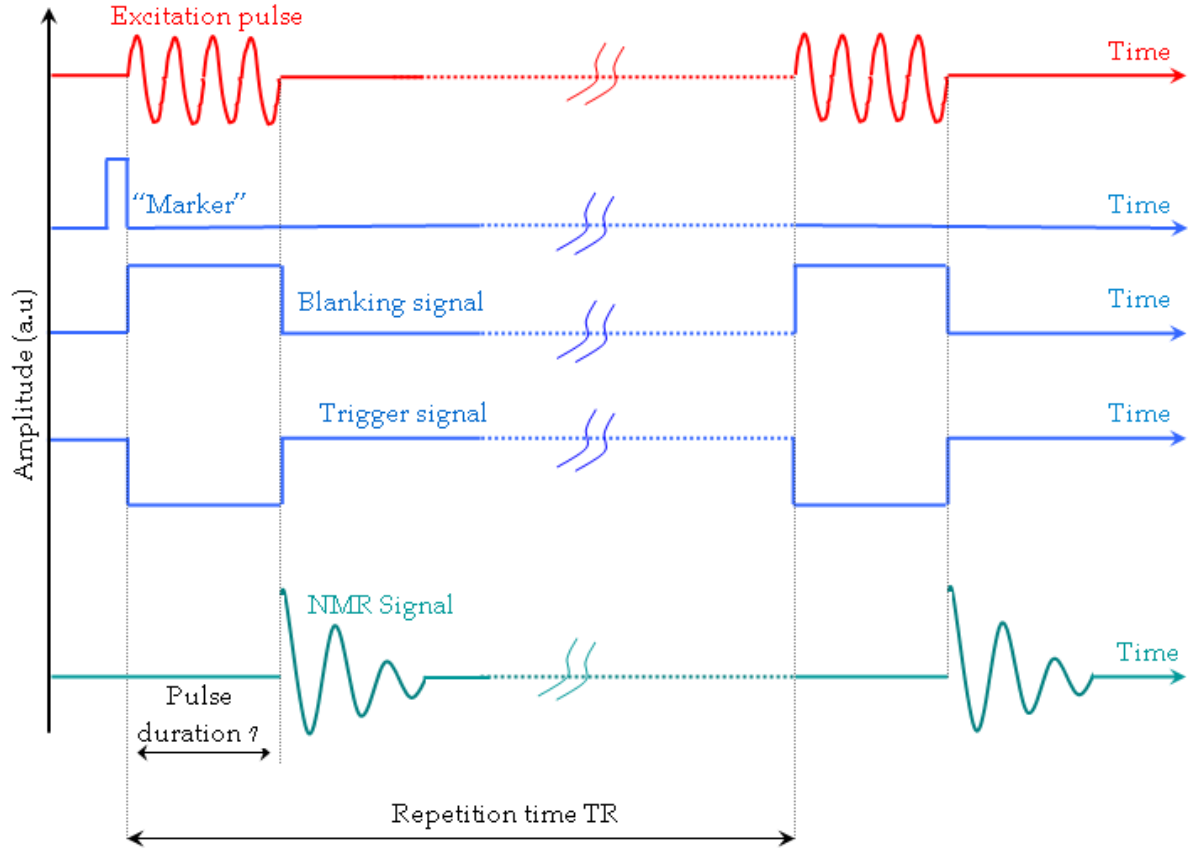

Figure 56 The timing-diagram of a typical one-pulse NMR experiment.

13.4 The mq-ProFiler [51]

The mq-ProFiler is a compact NMR relaxometer produced by Brucker. It is equipped with single-sided magnet and RF probes mainly built for performing 1H-NMR experiments within the first few millimeters below the surface of arbitrarily shaped samples. The mq-ProFiler utilizes NMR techniques, similar in principle to the high-resolution NMR and MRI, and analyzes the data in time-domain to predict physical and chemical properties of materials.[51]

This device is portable, but the field produced is high. Approximately 0.4 Tesla and the broadband frequency are between (2-65MHz). The frequency for ^{129}Xe at such a field is approximately ~4.2MHz (=11,777e6*0.4), hence it is suited for this device. The source of generation of the 0.4 Tesla B_0 field is unknown. The excitation's sequences are configurable as well as the amplitude of B_1 and the time of excitation τ. The technology is proprietary and requires back engineering to be better understood.[52]

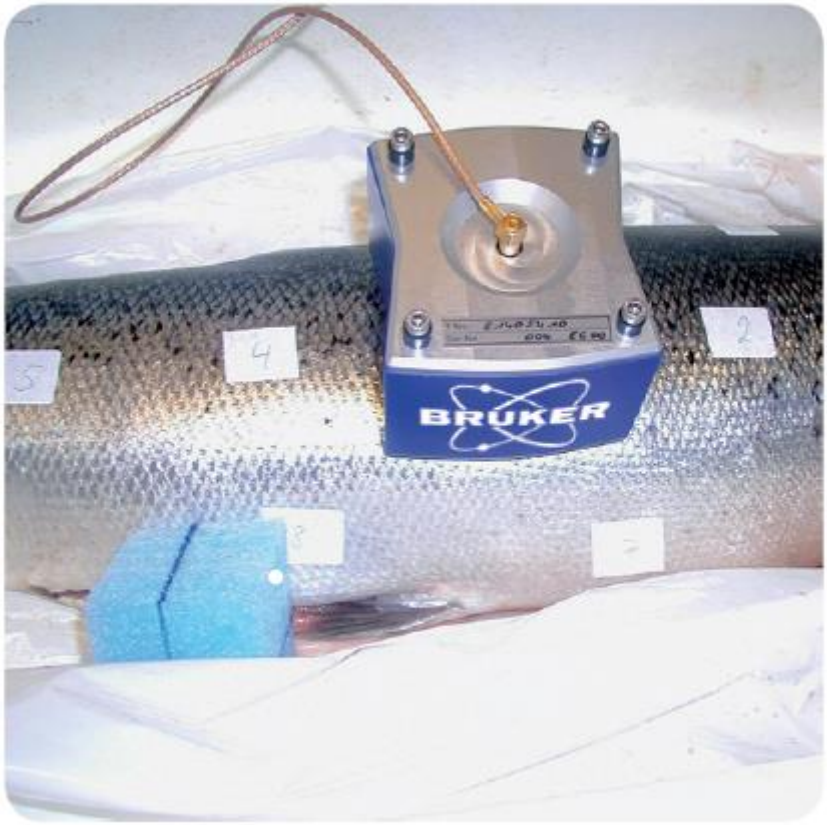

Figure 57 mq-ProFiler used in the determination of fat content in fresh fish and meat [52]

13.5 Opencore NMR

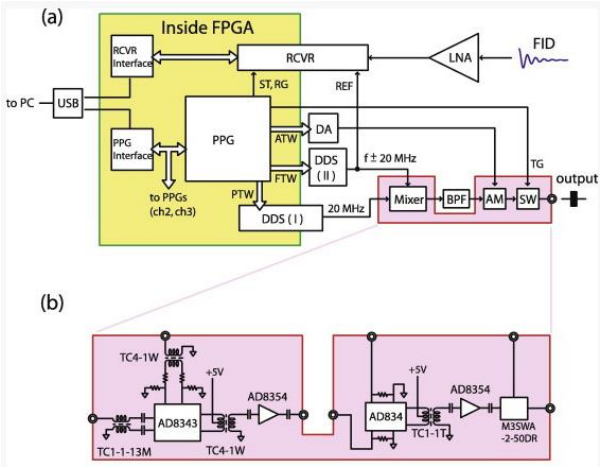

Figure 58 OPENCORE NMR schematic principle

"OPENCORE NMR is an open-source toolkit for implementing an NMR spectrometer. This console has the size of a laptop computer, making it easy to transport. The cost of its parts is very low compared to the prize of commercial systems. This integrated system has 3 radio frequency transmitting channels capable of operating at up to 600 MHz (14 T). It has been successfully combined with high-temperature superconducting magnets, as well as with a portable 1T permanent magnet. The toolkit comes with a multiplatform graphical user interface software to run the spectrometer.

Its key feature is that a single Field-Programmable Gate-Array (FPGA) chip does most digital jobs of the spectrometer. It allows building digital hardware modules, called core modules, by writing a software code in VHDL language. The FPGA is responsible for the pulse sequence controls, the digital part of DDS, the quadrature demodulation, filtering, and PC communication. The FPGA chip is complemented with several peripheral boards for USB communication, direct-digital synthesis (DDS), RF transmission and signal acquisition. Resources necessary for reproducing the FPGA-based NMR spectrometer are publicly available. They include source code of the modules, circuit diagrams, board drawings, control software, and technical documents

The OpenCore NMR spectrometer has not been designed to compete against commercial systems, but to complement them by being a test-bench for concepts that may require strong hardware modifications. Nevertheless, its performance can be as high as that of commercial systems. Some of the projects developed with the Opencore NMR spectrometer include: Magic-angle adjustment with X0-shimming, dynamic receiver-gain modulation, paramagnetic shimming, hetero-nuclear covariance spectroscopy employing a dual-receiver system, and Double-resonance Magic Angle Coil Spinning. The spectrometer has also been complemented with a field-gradient waveform generator to acquire 3D NMR images (MRI).

The OPENCORE NMR spectrometer facilitates setting up a system for non-conventional NMR experiments within a reduced development time. This work can promote novel and exciting NMR experiments by lowering the barrier for building a handmade NMR spectrometer." [53]

13.6 picoSpin™ 80 Series II NMR Spectrometer

Figure 59 picoSpin™ 80 Series II NMR Spectrometer during its manual method of operation [54]

"The picoSpin™ 80 NMR Spectrometer features a 2 Tesla magnet. The instrument's fluid capillary system is contained within a replaceable cartridge and only requires 40 microliters of a liquid sample. Its temperature-controlled permanent magnet does not require cryogens, eliminating the need for consumables or custom laboratory facilities." [54]

The operation costs are reduced to the consumable, which are estimate to $5k/yr. The purchase price of the device is of $60k. It is possible to program a unique excitation pulse. For application to this thesis, the process to inject and recycle the blood and the HP ^{129}Xe would need to be implemented. However, the functioning of the device is proprietary and thus unknown. They also have an existing proprietary signal processing software. As each blood is unique, the tube must be replaced to avoid cross contamination, therefore reducing the potential for automation of this process. The alignment of the spin of HP ^{129}Xe is unknown inside the device. The hardware and the software are proprietary; it needs to be reverse engineered to understand how the magnets are configured inside.

13.7 NMReady-60PRO

Figure 60 NMR 60 Pro [55]

The NMR 60 Pro is an NMR spectrometer all in one. It uses permanent magnet and produces a magnetic field of 1.4 T without cryogenic cooling. It is compatible with LabVIEW (via NMReadyCONNECT API). It has a resolution of 20 ppb (part per billion). It is possible to request the spectrometer's hardware to be tuned for HP ^{129}Xe. The excitations pulses can be modified. It has two channels of excitation. The following elements can be used for excitation: ^{1}H (60 MHz), ^{7}Li (24 MHz), ^{11}B (19 MHz), ^{13}C (15 MHz), ^{19}F (56 MHz), and ^{31}P (25 MHz). It is also possible to specify other elements and frequency without additional fee.

Figure 61 AUTOsample-60 mounted on an NMR 60 Pro [55]

The possibility is given to add an auto sampler on top of an NMR 60 Pro. With this configuration, 25 tubes can be tested one after another inside the NMR without human intervention. The time taken to introduce the test tube inside the device and the possibility to synchronize the injection of the HP ^{129}Xe need further research. This device does not consider the need to inject the HP ^{129}Xe into the blood after it has been entered the machine. This will necessitate further research.

The quotation of the NMRReady-60Pro and the AUTOsample-60:

nanalysis

Quotation

Mr. Nassim Augsburger
HES-SO VALAIS-WALLIS
Route du Rawil 47
Postfach 2134
1950 Sitten 2

Date: 14.08.2019
Quotation #: 20190814EU699

Thank you for your interest in the NMReady-60PRO, provided by Nanalysis Corp. As per your request we are pleased to submit the following budgetary quotation.

Product	Description	List Price	Qty	Discount	Extended Price
NMReady-60PRO*	60 MHz NMR spectrometer with built in computer - ^{1}H & ^{129}Xe - 1D experiments - 2D experiments - T_1, T_2 and Nutation - Perpetual, easy-to-use **NMReady software** for acquisition and processing	65,000.00	1	13,000.00	52,000.00
AUTOsample-60*	Autosampler - Up to 25 tubes - Simple mounting on top of NMReady-60 - Operated through onboard Software	11,000.00	1	1,100.00	9,900.00
12 Months additional warranty	Includes all parts, labour and depot to customer shipping. (Note: Customer is responsible for shipping the unit to the depot)	3,500.00	1	3,500.00	-
Accessories	Sample warmer, reference samples	500.00	1	500.00	-
Mestrelab	12 month license to MNova software.	-	1	-	-
Service**	Covered by Nanalysis for 1-year	6,000.00	1	6,000.00	-
Customs	Customs fees	300.00	1	-	300.00
Delivery	Delivery by DHL or FedEx	800.00	1	-	800.00
				Net Price EUR	**63,000.00**

* Manufacturer's Warranty, 12 months from date of purchase, includes all parts, labour and depot to customer shipping. (Note: Customer is responsible for shipping the unit to the depot)

NMReady Analytical Power - Right where You need it!

Nanalysis Corp. Unit 1 4600 – 5 Street NE Calgary, AB T2E 7C3 +1.403.769.9499

13.8 Helmholtz coils for field homogeneity

Figure 62 HC9 Helmholtz Coils and its PXI control system [56]

"Bartington Instruments' HC9 Helmholtz Coil system is designed to generate stable and homogeneous magnetic fields in up to three axes. The coil pairs generate a homogeneous magnetic field, up to ±1mT from DC to 440Hz and >±100µT at 5 kHz. The HC9 allows for testing of small sensors at higher fields and provides a homogeneous field to 1% in a volume of 1150cm^3, and homogeneous to 0.1% in a volume of 175cm^3. The PXI control system allows controlling the system from a LabVIEW™-based software, whilst compensation potentiometers are used to cancel the local DC magnetic field." [56]

This device can be used to generate and to homogenize B_0. For application to HP ^{129}Xe, the maximal frequency generated by this system is too low to generate the field B_1.

13.9 NDFEB HALBACH ARRAY

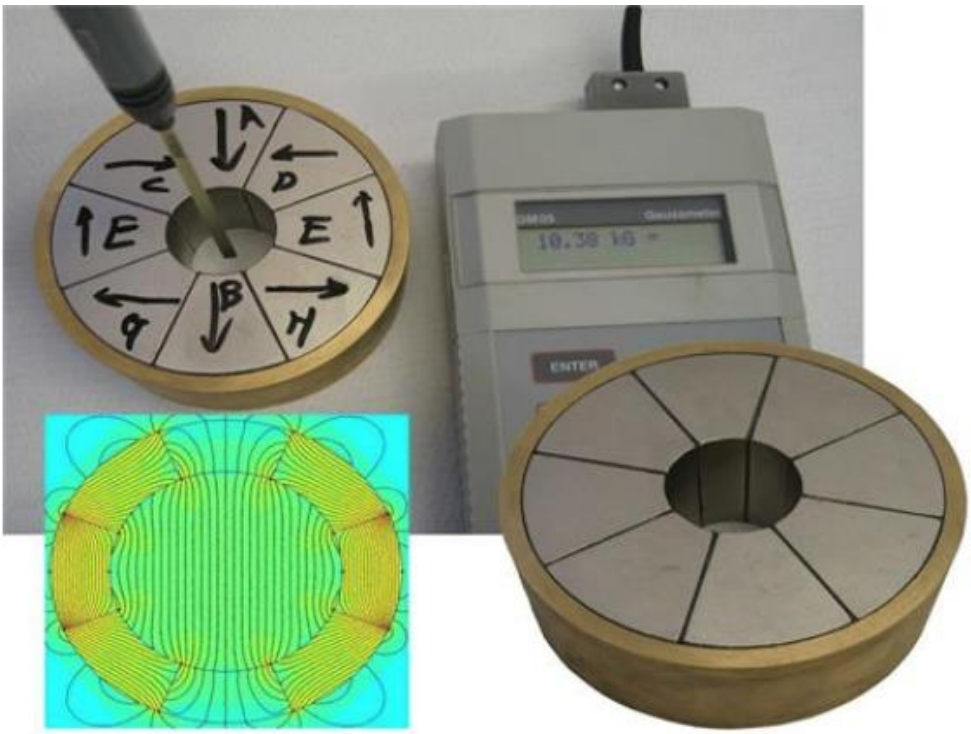

Figure 63 NDFEB HALBACH ARRAY [57]

"The NdFeB Halbach Array is a specialized magnetic assembly consisting of Neodymium Iron Boron (NdFeB, NIB, Neo) permanent magnets assembled in such a way as to provide a controlled (uniform and homogenous) and high magnetic field strength without the use of ferromagnetic materials.

This Halbach Array is a cylinder / ring version with a dipole (2 pole) pattern in the central air gap. The magnetic field within the ring is uniform (parallel field lines which are homogenous) across the entire central hole and of high strength (above 10000 Gauss or 1 Tesla), both being features of this style of Halbach Array. The NdFeB Halbach Array ring is made from 8 magnets (45-degree arc segments, each with a specific direction of magnetization). Each arc segment has the direction of magnetization such that the magnetic field traverses the central air gap and is then 'guided' through and around the magnet material itself.

The NdFeB Halbach Array we offer is a two-pole version that is 110mm in diameter with a 30mm diameter central hole. It is 40mm in axial length. It uses standard +80 deg C maximum recommended operating temperature NdFeB (Neodymium Iron Boron). The field in the center of the air gap is at least 10000Gauss / 1Tesla at ambient temperature. The outer protective sleeve is of brass construction.

We can manufacture other Halbach Arrays upon request. For example, the ring can be made from more arc segments (the higher the number of segments, the better the uniformity of field within the central air gap, but the assembly cost increases) or we can produce to a different magnetic field pattern (multiple pole pairs). Please be aware that the lead-time for making the Halbach Array is typically **11-12** weeks." [57]

13.10 ScopeFun + Red Pitaya

Comparison Table

	ScopeFun	PicoScope 3203D MSO	Red Pitaya	SmartScope	OpenScope
Open Source					
Firmware/Software	YES	No	YES	YES	YES
Hardware	YES	No	No	No	No
Primary Components					
FPGA	Xilinx Artix-7 XC7A35T	-	Xilinx Zynq 7010	Spartan-6 XC6SLX4	-
USB	USB 3.0	USB 3.0	USB 2.0	USB 2.0	USB 2.0
RAM	512 MB DDR3	-	512 MB DDR3	8 MB SDR	-
Oscilloscope					
Channels	2	2	2	2	2
Analog Bandwidth	100 MHz	50 MHz	40 MHz	30 MHz	2 MHz
Max. Real-time Sampling Speed	500 MSPS	1 GSPS	125 MSPS	100 MSPS	6.25 MSPS
Equivalent Time Sampling	YES (2.0 GSPS)	YES (2.5 Gsps)	No	No	No
Memory Depth	128 MS	64MS	16 KS	4 MS	32 KS
Resolution	10-bit	8-bit	14-bit	8-bit	12-bit
Min. Voltage Sensitivity	0.098 mV	0.156 mV	0.122 mV	0.625 mV	-
Input coupling	AC, DC, GND	AC, DC	DC	AC, DC	DC
Arbitrary Waveform Generator					
Channels	2	1	2	1	1
Update Rate	200 MSPS	20 MSPS	125 MSPS	50 MSPS	10 MSPS
Custom Signal Data Points	32 K	32 K	16 K	2 K	25 K
Output Range	±2 V	±2 V	±1 V	0 to +3.3 V	±1.5 V
Resolution	12-bit	12-bit	14-bit	8-bit	10-bit
Logic Analyzer					
Channels	12*	16	8*	8	10*
Sampling Speed	250 MSPS	500 MSPS	12 MSPS	100 MSPS	10 MSPS
Memory Depth	128 MS	64 MS	1 MS	4 MS	32 KS
Digital GPIO					
Channels	12*	-	16*	4	10*
Digital Pattern Generator	YES	No	No	YES	No
Digital Pattern Generator Buffer Size	32 KS	-	-	2 KS	-
Update Rate	250 MSPS	-	-	100 MSPS	-
Price	$650	$800	$360	$260	$99

* Digital channels share the same I/O pins.

Figure 64 Comparison table of different type of oscilloscope [58]

From the 5 oscilloscope and signal generators above, the two following choices are compatible with our application: Red Pitaya and Scopefun. One of the requirements is to have an open source software so that it can be modified to implement the digital logic of an NMR spectrometer. The resolution of the AWG and the oscilloscope needs to be at least 10 bits (1024 discrete values) to diminish the noise of quantification. The update rate needs to be 5 times greater than the Larmor frequency of HP ^{129}Xe at 1 Tesla for resolution reasons. This implies a sampling and receiving speed of at least 50 MSPS. Due to this, the **Red Pitaya STEMlab 125-14 board** listed above would not be suited for this application, however, the **Red Pitaya STEMlab 122.88-16 SDR** has a sampling and receive frequency of **122.88** Msps. This board's specifications and hardware has a high enough performance to meet the needed specifications.

Scopefun was under development at the time of this thesis, the hardware was partially developed and couldn't be reused in the analogic circuit design. Some software parts in the git project implemented an FFT algorithm on a remote server. In fact, it was under crowdfunding in

crowd supply (a website containing multiple breakthrough electronic projects). Scopefun was funded by the end of the thesis. [https://www.crowdsupply.com/] It will be useful to understand its design for the development of the ADC and DAC stages.

Furthermore, the Red Pitaya has an internet interface compatible with Matlab and LabVIEW. It is possible do develop your own application from the firmware to the application. There is a gallery of application to make this device truly multipurpose. A lot of different applications are conceived to measure development circuit for a low cost without the need to have different instruments for each purpose.

Furthermore, a spectrometer is already developed inside the multiple application they have. It is possible to have an LCR meter a bode analyzer and a vector network analyzer. They have also the possibility to simulate the characteristic of a component in frequency.

This could be a great help to use this tool in the development of the radio passive components needed to produce this spectrometer. In the case of tunable capacitors, the component can be measured and estimate great to the Red Pitaya. It could also produce the frequency response of any component for low amplitude signal while measuring the LCR circuit. This enable true tuning of an NMR spectrometer.

Lab-Tools.com have developed a spectrometer by using a Red Pitaya and an analogic circuit. Their device is sold for £6,000 plus VAT including the red pitaya and excluding the oscilloscope and the permanent magnet. This yellow box, produces an NMR spectrum and cost around £5000 with its proprietary software represented on the screen.

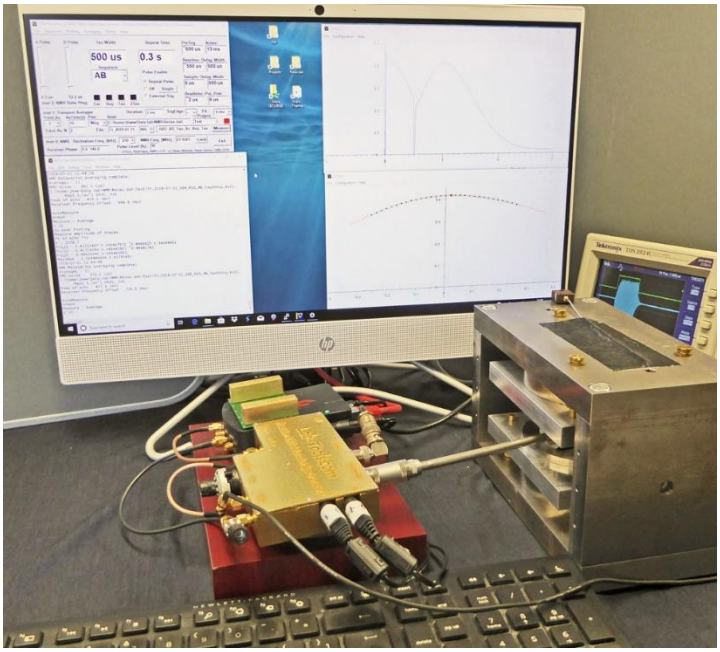

Figure 65 Red Pitaya + lab-tools interface [Source: lab-tools.com]

The Red Pitaya is a real “swiss knife” for electronic development at MF and for all its functionalities. Moreover, it is really affordable.